AD-A097 620 CNR INC NEEDHAM MA F/G 17/2
CHANNEL MEASUREMENT DECODING FOR TROPOSCATTER COMMUNICATIONS.(U)
FEB 81 D CHASE F30602-77-C-0182
UNCLASSIFIED RADC-TR-81-7 NL

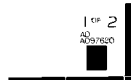

RADC-TR-81-7
Final Technical Report
February 1981

CHANNEL MEASUREMENT DECODING FOR TROPOSCATTER COMMUNICATIONS

CNR, Inc.

David Chase

ROME AIR DEVELOPMENT CENTER
Air Force Systems Command
Griffiss Air Force Base, New York 13441

This report has been reviewed by the RADC Public Affairs Office (PA) and is releasable to the National Technical Information Service (NTIS). At NTIS it will be releasable to the general public, including foreign nations.

RADC-TR-81-7 has been reviewed and is approved for publication.

APPROVED: Paul Sierak

PAUL SIERAK
Project Engineer

APPROVED: Fred I. Diamond

FRED I. DIAMOND, Technical Director
Communications and Control Division

FOR THE COMMANDER: John P. Huss

JOHN P. HUSS
Acting Chief, Plans Office

If your address has changed or if you wish to be removed from the RADC mailing list, or if the addressee is no longer employed by your organization, please notify RADC (DCCT), Griffiss AFB NY 13441. This will assist us in maintaining a current mailing list.

Do not return this copy. Retain or destroy.

UNCLASSIFIED

SECURITY CLASSIFICATION OF THIS PAGE (When Data Entered)

REPORT DOCUMENTATION PAGE	READ INSTRUCTIONS BEFORE COMPLETING FORM
1 REPORT NUMBER: RADC-TR-81-7	2 GOVT ACCESSION NO.: AD-A097620
	3 RECIPIENT'S CATALOG NUMBER:
4 TITLE (and Subtitle): CHANNEL MEASUREMENT DECODING FOR TROPOSCATTER COMMUNICATIONS	5 TYPE OF REPORT & PERIOD COVERED: Final Technical Report
	6 PERFORMING ORG. REPORT NUMBER: N/A
7 AUTHOR(s): David Chase	8 CONTRACT OR GRANT NUMBER(s): F30602-77-C-0182
9 PERFORMING ORGANIZATION NAME AND ADDRESS: CNR, Inc. 220 Reservoir Street Needham MA 02194	10 PROGRAM ELEMENT, PROJECT, TASK AREA & WORK UNIT NUMBERS: 62702F 45192147
11 CONTROLLING OFFICE NAME AND ADDRESS: Rome Air Development Center (DCCT) Griffiss AFB NY 13441	12 REPORT DATE: February 1981
	13 NUMBER OF PAGES: 113
14 MONITORING AGENCY NAME & ADDRESS (if different from Controlling Office): Same	15 SECURITY CLASS. (of this report): UNCLASSIFIED
	15a DECLASSIFICATION/DOWNGRADING SCHEDULE: N/A

16 DISTRIBUTION STATEMENT (of this Report)

Approved for public release; distribution unlimited

17 DISTRIBUTION STATEMENT (of the abstract entered in Block 20, if different from Report)

Same

18 SUPPLEMENTARY NOTES

RADC Project Engineer: Paul Sierak (DCCT)

19 KEY WORDS (Continue on reverse side if necessary and identify by block number)

Troposcatter Communication
Channel Measurement Decoding
Soft Decoding
Interleaved Golay Code

20 ABSTRACT (Continue on reverse side if necessary and identify by block number)

The object of this program is to theoretically investigate and experimentally verify the performance improvement possible by the use of channel-measurement (soft-decision) information when decoding an interleaved (24,12) Golay code. The experimental results obtained during this effort indicate that under certain conditions, such as pulse jamming, significant gains can be achieved by the use of channel measurement decoding. For typical multipath profiles, coding gains in the 5 to 10 (over)

DD FORM 1 JAN 73 1473 EDITION OF 1 NOV 65 IS OBSOLETE

UNCLASSIFIED

SECURITY CLASSIFICATION OF THIS PAGE (When Data Entered)

dB range have been achieved by fairly simple binary decoding techniques. Unfortunately, the predicted theoretical gains due to the use of channel measurement decoding have not been achieved by the experimental results. While channel measurement decoding did offer a 3-dB gain over binary decoding for flat fading, this gain is well below the theoretical prediction of 7.2 dB. The discrepancy between the theoretical experimental results is still an open question, which may be resolved by future work in this area. Nevertheless, in the presence of pulse jamming, channel measurement decoding doubled the effective pulse duration that can be handled by the Golay code. This result is in agreement with theory and a strong indication of the importance of optimum decoding techniques in an ECCM environment.

SUMMARY

The object of this program is to theoretically investigate and experimentally verify the performance improvement possible by the use of channel-measurement (soft-decision) information when decoding an interleaved (24,12) Golay code. The experimental results obtained during this effort indicate that under certain conditions, such as pulse jamming, significant gains can be achieved by the use of channel measurement decoding. For typical multipath profiles, coding gains in the 5 to 10 dB range have been achieved by fairly simple binary decoding techniques. Unfortunately, the predicted theoretical gains due to the use of channel measurement decoding have not been achieved by the experimental results. While channel measurement decoding did offer a 3-dB gain over binary decoding for flat fading, this gain is well below the theoretical prediction of 7.2 dB. The discrepancy between the theoretical and experimental results is still an open question, which may be resolved by future work in this area. Nevertheless, in the presence of pulse jamming, channel measurement decoding doubled the effective pulse duration that can be handled by the Golay code. This result is in agreement with theory and a strong indication of the importance of optimum decoding techniques in an ECCM environment.

TABLE OF CONTENTS

LIST OF TABLES

LIST OF TABLES (Continued)

LIST OF FIGURES

LIST OF FIGURES (Continued)

LIST OF FIGURES (Continued)

EVALUATION

This report summarizes work aimed at evaluating the performance obtainable over the tactical troposcatter channel by utilizing a new channel measurement or soft decision decoder in conjunction with the previously built Interleaved Golay (24.12) encoder. Performance results indicate minimal improvement over the previous hard decision or binary decoder used to decode the Interleaved Golay (24,12) encoder. Within the cost constraints of this effort the question as to whether the problem of not confirming the expected results lies within the hardware implementation (MLT Modem, Interleaver, Golay (24,12) Encoder, Channel Measurement Decoder) or in theoretical estimates of performance is still open.

Previous performance of the Maximum Likelihood Modem used in conjunction with the Interleaved Golay (24,12) encoder with hard decoding has certainly indicated substantial performance improvement in the tactical troposcatter communications arena. Although the performance improvements via channel measurement decoding is still undecided, key data on the effectiveness of this decoding technique in the face of pulse jamming, does improve our arsenal of techniques utilizable against enemy jamming of tactical troposcatter links. Based on this, it is important to note that a bandwidth efficient modem (MLT Modem), is the key to unlocking the benefits coding brings to the tactical troposcatter arena whether under normal operation or in a jamming environment.

PAUL SIERAK
Project Engineer

SECTION 1

INTRODUCTION

The object of this program is to theoretically investigate and experimentally verify the performance improvement possible by the use of channel-measurement (soft-decision) information when decoding an interleaved (24,12) Golay code. During the previous troposcatter communications contract, F30602-74-C-0133 [1.1],[1,2], a hard decoder for a (24,12) Golay code was implemented; experimental results obtained indicated that significant performance gains are possible by hard decoding even with delays as short as 138 ms. This program is concerned with obtaining bit reliability information from the maximum-likelihood demodulator and using this information to enhance the performance of the (24,12) Golay code by implementing an effective soft-decision decoding algorithm [1.3]. The equipment developed under Contract No. F30602-74-C-0133 is modified to include this additional mode of operation, with the original mode of operation still being retained.

The theoretical coding gains when bit errors occur independently (no constraint on decoding delay) is determined in Section 2 and is summarized in Table 1-1. This table illustrates that as the available diversity increases, be it implicit (in-band multipath) or explicit (space or frequency diversity), the coding gains decrease. Fortunately, the estimated loss in performance due to correlated bit errors also decreases as the order of diversity increases, as indicated in Table 1-2. These two tables indicate that even for highly correlated bit errors channel-measurement decoding should offer at least an additional 2-dB coding gain in addition to the 5- to 7-dB coding gain already achieved by binary decoding. These predictions are based on the assumption that the available diversity is 3 or 4 and that $B\tau = 0.01$. For the Golay code, the decoding delay is given by $T = 23\tau$, so that $B\tau = 0.01$, corresponding to a decoding delay of

$$T = \frac{230}{B} \text{ ms}$$

TABLE 1-1

THEORETICAL CODING GAINS AT A BIT ERROR PROBABILITY OF 10^{-5}

Available Diversity	Binary Decoding	Channel Measurement Decoding	Difference Between Binary and Channel Measurement Decoding
1	26.4 dB	33.6 dB	7.2 dB
2	12.4 dB	16.4 dB	4.0 dB
3	8.4 dB	11.8 dB	3.4 dB
4	6.4 dB	9.3 dB	2.9 dB
8	4.0 dB	6.4 dB	2.4 dB

TABLE 1-2

ESTIMATED LOSS IN PERFORMANCE DUE TO CORRELATED BITS AT A DECODED ERROR RATE OF 10^{-5}

Order of Diversity	$B\tau = 0.01$	$B\tau = 0.02$	$B\tau = 0.05$	$B\tau = 0.2$
1	10.4 dB	8.1 dB	4.5 dB	0.7 dB
2	3.2 dB	3.0 dB	2.5 dB	0.6 dB
3	1.4 dB	1.3 dB	1.2 dB	0.5 dB
4	1.0 dB	0.8 dB	0.7 dB	0.4 dB
8	0.3 dB	0.3 dB	0.3 dB	0.2 dB

Thus, for a fading bandwith of $B = 5$ Hz, a decoding delay of only 46 ms is required for $B\tau = 0.01$.

The actual experimental results are presented in Section 3. The most encouraging results were obtained for a test which simulated pulse interference. This preliminary test was performed to determine the maximum pulse duration which can be corrected with and without channel-measurement information. A separation of $\tau = 48$ ms between code digits was used for this experiment. As the pulse width was increased, the performance of the binary decoder started to deteriorate for pulse durations exceeding 140 ms. The channel-measurement decoder was able to operate error-free for pulse durations up to 280 ms. These results agree very well with theory since a triple error-correcting binary decoder should operate successfully with pulses of duration less than $3\tau = 144$ ms. The channel-measurement decoder should double the error-correcting capabilities [1.3] or, equivalently, operate with pulse durations of approximately twice the length handled by a binary decoder.

The experimental results for the three multipath profiles considered in Section 2 fell considerably below that predicted by theory. A 3-dB gain, due to the use of channel-measurement information, was obtained for the flat fading channel. This gain is approximately 4 dB less than predicted by theory. The gains due to the use of channel-measurement information for profiles 3 and 5 were quite small and fall a few dB below that predicted by theory.

This discrepancy between theory and experimental results remains an open question which should be resolved by future work in this area.

REFERENCES

[1.1] CNR, Inc., "Troposcatter Interleaver Study Report," Phase Report, RADC-TR-75-19, February 1975. AD#A008523.

[1.2] CNR, Inc., "Troposcatter Interleaver," Final Technical Report for Rome Air Development Center, RADC-TR-76-213, July 1976. AD#A030054

[1.3] D. Chase, "A Class of Algorithms for Decoding Block Codes with Channel Measurement Information," IEEE Trans. on Information Theory, Vol. IT-18, January 1972, pp. 170 - 182.

SECTION 2

THEORETICAL PERFORMANCE PREDICTIONS

In this section theoretical performance estimates are obtained for the improvement in performance when channel measurement decoding of the Golay code is used for tactical troposcatter communications. These theoretical results are used to predict the performance gains for the multipath profiles considered in Rome Air Development Center Contract No. F30602-74-C-0137 [2.1], [2.2].

The first portion of this section gives the ultimate performance possible if decoding delay is not a constraint, i.e., the performance is given when code bits are statistically independent. Performance with a decoding delay constraint, which introduces dependent errors, is estimated in Section 2.2. An important result included in Section 2.2 is a simulation illustrating that for a completely correlated (zero delay) Golay code, which is decoded with channel measurement information, a coding gain of 2.5 dB is achieved at a bit error probability of 10^{-5} when a quad diversity channel is assumed. This result implies that even a signal diversity channel, with a fourth-order in-band diversity, can satisfy the above conditions. Thus, it is anticipated that significant performance gains can be achieved with minimum decoding delay. Finally, in Section 2.3, techniques for obtaining meaningful channel measurement information for use by the Golay decoder are presented.

2.1 Performance with Independent Code Bits

The ultimate performance gains possible for the Golay code with binary and channel measurement decoding are obtained under the assumption that code bits are interleaved sufficiently such that errors occur independently. Under this assumption, the performance is readily obtainable by the equations given ir [2.3]. The performance results for binary decoding are given by Eq. (22) of [2.3], which is closely approximated by

$$P_b \simeq 1771\ p^4 \tag{2.1}$$

This upper bound on decoded bit error probability is quite tight for values of raw (undetected) bit error rates p below 10^{-2}, and, thus, is sufficient to estimate decoded error probabilities of 10^{-5}. For channel measurement decoding, Eq. (21) in [2.3] for the Golay code becomes

$$P_b \approx 253\, P_r[8^{th}\text{-order diversity}] \tag{2.2}$$

where $P_r[8^{th}$-order diversity] is the performance for a given channel under the assumption that 8^{th}-order (time) diversity is available. Thus, if the channel without coding behaves as a dual-diversity channel, the use of the Golay code with channel measurement decoding will increase the effective diversity to that of a 16^{th}-order system. Note, of course, that the performance with coding has a multiplicative factor of 253; when plotted as a function of E_b/N_0, the performance curve must be penalized by 3 dB for the rate-1/2 code. Nevertheless, Figures 2.1 through 2.5 indicate the significant coding possible by use of this code. These results are for a flat Rayleigh fading channel with the order of diversity varying from L=1 on Figure 2.1 to L=8 on Figure 2.5. Results of this nature are also useful for predicting the performance possible when in-band diversity is present due to multipath or if space/frequency diversity is actually available. Table 2-1 summarizes the theoretical coding gains at 10^{-5} for binary decoding and for a practical channel measurement decoding algorithm such as algorithm 2 in [2.4].

For completeness, the same performance curves are also plotted on Figures 2.6 through 2.10 as a function of the signal-to-noise ratio per transmitted (encoded) bits, i.e., as a function of E_t/N_0. The signal-to-noise ratio per transmitted (encoded) bit is given by:

$$\frac{E_t}{N_0} = \frac{P_r}{N_0 D} \tag{2.3}$$

where P_r is the received power, N_0 is the noise power density per Hz, and D is the transmitted data rate. When coding is not used,

$$\frac{E_t}{N_0} = \frac{E_b}{N_0} \quad \text{(no coding)} \tag{2.4}$$

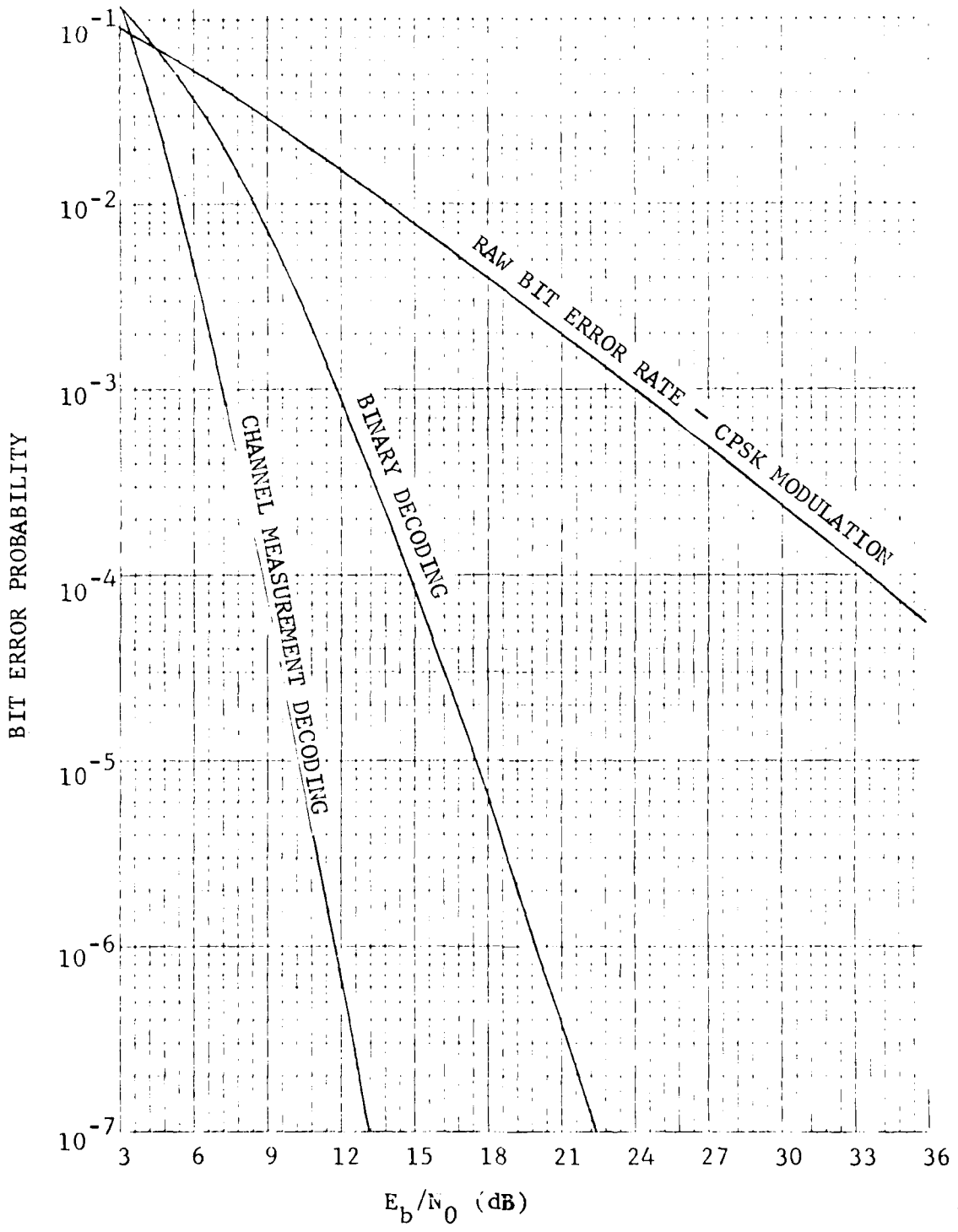

Figure 2.1 Coding Performance as a Function of the SNR per Information Bit - Order of Diversity: L=1

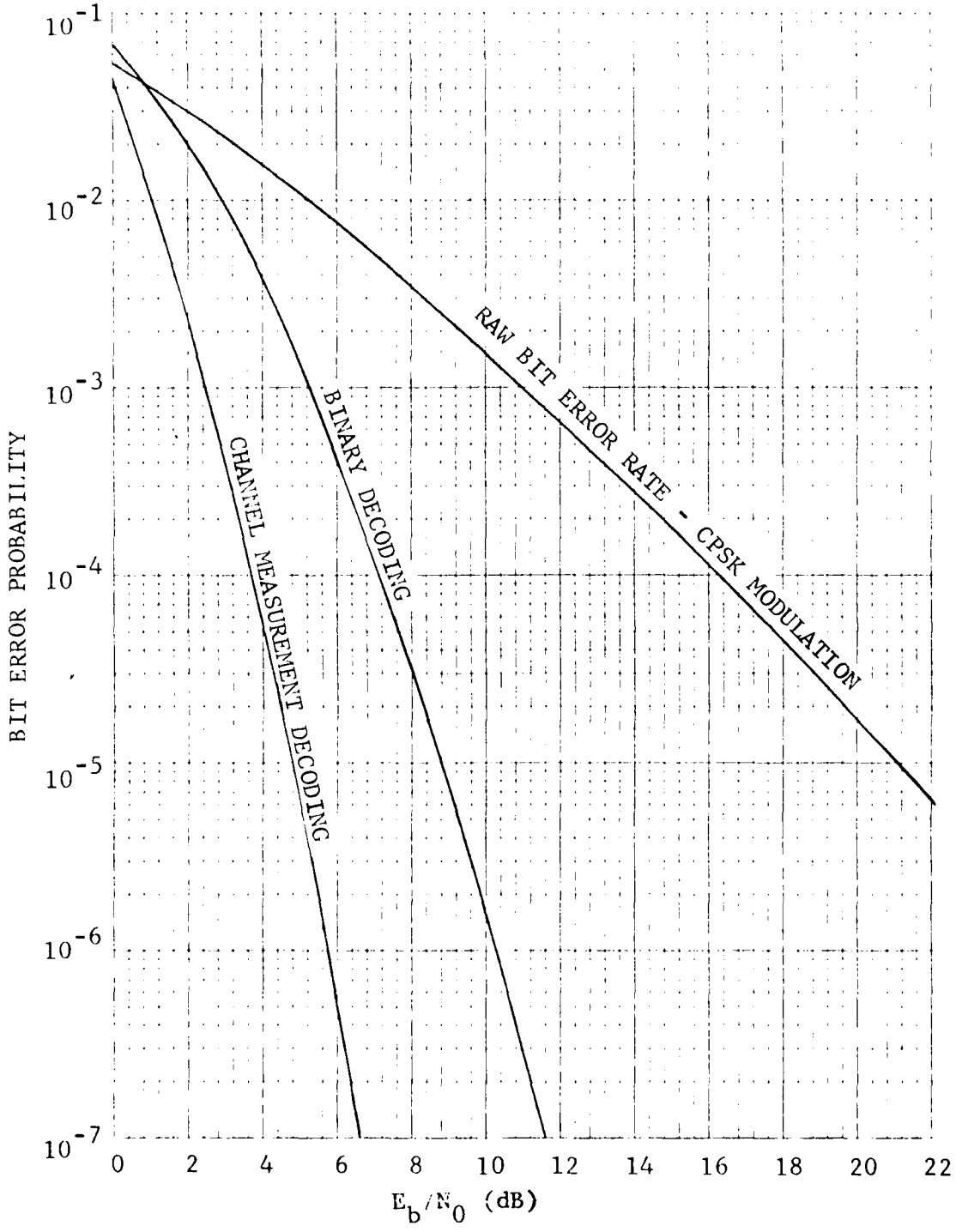

Figure 2.2 Coding Performance as a Function of the SNR per Information Bit - Order of Diversity: L=2

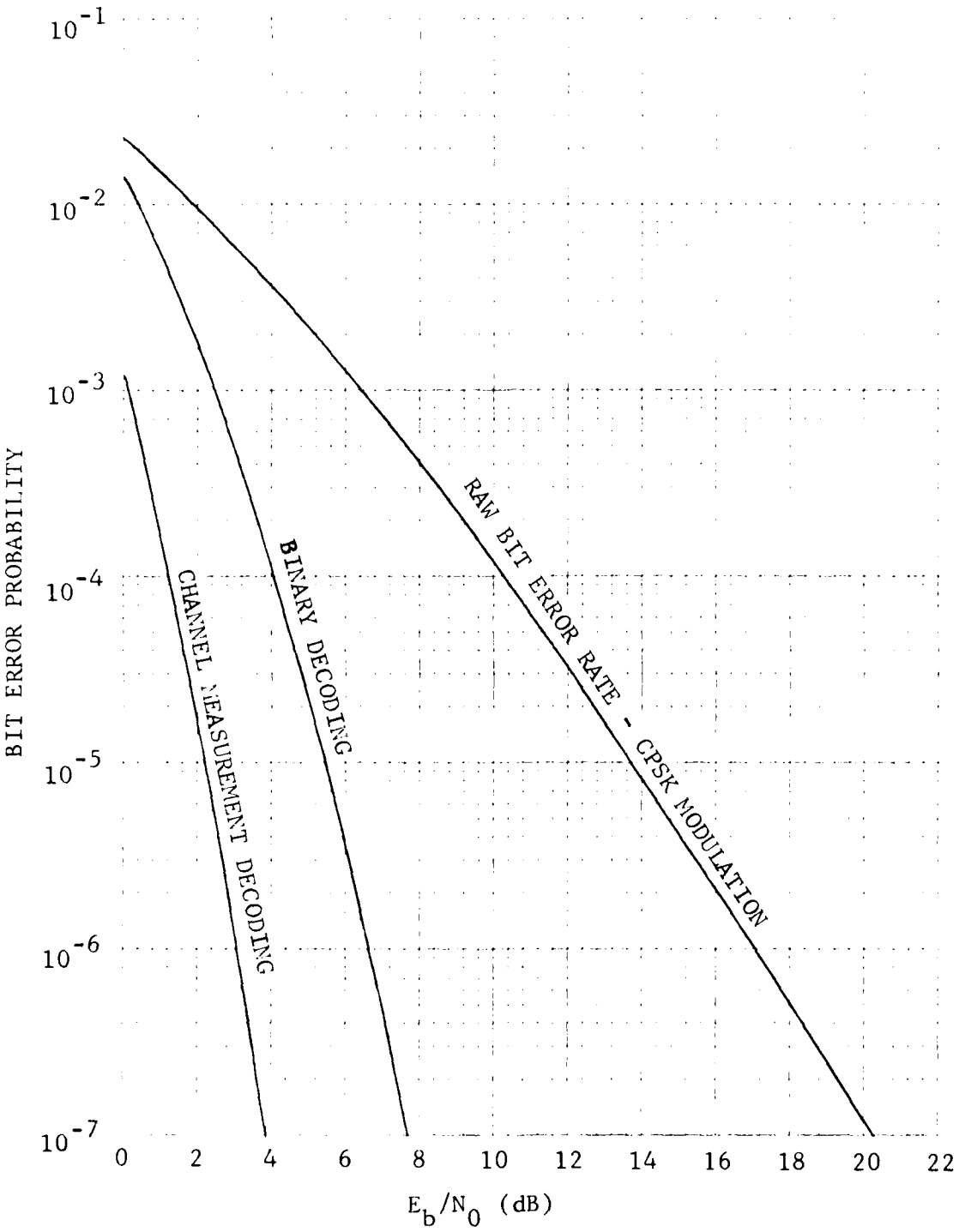

Figure 2.3 Coding Performance as a Function of the SNR per Information Bit - Order of Diversity: L=3

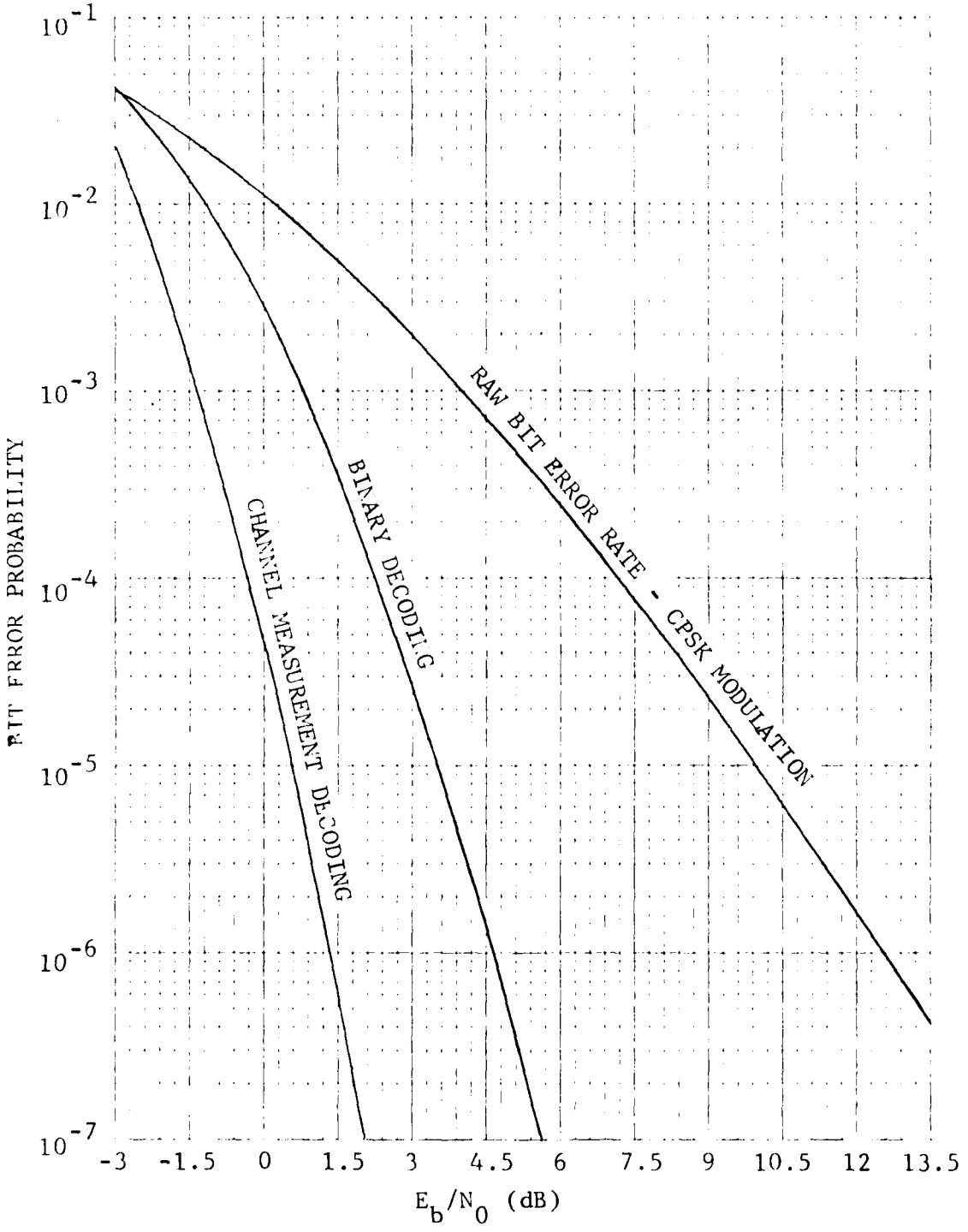

Figure 2.4 Coding Performance as a Function of the SNR per Information Bit - Order of Diversity: L=4

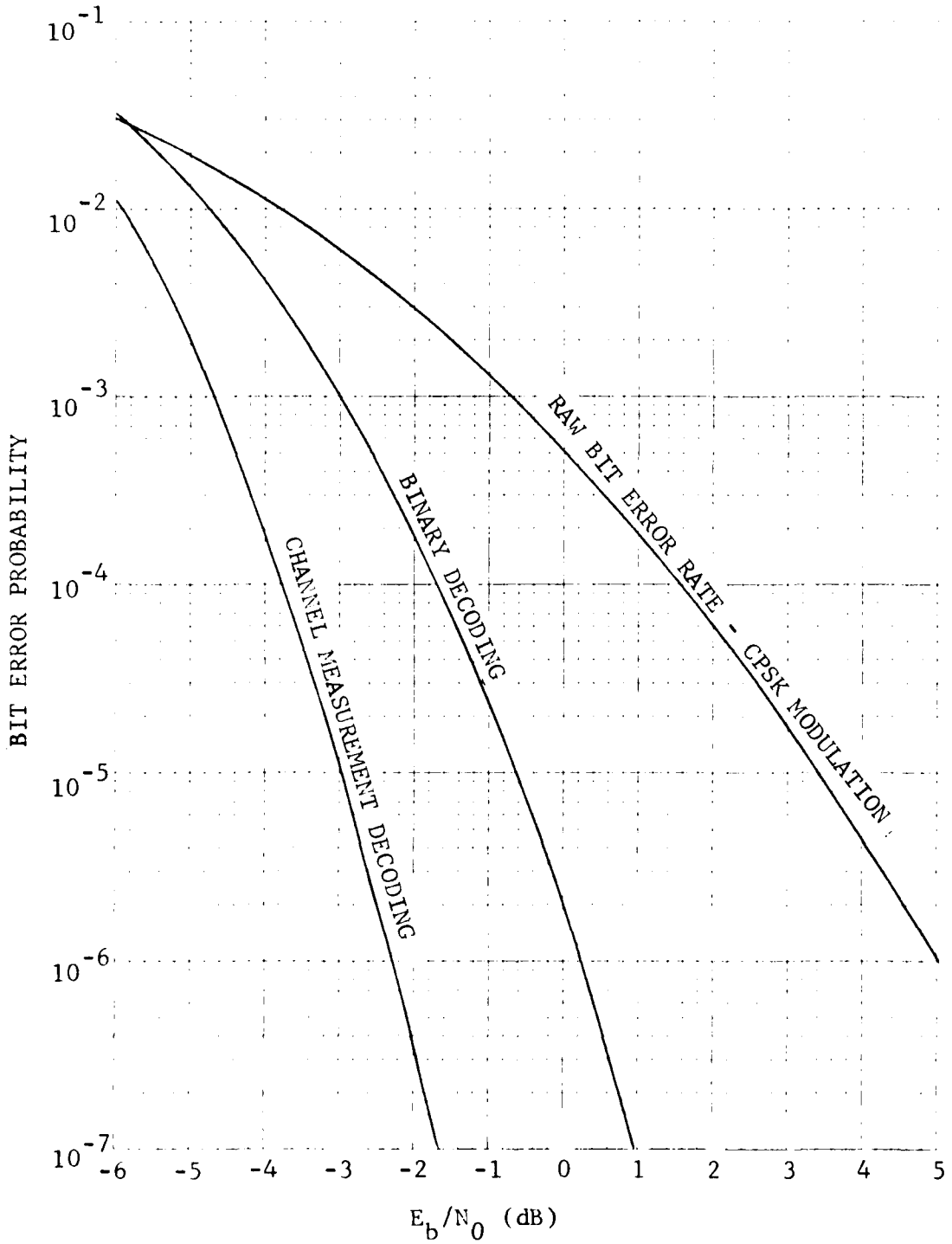

Figure 2.5 Coding Performance as a Function of the SNR per Information Bit - Order of Diversity: L=8

TABLE 2-1

THEORETICAL CODING GAINS AT A BIT ERROR PROBABILITY OF 10^{-5}

Available Diversity	Binary Decoding	Channel Measurement Decoding	Difference Between Binary and Channel Measurement Decoding
1	26.4 dB	33.6 dB	7.2 dB
2	12.4 dB	16.4 dB	4.0 dB
3	8.4 dB	11.8 dB	3.4 dB
4	6.4 dB	9.3 dB	2.9 dB
8	4.0 dB	6.4 dB	2.4 dB

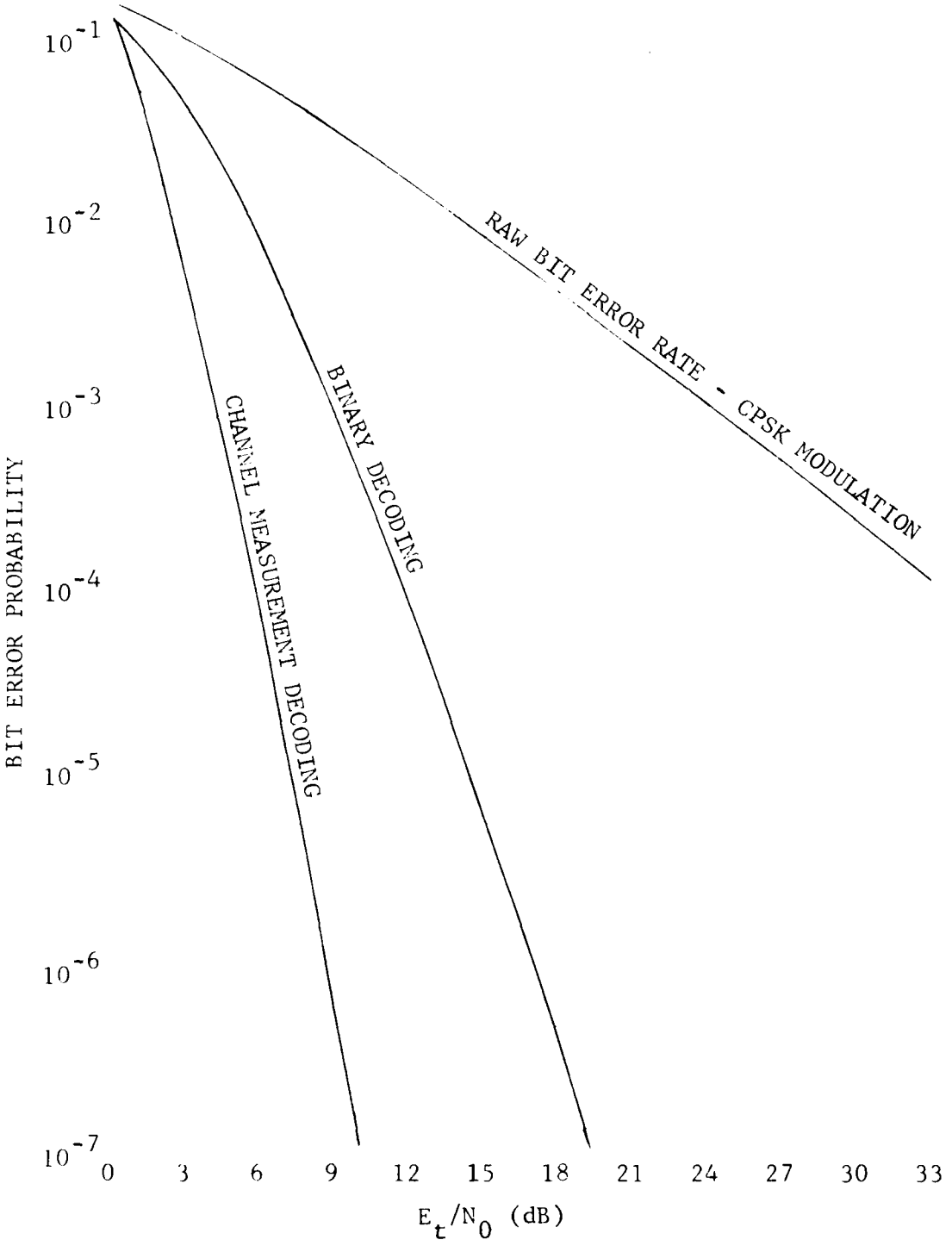

Figure 2.6 Coding Performance as a Function of the SNR per Encoded Bit - Order of Diversity: L=1

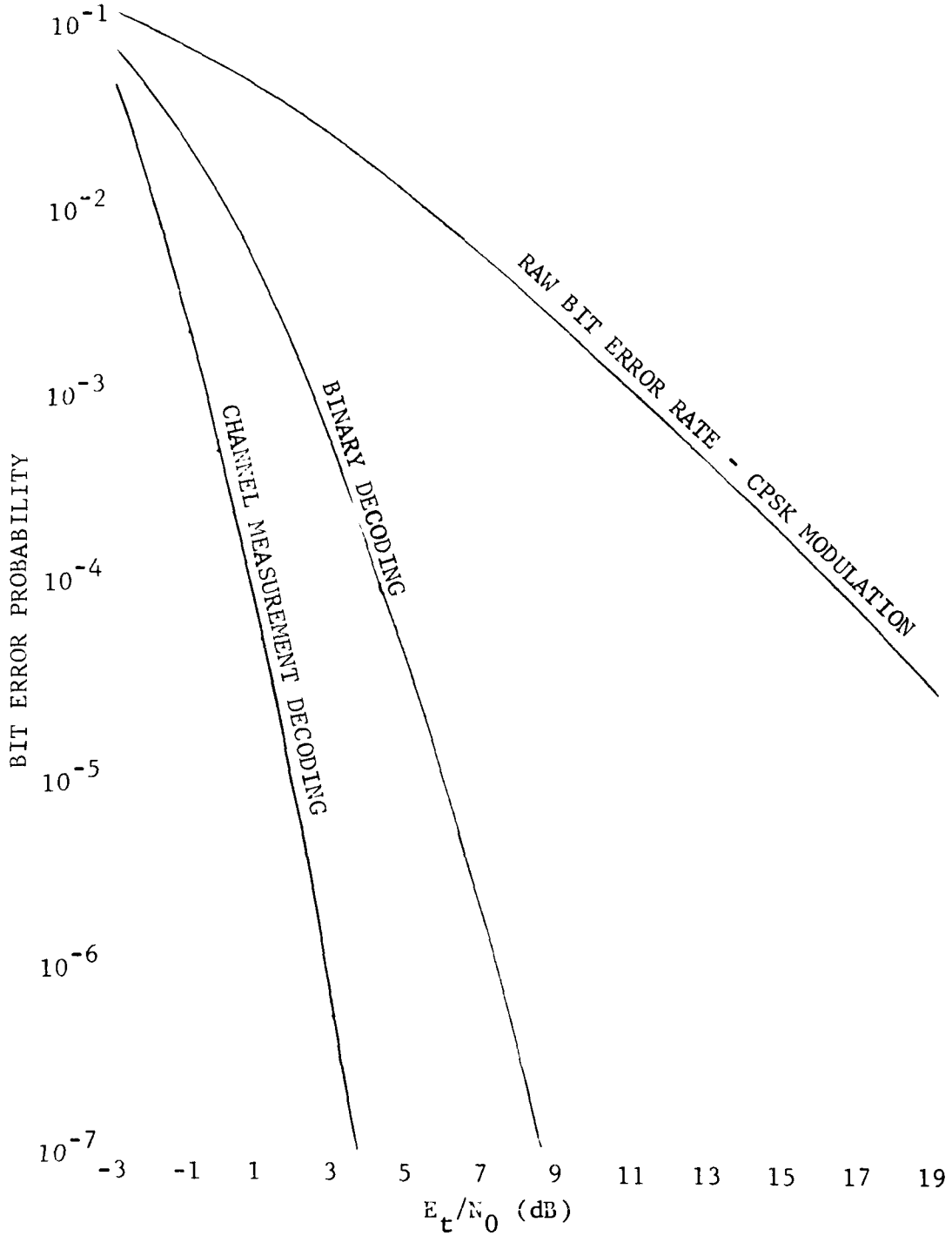

igure 2.7 Coding Performance as a Function of the SNR per Encoded Bit - Order of Diversity: L=2

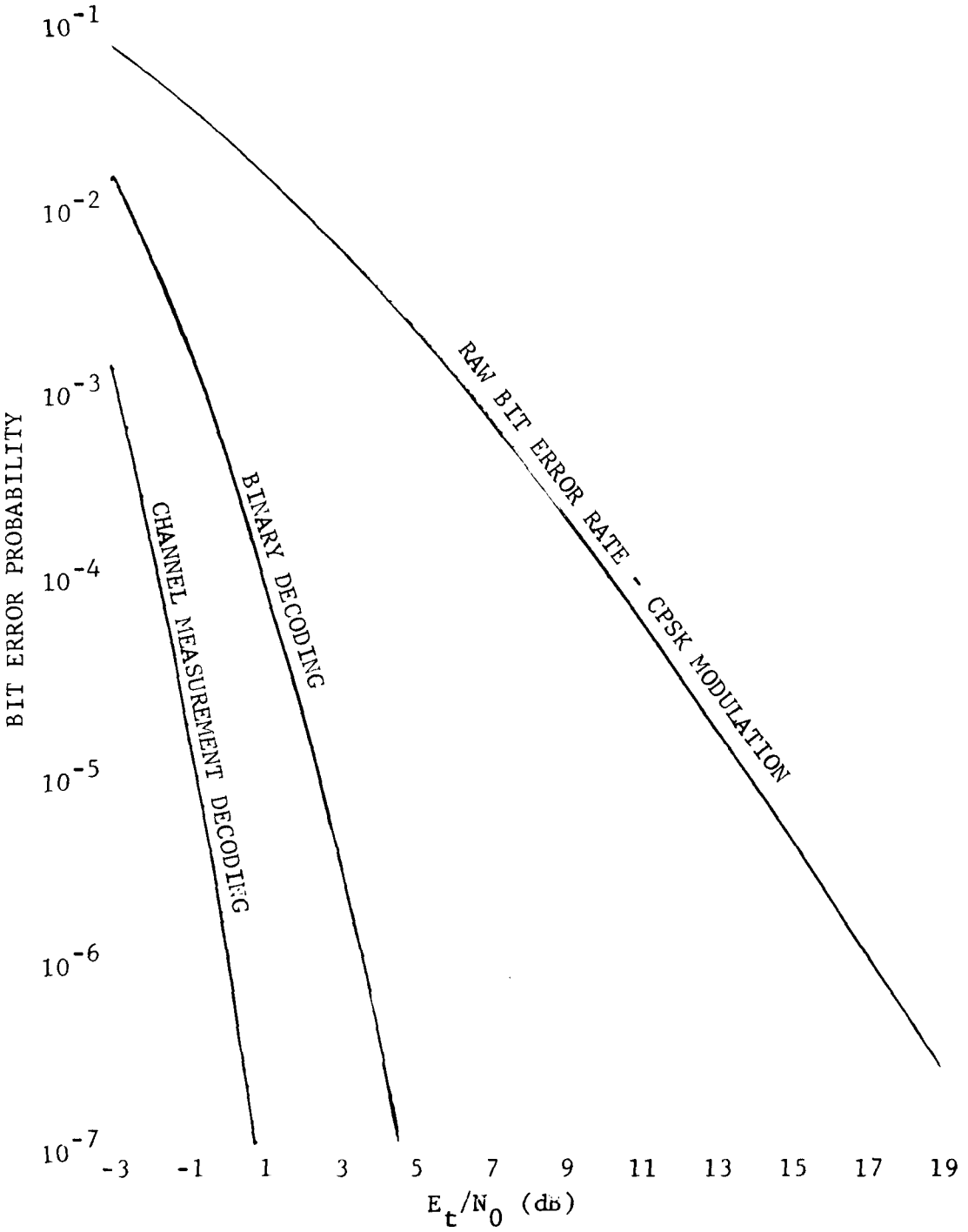

Figure 2.8 Coding Performance as a Function of the SNR per Encoded Bit - Order of Diversity: L=3

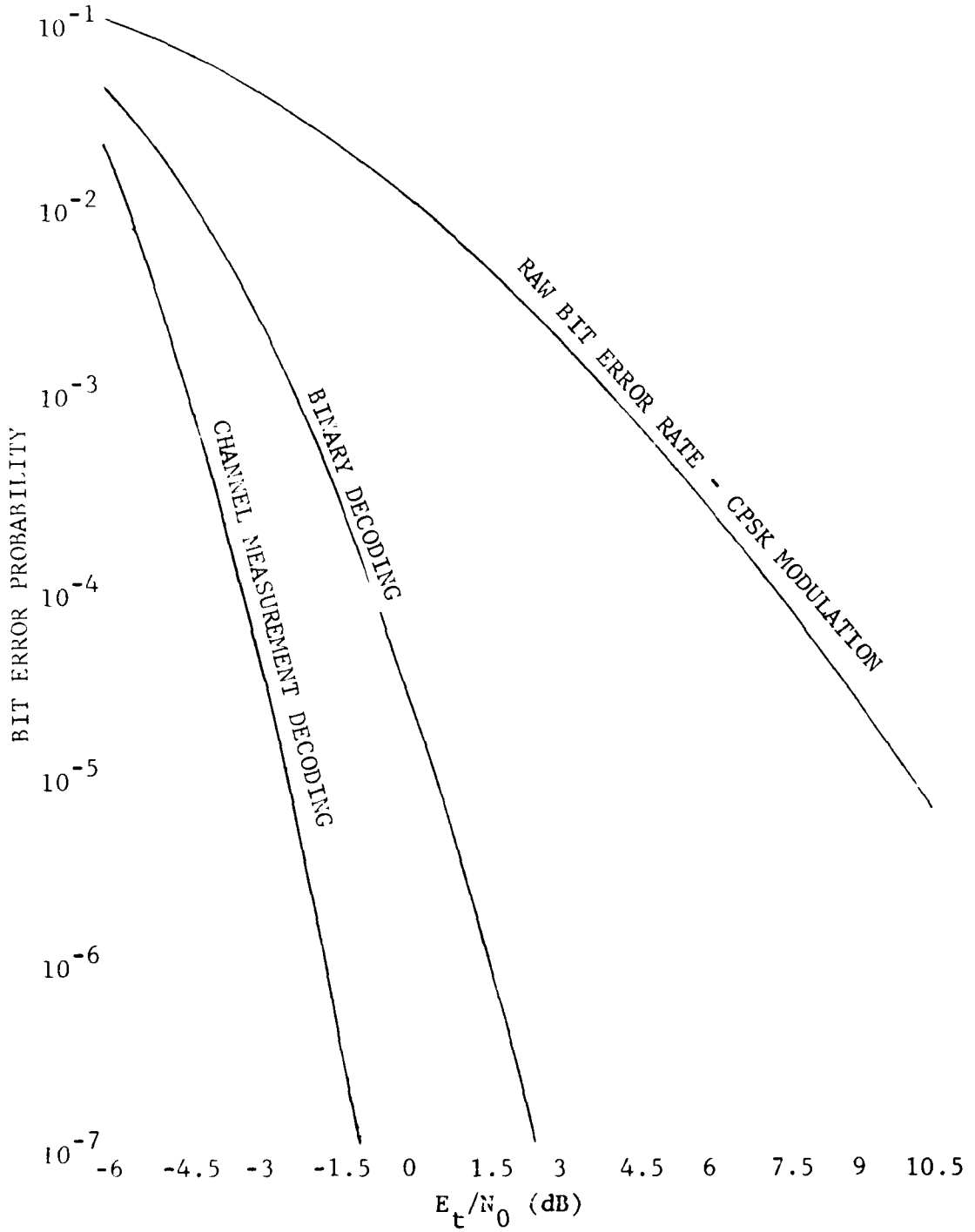

Figure 2.9 Coding Performance as a Function of the SNR per Encoded Bit - Order of Diversity: L=4

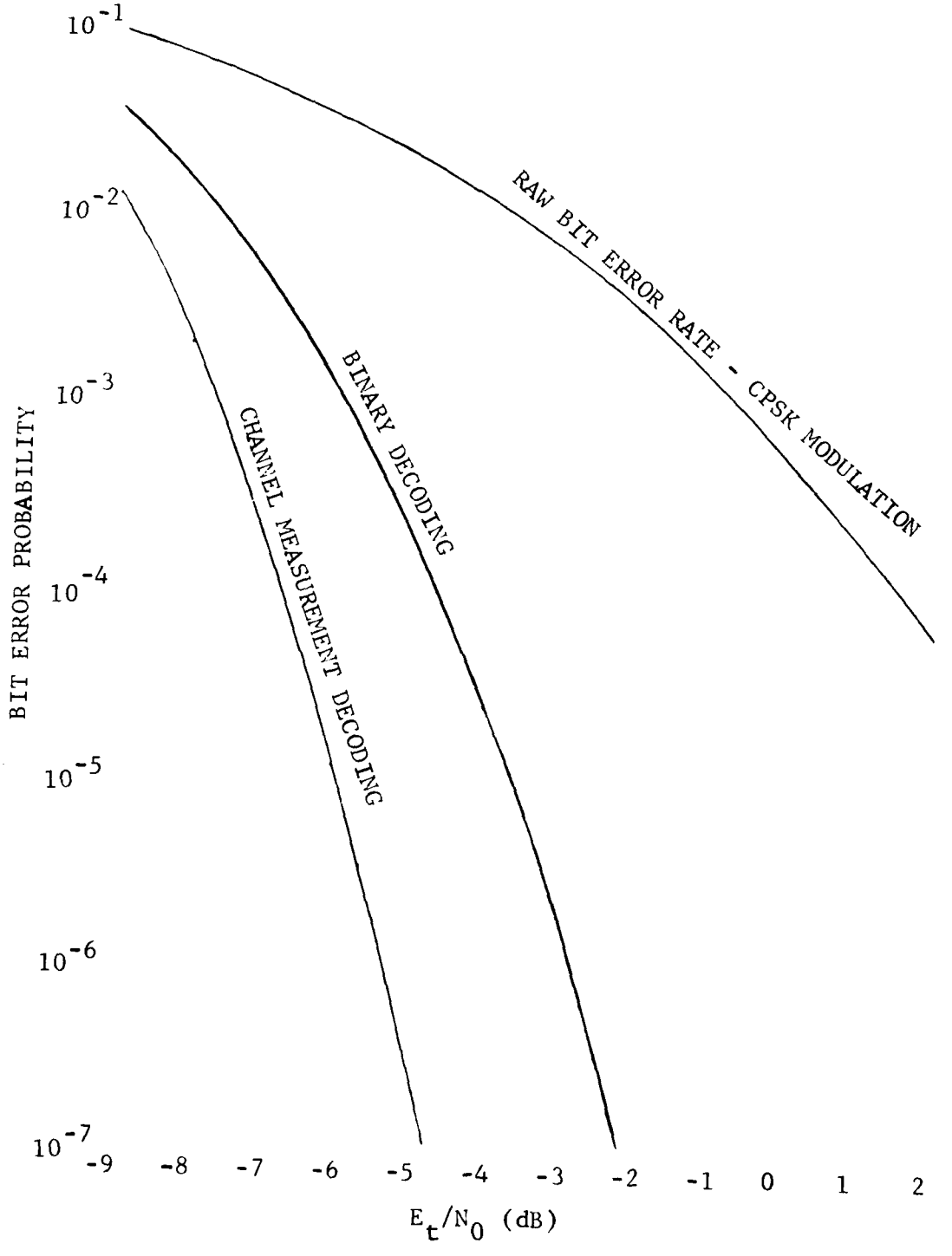

igure 2.10 Coding Performance as a Function of the SNR per Encoded Bit - Order of Diversity: L=8

However, in our case, the actual information data rate is R b/s which is less than D b/s because of the redundancy inserted by the error-correcting code. Since the code rate is given as

$$r = \frac{R}{D} = \frac{1}{2} \tag{2.5}$$

we have

$$\frac{E_b}{N_0} \doteq \frac{P_r}{N_0 R} = \left(\frac{E_t}{N_0}\right)\frac{1}{r} \qquad \text{(with coding)} \tag{2.6}$$

For system performance evaluation, a plot as a function of E_b/N_0 is desirable. However, for testing coding, a plot of error probability as a function of E_t/N_0 is convenient since the raw bit rate before and after decoding is shown at the same signal-to-noise ratio. A block diagram of the interleaved Golay code and modem is illustrated in Figure 2.11.

2.2 Performance Estimate with Dependent Code Bits

The purpose of this section is to investigate the performance of these coding schemes when a limited amount of storage is available or, equivalently, when a constraint on data delay is imposed.

When the bit separation for the interleaved code is not large enough, there is correlation between bits within a code block at the output of the deinterleaver. To a first approximation, which agrees quite well with experimental results, we will assume that a given bit depends on its adjacent bits only and is independent of bits which are nonadjacent. Thus, a model for this situation is given by a Markov chain, as shown in Figure 2.12. There are two possible states in the Markov chain: state 0, the good state; and state 1, the bad state. In other words, when a bit error is incorrect, the chain enters state 1 and when a bit is received correctly, it enters state 0. The conditional probabilities are given by:

$$s = \Pr\{\text{present bit is incorrect} \mid \text{previous bit is correct}\} \tag{2.7}$$

and

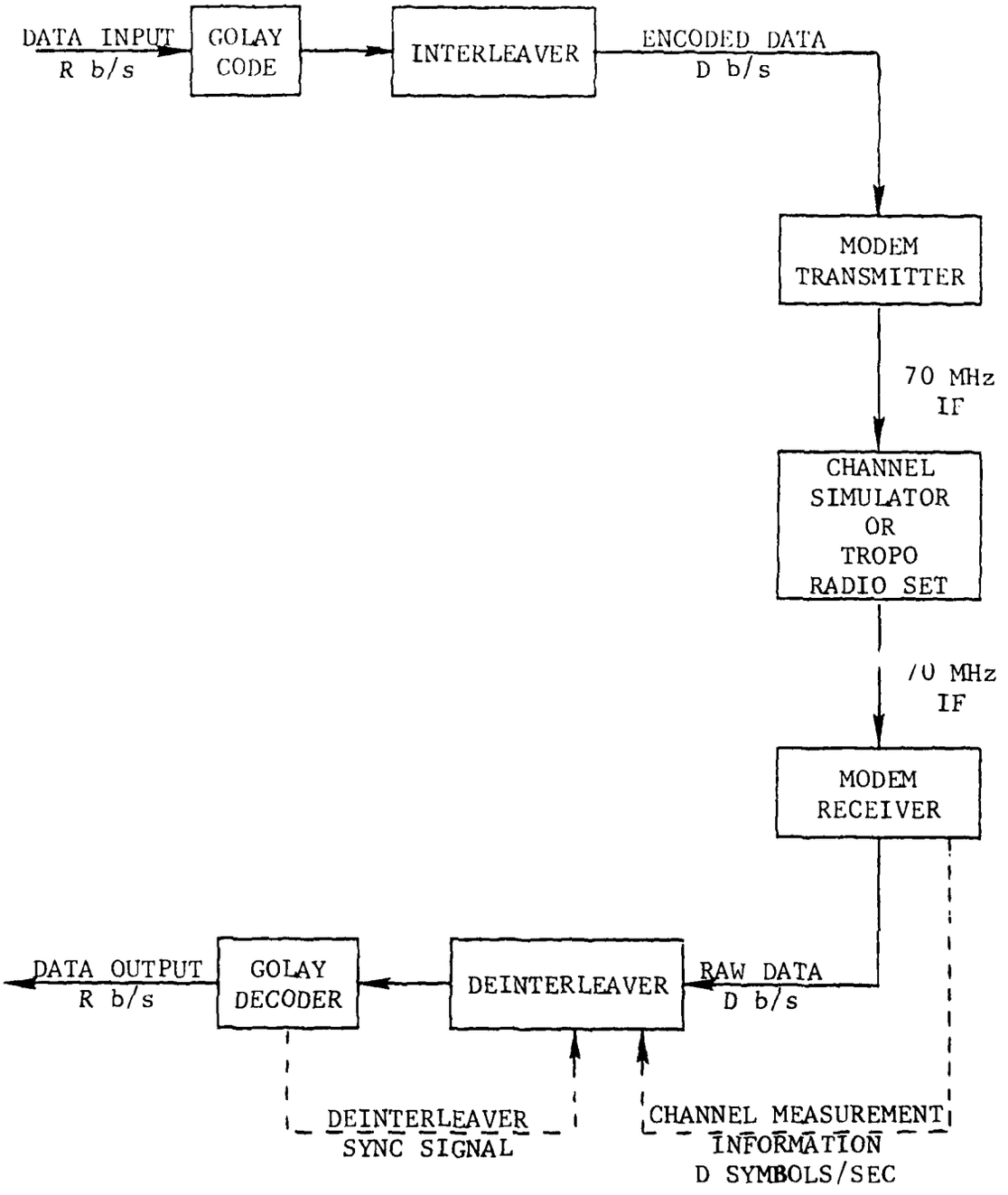

Figure 2.11 Block Diagram of a Tropo System Utilizing an Interleaved Code

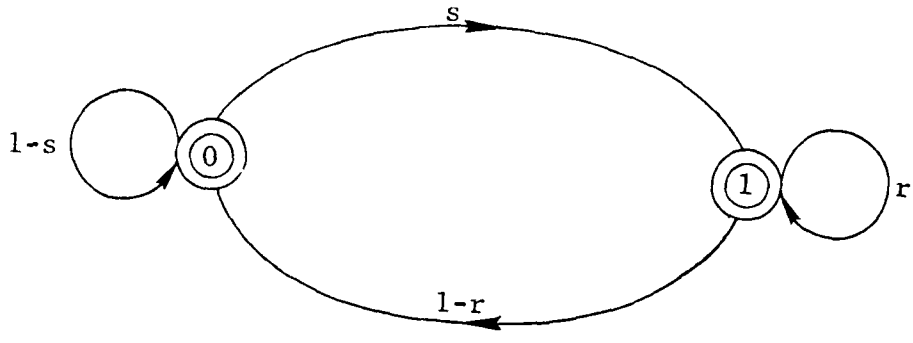

Figure 2.12 Markov Chain Model for a Correlated Bit Stream

$$r = \Pr\{\text{present bit is incorrect} \mid \text{previous bit is incorrect}\} \tag{2.8}$$

It is obvious that the bit error rate p is just the probability of the chain being in state 1. The transition matrix of the Markov chain is given by:

$$A = \begin{bmatrix} 1-s & 1-r \\ s & r \end{bmatrix} \tag{2.9}$$

The steady-state probability distribution is

$$\Pr\{\text{state } 0\} = 1 - p \tag{2.10}$$

$$\Pr\{\text{state } 1\} = p = \text{bit error rate} \tag{2.11}$$

so that

$$A\begin{bmatrix} 1-p \\ p \end{bmatrix} = \begin{bmatrix} 1-p \\ p \end{bmatrix} \tag{2.12}$$

For L=1 (no diversity), the joint density of R_1R_2, where R_1 and R_2 are two correlated envelope values, is given by [2.5]:

$$f(R_1R_2) = \frac{R_1R_2}{\sigma_1^2\sigma_2^2(1-\rho^2)} I_0\left[\frac{\rho R_1R_2}{(1-\rho^2)\sigma_1\sigma_2}\right] \exp\left[-\frac{1}{2(1-\rho^2)}\left(\frac{R_1^2}{\sigma_1^2}+\frac{R_2^2}{\sigma_2^2}\right)\right] \tag{2.13}$$

where ρ is the correlation between the two underlying complex Gaussian random vectors and σ_i^2 is the power in one component of either vector. ρ is related to the bit separation τ by the relation

$$\rho = \exp\left(-\frac{\pi^2 B^2 \tau^2}{2}\right) \tag{2.14}$$

where B is the rms bandwidth of a fading path. $I_0(x)$ is the zero-order modified Bessel function of the first kind. Assuming that the average power remains constant in time and that each path has unity average power, then $\sigma_i^2 = 1/2$, and

$$f(R_1 R_2) = \frac{4R_1R_2}{1-\rho^2} I_0\left(\frac{2\rho}{1-\rho^2} R_1R_2\right) \exp\left[-\frac{1}{1-\rho^2}\left(R_1^2 + R_2^2\right)\right] \tag{2.15}$$

Thus, defining $S_i = R_i^2$ to be the power in the i^{th} baud,

$$f(S_1S_2) = \frac{1}{1-\rho^2} I_0\left(\frac{2\rho}{1-\rho^2}\sqrt{S_1S_2}\right) \exp\left[-\frac{1}{1-\rho^2}(S_1 + S_2)\right] \tag{2.16}$$

Obtain the joint moment generating function defined by

$$\begin{aligned}
\varphi_{\underline{S}}(\underline{p}) &= E\left[\exp\left(-\langle \underline{p}, \underline{S}\rangle\right)\right] = E\left[\exp\left(-p_1S_1 - p_2S_2\right)\right] \\
&= \frac{1}{1-\rho^2}\int_0^\infty dS_1 \int_0^\infty dS_2\, I_0\left(\frac{2\rho}{1-\rho^2}\sqrt{S_1S_2}\right) \exp\left[-\left(\frac{1}{1-\rho^2} + p_1\right)S_1 \right. \\
&\qquad \left. -\left(\frac{1}{1-\rho^2} + p_2\right)S_2\right] \\
&= \frac{1}{1-\rho^2}\int_0^\infty dS_2 \exp\left[-\left(\frac{1}{1-\rho^2} + p_2\right)S_2\right] \int_0^\infty dS_1\, I_0\left(\frac{2\rho\sqrt{S_2}}{1-\rho^2} S_1^{\frac{1}{2}}\right) \\
&\quad \cdot \exp\left[-\left(\frac{1}{1-\rho^2} + p_1\right)S_1\right]
\end{aligned} \tag{2.17}$$

$$\varphi_{\underline{S}}(\underline{p}) = \frac{1}{1-\rho^2}\int_0^{\infty} dS_2 \exp\left[-\left(\frac{1}{1-\rho^2}+p_2\right)S_2\right] \frac{\exp\left[\frac{\rho^2}{(1-\rho^2)^2}S_2 \Big/ \frac{1}{1-\rho^2}+p_1\right]}{\frac{1}{1-\rho^2}+p_1}$$

$$= \frac{1}{1+p_1(1-\rho^2)}\int_0^{\infty} dS_2 \exp\left\{-S_2\left[\frac{1}{1-\rho^2}+p_2-\frac{\rho^2}{1-\rho^2+p_1(1-\rho^2)^2}\right]\right\}$$

$$= \frac{1}{1+p_1(1-\rho^2)} \frac{1-\rho^2}{1+p_2(1-\rho^2)-\frac{\rho^2}{1+p_1(1-\rho^2)}}$$

$$= \frac{1-\rho^2}{\left[1+p_1(1-\rho^2)\right]\left[1+p_2(1-\rho^2)\right]-\rho^2} \qquad \text{(2.17 Cont.)}$$

Let $1-\rho^2=\mu$, then

$$\varphi_{\underline{S}}(\underline{p}) = \frac{\mu}{1+p_1p_2\mu^2+(p_1+p_2)\mu-\rho^2}$$

$$= \frac{1}{1+p_1+p_2+p_1p_2\mu} \qquad (2.18)$$

For L^{th}-order diversity maximal ratio combining,

$$S_1 = \sum_1^L r_k^{(1)^2} \qquad S_2 = \sum_1^L r_k^{(2)^2} \qquad (2.19)$$

where $r_k^{(i)}$ is the envelope value for the k^{th} path for bit i.

$$\therefore \quad \varphi_{\underline{S}}(\underline{p};L) = E\left[\exp\left(-\langle p,S\rangle\right)\right]$$

$$= E\left[\exp\left(-\sum_{1}^{L} p_1 r_k^{(1)2} - \sum_{1}^{L} p_2 r_k^{(2)2}\right)\right]$$

$$= \prod_{K=1}^{L} E\left[\exp\left(-p_1 r_k^{(1)2} - p_2 r_k^{(2)2}\right)\right] \text{ by independence of paths}$$

$$= \left[\varphi_{\underline{S}}(\underline{p})\right]^L$$

$$= \frac{1}{\left[1 + p_1 + p_2 + p_1 p_2 \mu\right]^L} \tag{2.20}$$

This can be inverted to yield:

$$f(\underline{S};L) = \frac{1}{1-\rho^2}\,\frac{1}{\rho^{L-1}}\,\frac{\left(\sqrt{S_1 S_2}\right)^{L-1}}{(L-1)!}\exp\left(-\frac{S_1+S_2}{1-\rho^2}\right) I_{L-1}\left(\frac{2\rho}{1-\rho^2}\sqrt{S_1 S_2}\right) \tag{2.21}$$

Alternately defining $\begin{pmatrix} x \\ y \end{pmatrix} = \begin{pmatrix} \sqrt{S_1} \\ \sqrt{S_2} \end{pmatrix}$, we obtain

$$f(x,y;L) = \frac{4}{1-\rho^2}\,\frac{1}{\rho^{L-1}}\,\frac{(xy)^L}{(L-1)!}\exp\left(-\frac{x^2+y^2}{1-\rho^2}\right) I_{L-1}\left(\frac{2\rho}{1-\rho^2}\,xy\right) \tag{2.22}$$

where $I_{L-1}(x)$ is the L-1th-order modified Bessel function.

Given x and y, then the probability of a double error in additive noise with variance σ^2 is

$$P(e_1e_2|x,y) = \int_{-\infty}^{-x} \frac{1}{\sqrt{2\pi}\,\sigma} \exp\left(-\frac{n_1^2}{2\sigma^2}\right) dn_1 \int_{-\infty}^{-y} \frac{1}{\sqrt{2\pi}\,\sigma} \exp\left(-\frac{n_2^2}{2\sigma^2}\right) dn_2$$

$$= Q\left(\frac{x}{\sigma}\right) Q\left(\frac{y}{\sigma}\right) \tag{2.23}$$

where

$$Q(z) = \int_z^{\infty} \frac{1}{\sqrt{2\pi}} \exp\left(-\frac{t^2}{2}\right) dt \tag{2.24}$$

the probability that a unit normal exceeds the argument. Thus,

$$P(e_1e_2) = E_{x,y}\left[P(e_1e_2|x,y)\right]$$

$$= \int_0^{\infty}\int_0^{\infty} Q\left(\frac{x}{\sigma}\right) Q\left(\frac{y}{\sigma}\right) \frac{4}{1-\rho^2} \frac{(xy)^L}{(L-1)!\rho^{L-1}} \exp\left(-\frac{x^2+y^2}{1-\rho^2}\right)$$

$$\cdot\, I_{L-1}\left(\frac{2\rho}{1-\rho^2}\, xy\right) dx\, dy \tag{2.25}$$

A power series expansion for $I_{L-1}\left(\frac{2\rho}{1-\rho^2}\, xy\right)$ is:

$$I_{L-1}\left(\frac{2\rho}{1-\rho^2}\, xy\right) = \left(\frac{\rho xy}{1-\rho^2}\right)^{L-1} \sum_{K=0}^{\infty} \frac{\left[\frac{\rho^2x^2y^2}{(1-\rho^2)^2}\right]^K}{K!\;\Gamma(L+K)} \tag{2.26}$$

The integral, therefore, is:

$$P(e_1 e_2) = \int_0^\infty \int_0^\infty Q\left(\frac{x}{\sigma}\right) Q\left(\frac{y}{\sigma}\right) \frac{4}{1-\rho^2} \frac{(xy)^L}{(L-1)!\ \rho^{L-1}} \exp\left(-\frac{x^2+y^2}{1-\rho^2}\right)\left(\frac{\rho xy}{1-\rho^2}\right)^{L-1}$$

$$\cdot \sum_{K=0}^{\infty} \frac{\left[\frac{\rho^2 x^2 y^2}{(1-\rho^2)^2}\right]^K}{K!\ \Gamma(L+K)}\ dx\ dy$$

$$= \frac{4}{(1-\rho^2)^L} \frac{1}{(L-1)!} \sum_{K=0}^{\infty} \frac{\left[\frac{\rho^2}{(1-\rho^2)^2}\right]^K}{K!\ \Gamma(L+K)} \int_0^\infty \int_0^\infty Q\left(\frac{x}{\sigma}\right) Q\left(\frac{y}{\sigma}\right)$$

$$\cdot (xy)^{2L+2K-1} \exp\left(-\frac{x^2+y^2}{1-\rho^2}\right) dx\ dy$$

$$= \frac{4}{(1-\rho^2)^L} \frac{1}{(L-1)!} \sum_{K=0}^{\infty} \frac{\left[\frac{\rho^2}{(1-\rho^2)^2}\right]^K}{K!\ \Gamma(L+K)} \left[\int_0^\infty Q\left(\frac{x}{\sigma}\right) x^{2L+2K-1}\right.$$

$$\left. \cdot \exp\left(\frac{-x^2}{1-\rho^2}\right) dx\right]^2$$

(2.27)

The squared integral may be reduced in the following way:

For a diversity channel with signal-to-noise ratio per path of γ, with binary CPSK modulation, the probability of error given S, the normalized total signal strength, is:

$$Q\left(\sqrt{\frac{2S}{N_0}}\right) = Q\left(\sqrt{2\gamma\ S}\right) \tag{2.28}$$

The distribution of S is a 2L degree of freedom χ^2 random variable. Thus,

$$f(S) = \frac{S^{L-1}}{(L-1)!}\, e^{-S} \tag{2.29}$$

and

$$Pe = \int_0^\infty \frac{S^{L-1}}{(L-1)!}\, e^{-S}\, Q\left(\sqrt{2\gamma\ S}\right) ds \tag{2.30}$$

where Pe is the bit error rate for the L^{th}-order diversity channel. Letting $S = (x^2)/(1-\rho^2)$, we have

$$Pe = \int_0^\infty \frac{x^{2L-2}}{(L-1)!} \exp\left(\frac{-x^2}{1-\rho^2}\right) Q\left(\sqrt{\frac{2\gamma}{1-\rho^2}}\, x\right) \frac{2x\, dx}{\left(1-\rho^2\right)^L} \tag{2.31}$$

Thus, for $L+K^{th}$-order diversity,

$$Pe = \frac{1}{\left(1-\rho^2\right)^{L+K}} \left[\int_0^\infty \frac{2x^{2L+2K-1}\, dx}{(L+K-1)!} \exp\left(\frac{-x^2}{1-\rho^2}\right) Q\left(\sqrt{\frac{2\gamma}{1-\rho^2}}\, x\right)\right] \tag{2.32}$$

$\therefore$ The integral in (2.27) is $\left[\frac{\left(1-\rho^2\right)^{L+K}}{2}(L+K-1)!\right] \times Pe$

for $L+K^{th}$-order diversity, where $\gamma = \frac{1-\rho^2}{2\sigma^2}$.

Therefore, the desired probability is:

$$P(e_1 e_2) = \frac{4}{\left(1-\rho^2\right)^L} \frac{1}{(L-1)!} \sum_0^\infty \frac{\rho^{2K}}{\left(1-\rho^2\right)^{2K}} \frac{1-\rho^{2\,2L+2K}}{4}$$

$$\cdot \frac{[(L+K-1)!]^2}{K!\ \Gamma(L+K)} Pe^2\left(L+K^{th};\gamma = \frac{1-\rho^2}{2\sigma^2}\right)$$

$$= \left(1-\rho^2\right)^L \sum_0^\infty \rho^{2K} \frac{(L+K-1)!}{K!\ (L-1)!} Pe^2\left(L+K^{th};\gamma = \frac{1-\rho^2}{2\sigma^2}\right)$$

$$= \left(1-\rho^2\right)^L \sum_0^\infty \binom{L+K-1}{K} \rho^{2K} Pe^2\left(L+K^{th};\gamma = \frac{1-\rho^2}{2\sigma^2}\right) \qquad (2.33)$$

Since $\sigma^2 = \frac{1}{2\gamma'}$, where γ' is the signal-to-noise ratio of a single path, then

$$P(e_1 e_2) = \left(1-\rho^2\right)^L \sum_0^\infty \binom{L+K-1}{K} \rho^{2K} Pe^2\left[L+K^{th}, \gamma'(1-\rho^2)\right] \qquad (2.34)$$

where

$$Pe\left[L+K^{th};\gamma'(1-\rho^2)\right] = \frac{1}{2}\left\{1 - \sqrt{\frac{\gamma'(1-\rho^2)}{1+\gamma'(1-\rho^2)}} \sum_0^{L+K-1} \binom{2j}{j} \cdot \left(\frac{1}{4\left[1+\gamma'(1-\rho^2)\right]}\right)^j\right\} \qquad (2.35)$$

and γ' is the SNR per path [2.6].

As a check, observe that as $\rho \to 0$ only the first term in the outer sum is retained, so that

$$P(e_1e_2) = \binom{L-1}{0} Pe^2\left(L^{th}\text{-order diversity};\gamma'\right)$$

$$= Pe^2\left(L^{th};\gamma^2\right) = p^2 \tag{2.36}$$

which is exactly the result expected for independent bits.

The limit as $\gamma' \to \infty$ is now found. The probability of bit error in L^{th}-order diversity approaches

$$p \to \frac{\binom{2L-1}{L}}{\gamma'^{L}} \tag{2.37}$$

Thus,

$$P(e_1e_2) = \left(1-\rho^2\right)^L \sum_0^\infty \binom{L+K-1}{K} \rho^{2K} \frac{\binom{2L+2K-1}{L+K}^2}{\gamma'^{2L+2K}\left(1-\rho^2\right)^{2L+2K}}$$

$$= \left(1-\rho^2\right)^L \sum_0^\infty \binom{L+K-1}{K} \rho^{2K} \frac{\binom{2L+2K-1}{L+K}^2}{\left[\gamma'(1-\rho)^2\right]^{2L+2K}} \tag{2.38}$$

at high SNR only the $zero^{th}$ term contributes so that

$$P(e_1e_2) \to \left(1-\rho^2\right)^L \frac{\binom{2L-1}{L}^2}{\gamma'^{2L}\left(1-\rho^2\right)^{2L}}$$

$$= \frac{\binom{2L-1}{L}^2}{\gamma'^{2L}\left(1-\rho^2\right)^{L}}$$

$$= \frac{p^2}{\left(1-\rho^2\right)^L} \tag{2.39}$$

Thus r, the conditional probability, is given by:

$$r = \frac{P(e_1 e_2)}{p} = \frac{p}{(1-\rho^2)^L} \tag{2.40}$$

for high SNR.

The value of s follows directly from the steady-state Markov properties or, equivalently, can be obtained directly from the joint probability space as

$$s = P(e_2 | \bar{e}_1) = \frac{P(\bar{e}_1 e_2)}{1 - P(e_1)} = \frac{P(e_2) - P(e_1 e_2)}{1 - P(e_1)} = \frac{p - pr}{1 - p} \tag{2.41}$$

When $B\tau$ (or, equivalently, ρ) and p are specified, we can generate all possible error probabilities iteratively by the following relations:

$$f_0(N,i) = s\, f_1(N-1,i-1) + (1-s)\, f_0(N-1,i) \tag{2.42}$$

$$f_1(N,i) = r\, f_1(N-1,i-1) + (1-r)\, f_0(N-1,i) \tag{2.43}$$

where $f_S(N,i)$ is the probability of having i errors among N bits assuming start at state S. To initialize the iteration procedure, we have

$$f_0(i,i) = s\, r^{i-1} \tag{2.44}$$

$$f_1(i,i) = r^i \tag{2.45}$$

$$f_0(N,0) = (1-s)^N \tag{2.46}$$

$$f_1(N,0) = (1-r)(1-s)^{N-1} \tag{2.47}$$

Once $f_S(N,i)$ are computed for all i, then the block error rate P for a block code can be computed as

$$p = 1 - p \sum_{i=0}^{e} f_1(N,i) - (1-p) \sum_{i=0}^{e} f_0(N,i)$$

$$= p \sum_{i=e+1}^{N} f_1(N,i) + (1-p) \sum_{i=e+1}^{N} f_0(N,i) \qquad (2.48)$$

where e is the number of errors within a code block which can be corrected.

Let us denote ρ_i as the average number of decoded errors when the actual number of channel errors is i. It is obvious that

$$\beta_i = 0 \quad \text{for} \quad 0 \le i \le e \qquad (2.49)$$

Once the ρ's are known, the decoded bit error rate, p_b, for the block code is given by

$$p_b = \frac{1}{N} \sum_{i=e+1}^{N} \beta_i \left[p\, f_1(N,i) + (1-p)\, f_0(N,i) \right] \qquad (2.50)$$

The exact value of β_i depends on the weight distribution of the code. Unfortunately, the weight distributions of block codes are, in general, hard to obtain. In this case, some approximate values for β_i can be obtained if the numbers of codewords for a few of the lowest weights are known. For the case of the Golay (24,12) code, the entire weight distribution is known; thus, all the values for ρ_i can be computed.

The value β_i in Table 2-2 are obtained from:

$$\beta_i = \left[\sum_{k=i-e}^{i+e} k\, n_k \cdot m_k + i \left[\binom{N}{i} - n_k m_k \right] \right] \Big/ \binom{N}{i}$$

$$= \frac{1}{\binom{N}{i}} \sum_{k=i-e}^{i+e} (k-i)\, n_k m_k + i \qquad (2.51)$$

TABLE 2-2

WEIGHT DISTRIBUTION AND β_i OF GOLAY (24,12) CODE

i	n_i = Number of Codeword of Weight i	β_i
0	1	0
1 - 3	0	0
4	0	4
5	0	8
6	0	120/19
7	0	8
8	759	8
9	0	2637/323
10	0	3256/323
11	0	3656/323
12	2576	12
13	0	4096/323
14	0	4496/323
15	0	5115/323
16	759	16
17	0	16
18	0	336/19
19	0	16
20	0	20
21 - 23	0	24
24	1	24

where n_k is the number of codewords of weight k, and m_k is the number of ways that a codeword of weight k becomes weight i after committing e or fewer errors.

Figures 2.13 through 2.17 illustrate the decoded bit error rate for binary decoding of the Golay (24,12) code as a function of the signal-to-noise ratio per transmitted digit using $B\tau$ as a parameter for a flat fading Rayleigh channel with the order of diversity varying from one to eighth-order.

For the Golay code, the parameter τ is related to the total decoding delay T by

$$T = 23\tau \tag{2.52}$$

For example, if there is a 50-ms decoding delay, with a typically two-sided rms fading bandwidth (Doppler spread) of 5 Hz, we have

$$B\tau = 5 \times \frac{0.050}{23} \approx 0.01 \tag{2.53}$$

The loss in performance due to correlated bits for $B\tau = 0.01$, as well as other representative values, is given in Table 2-3. This loss must be subtracted from the coding gains given in Table 2-1 which assumes that $B\tau \to \infty$.

Table 2-4 illustrates the estimated coding gains for $B\tau = 0.01$ for binary and channel measurement decoding. These results indicate that, as the order of diversity increases, the required decoding delay decreases quite rapidly in the region of low SNR. It is of interest to determine if diversity alone (without any decoding delay) can improve the effectiveness of coding. This question is particularly relevant since it has been shown [2.7] that, on a flat fading channel with no diversity, coding is ineffective when all code bits are completely correlated. Figure 2.18 verifies this result for the special case of the Golay code which has been simulated for both binary and channel measurement decoding. When dual diversity is available (see Figure 2.19), the use of a binary decoding algorithm results in a 1/2-dB loss at 10^{-5}, but the use of a channel measurement decoding algorithm results in a 1-dB gain at 10^{-5}.

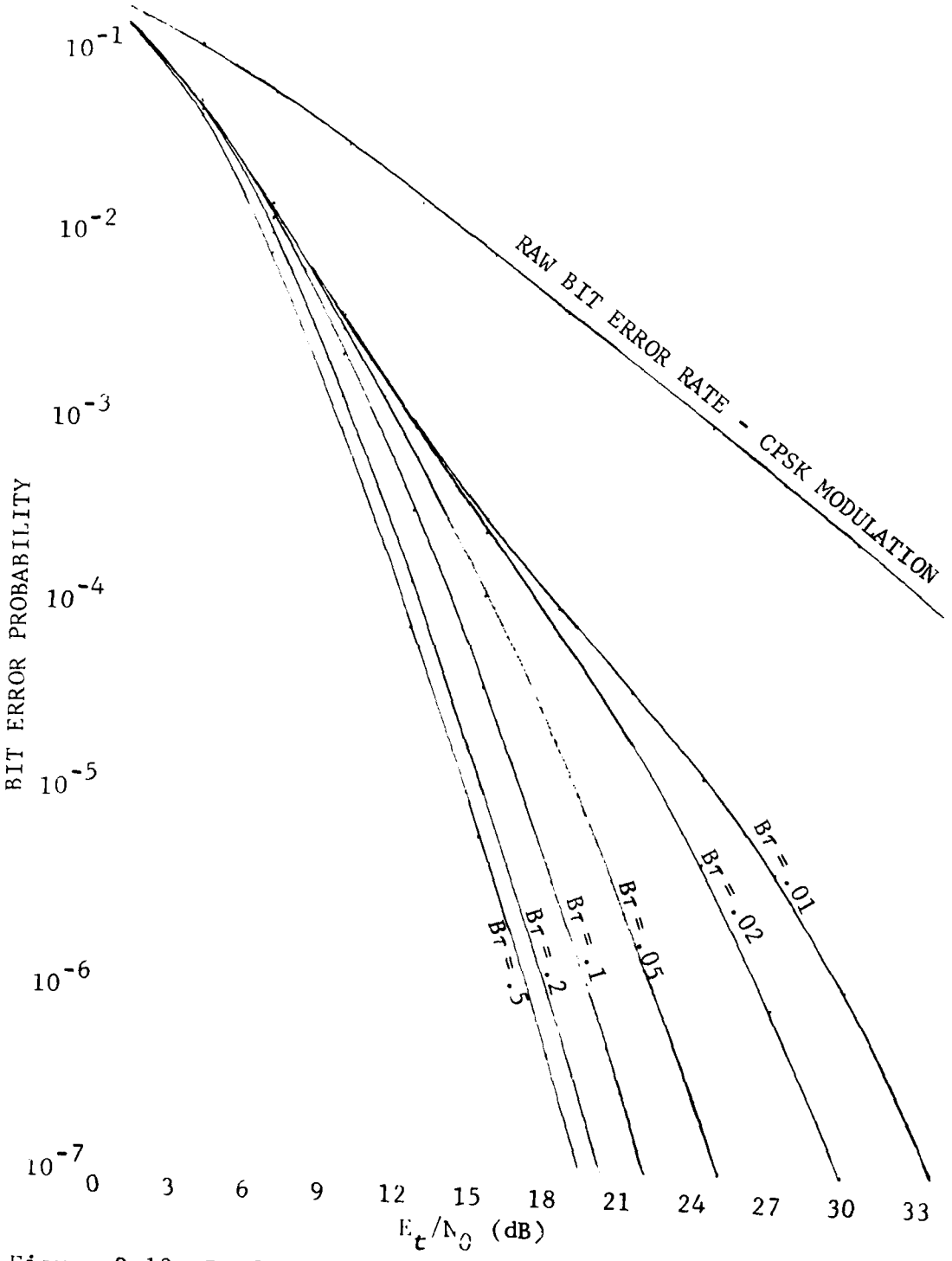

Figure 2.13 Performance for Binary Decoding of the Golay Code with Dependent Digits - Order of Diversity: L=1

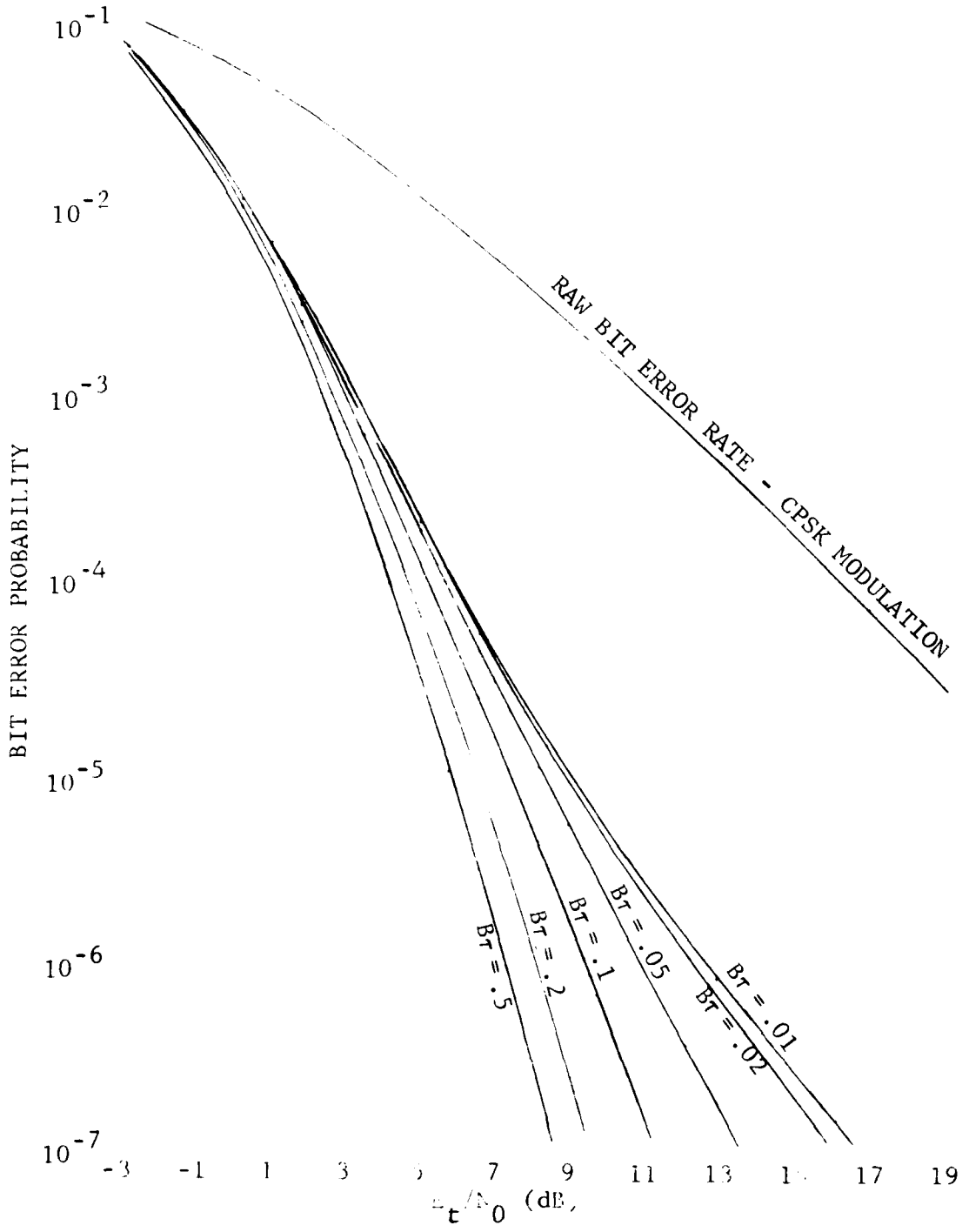

Figure 2.14 Performance for Binary Decoding of the Golay Code with Dependent Digits - Order of Diversity: L=2

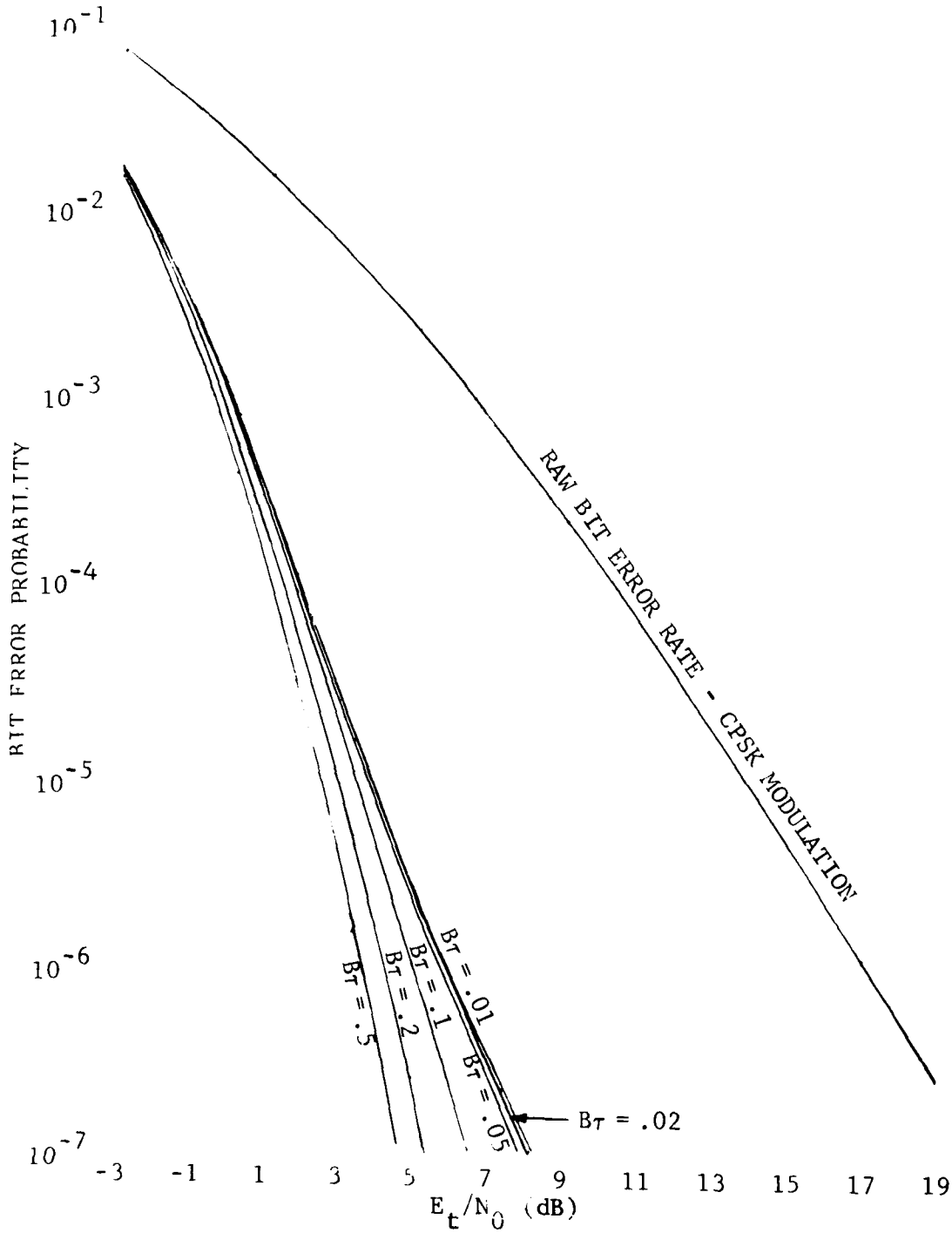

Figure 2.15 Performance for Binary Decoding of the Golay Code with Dependent Digits - Order of Diversity: L=3

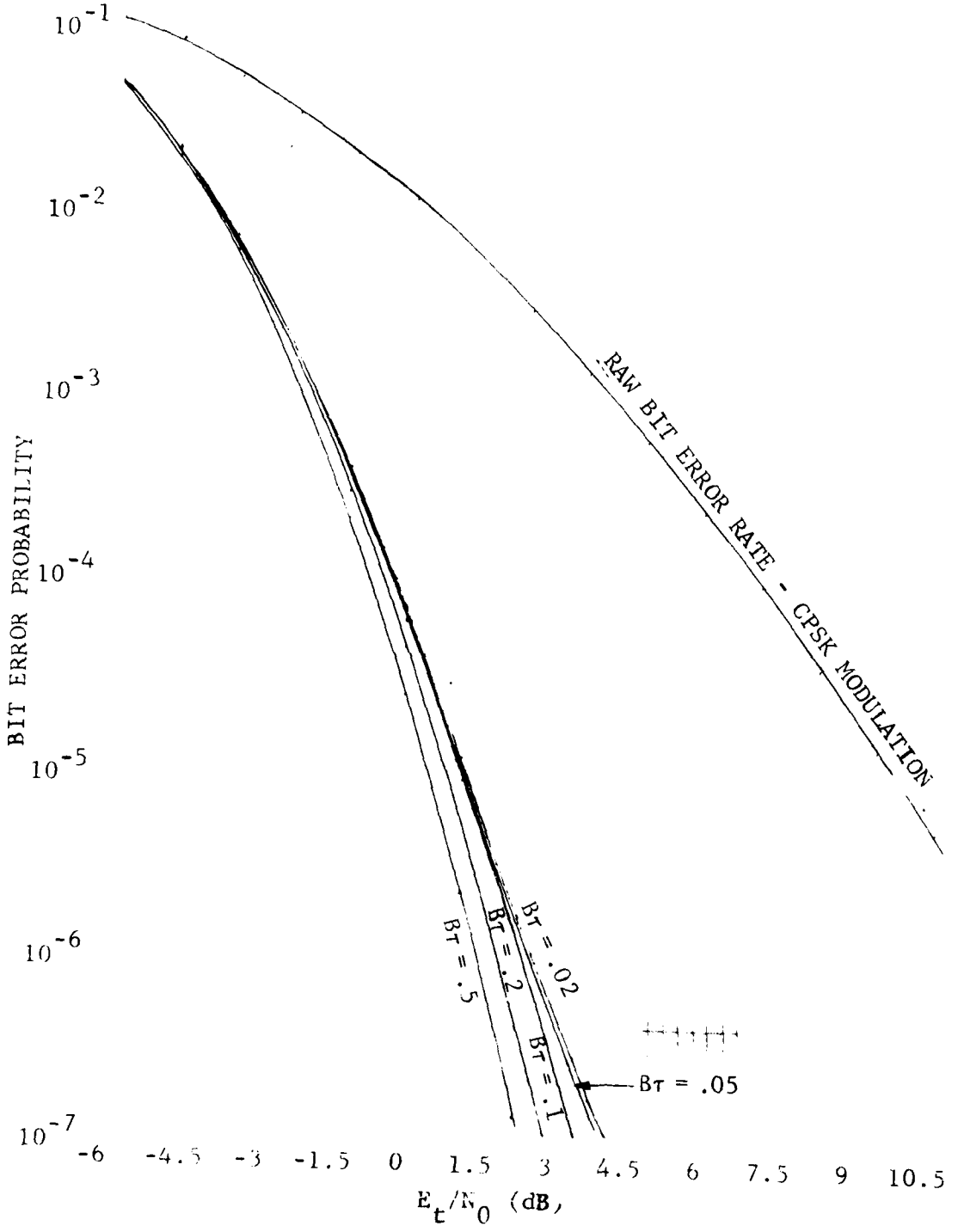

Figure 2.16 Performance for Binary Decoding of the Golay Code with Dependent Digits - Order of Diversity: L=4

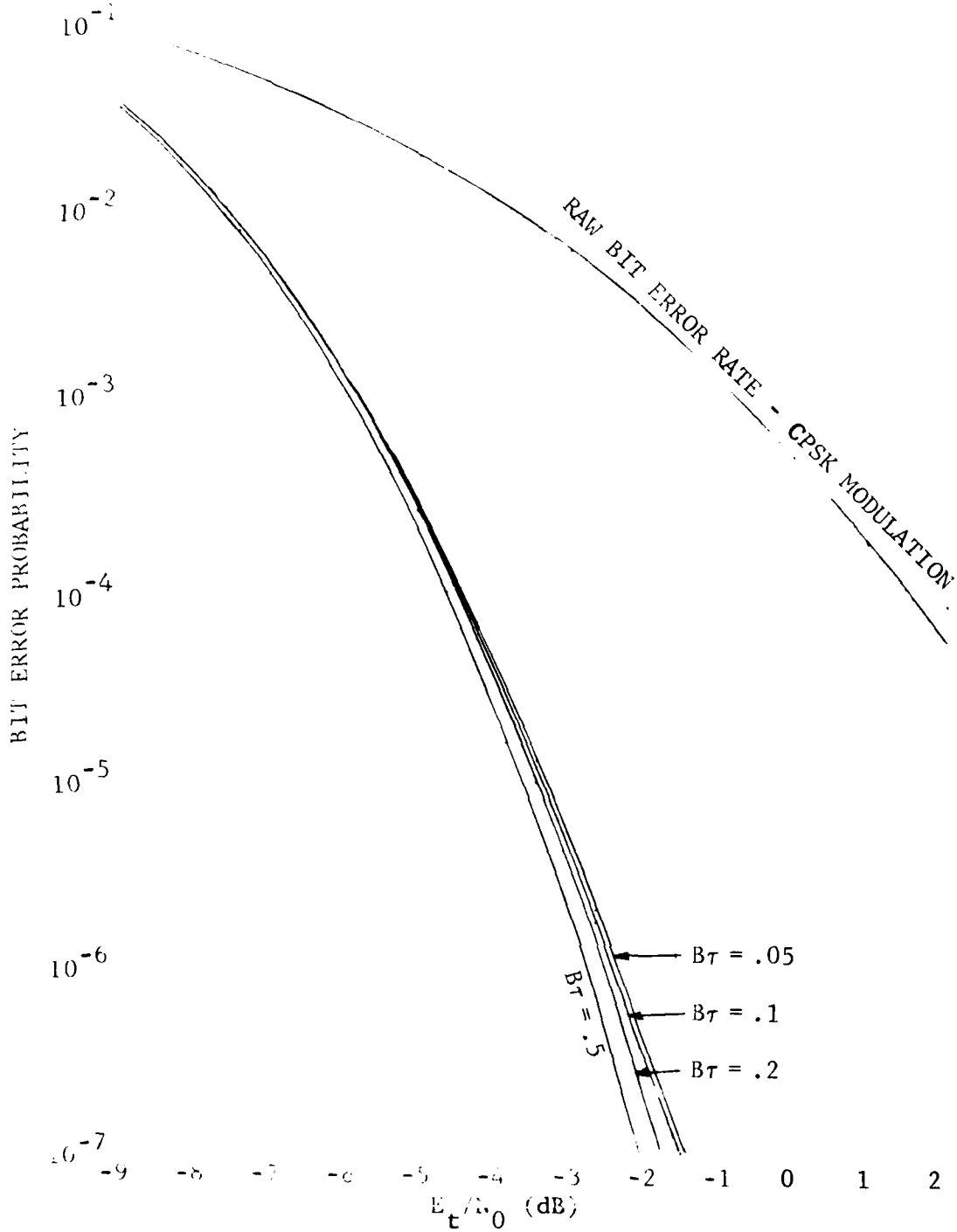

Figure 2.17 Performance for Binary Decoding of the Golay Code with Dependent Digits - Order of Diversity: L=8

TABLE 2-3

ESTIMATED LOSS IN PERFORMANCE DUE TO CORRELATED BITS AT A DECODED ERROR RATE OF 10^{-5}

Order of Diversity	$B\tau = 0.01$	$B\tau = 0.02$	$B\tau = 0.05$	$B\tau = 0.2$
1	10.4 dB	8.1 dB	4.5 dB	0.7 dB
2	3.2 dB	3.0 dB	2.5 dB	0.6 dB
3	1.4 dB	1.3 dB	1.2 dB	0.5 dB
4	1.0 dB	0.8 dB	0.7 dB	0.4 dB
8	0.3 dB	0.3 dB	0.3 dB	0.2 dB

TABLE 2-4

ESTIMATED CODING GAINS FOR $B\tau = 0.01$ AT A BIT ERROR PROBABILITY OF 10^{-5}

Available Diversity	Binary Decoding	Channel Measurement Decoding	Loss Assumed Due to Correlated Code Bits
1	16.0 dB	23.2 dB	10.4 dB
2	9.2 dB	13.2 dB	3.2 dB
3	7.0 dB	10.4 dB	1.4 dB
4	5.4 dB	8.3 dB	1.0 dB
8	3.7 dB	6.1 dB	0.3 dB

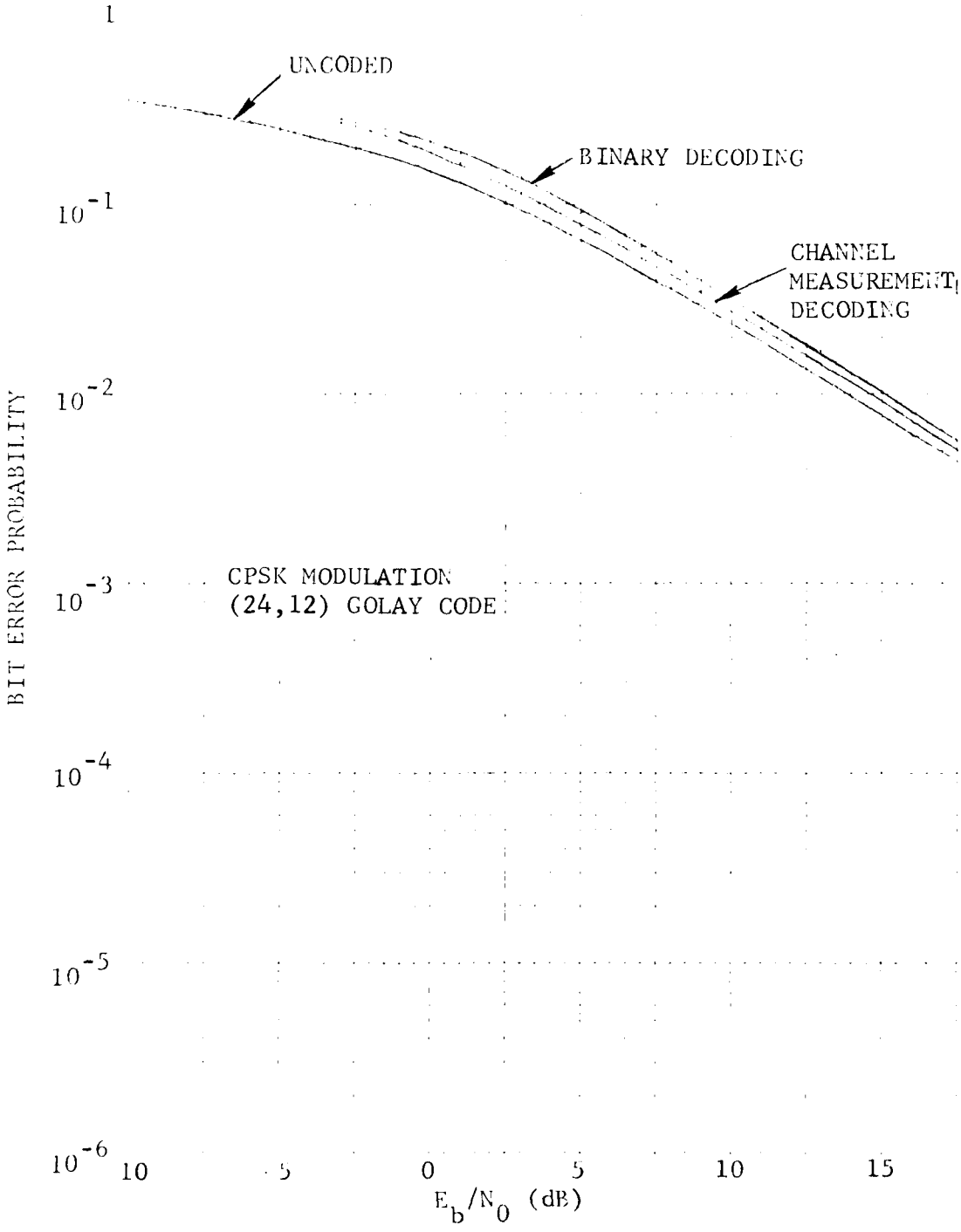

Figure 2.18 Simulated Results for a Flat Fading Channel with No Diversity and Completely Correlated Code Bits

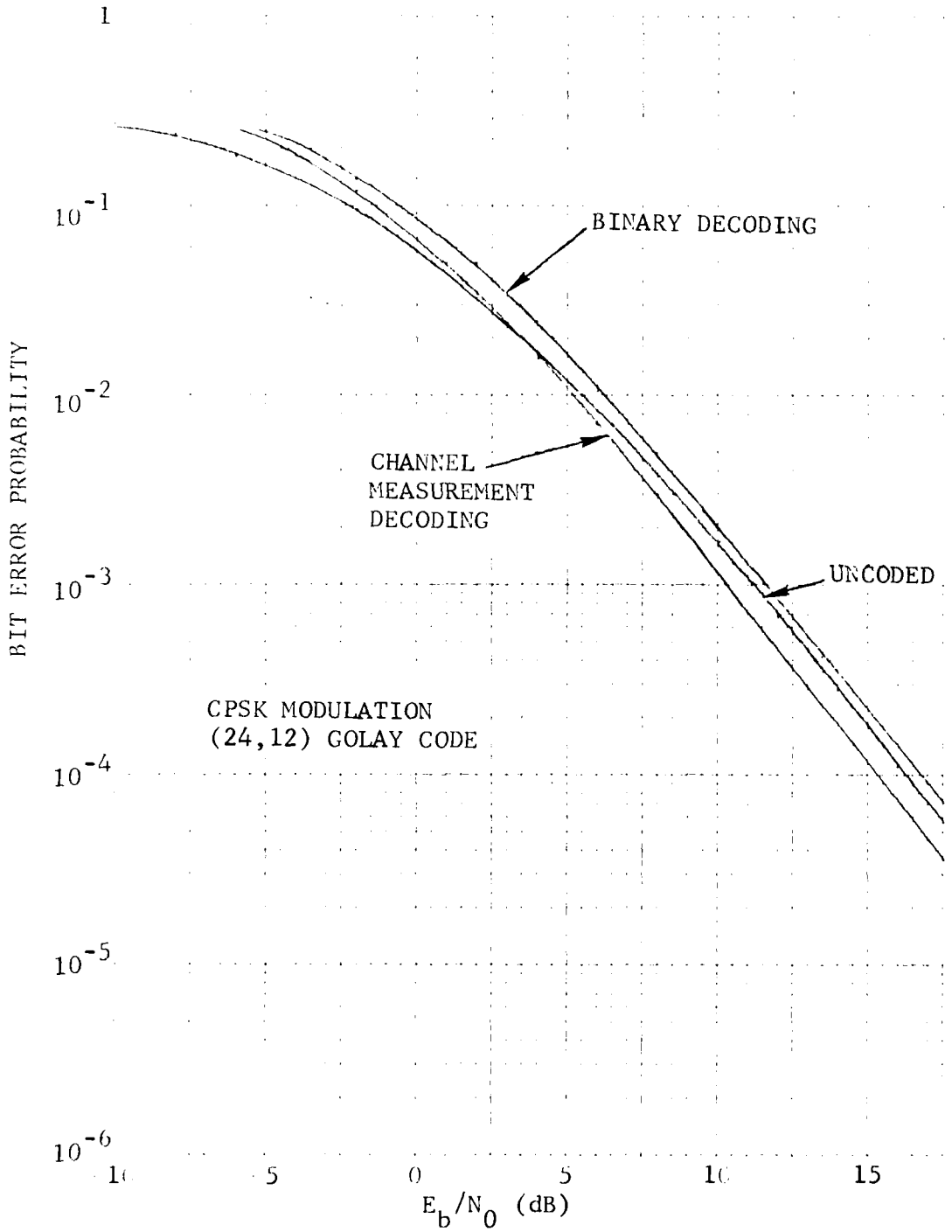

Figure 2.19 Simulated Results for a Flat Fading Channel with Dual Diversity and Completely Correlated Code Bits

For triple diversity, shown on Figure 2.20, the binary decoder shows no loss and the channel measurement decoder shows a gain of 1.5 dB. Finally, on Figure 2.21, we see that for quad diversity, a 2.5-dB coding gain is obtainable by channel measurement decoding when all code bits are completely correlated. These results are summarized in Table 2-5.

To estimate the benefits of channel measurement decoding over binary decoding for actual multipath profiles, one must estimate the amount of in-band diversity; then the results in Tables 2-1, 2-3, 2-4, and 2-5 may be used. For example, for flat fading (L=1) a gain of 7.2 dB (see Table 2-1) should be achievable when there is sufficient decoding delay. For a very short decoding delay, Table 2-5 illustrates that channel measurement decoding offers only a 0.5-dB gain over conventional binary decoding. For the multipath profiles considered in Section 3, profiles 3 and 5, the effective amount of combined diversity is a function of the actual signal-to-noise ratio. In the region of interest, L=3 represents an adequate approximation for profiles 3 and 5. Again using Table 2-1, channel measurement decoding should offer a gain of 3.4 dB over binary decoding when the decoding delay is sufficiently large so that the independent code bit assumption can be made.

2.3 Abstraction of Channel Measurement Information

In this section the problem of obtaining meaningful channel measurement (soft-decision) information to be used by an error-correcting decoder is addressed. Several coding and modulation formats will be considered, starting with fairly simple examples and progressing to more difficult coding and modulation formats. When the optimum structure for obtaining channel measurement information cannot be found, or is too difficult to implement, a practical suboptimum structure is developed.

2.3.1 Binary Antipodal (Biphase) Modulation over the White Gaussian Noise Channel

Figure 2.22 represents a block diagram of a communications system employing error-correction coding. For this case, the encoded digit X_i is transmitted as:

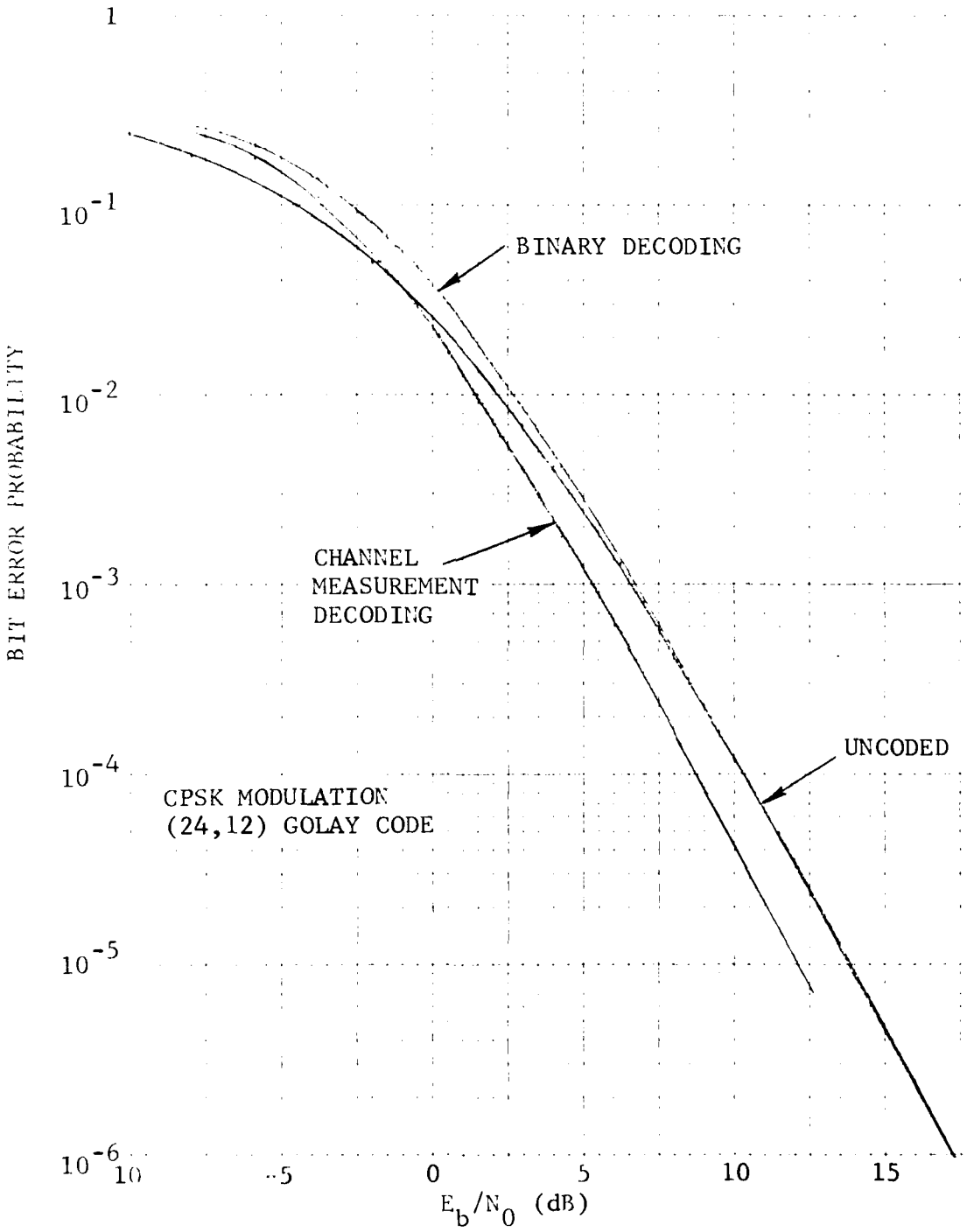

Figure 2.20 Simulated Results for a Flat Fading Channel with Triple Diversity and Completely Correlated Code Bits

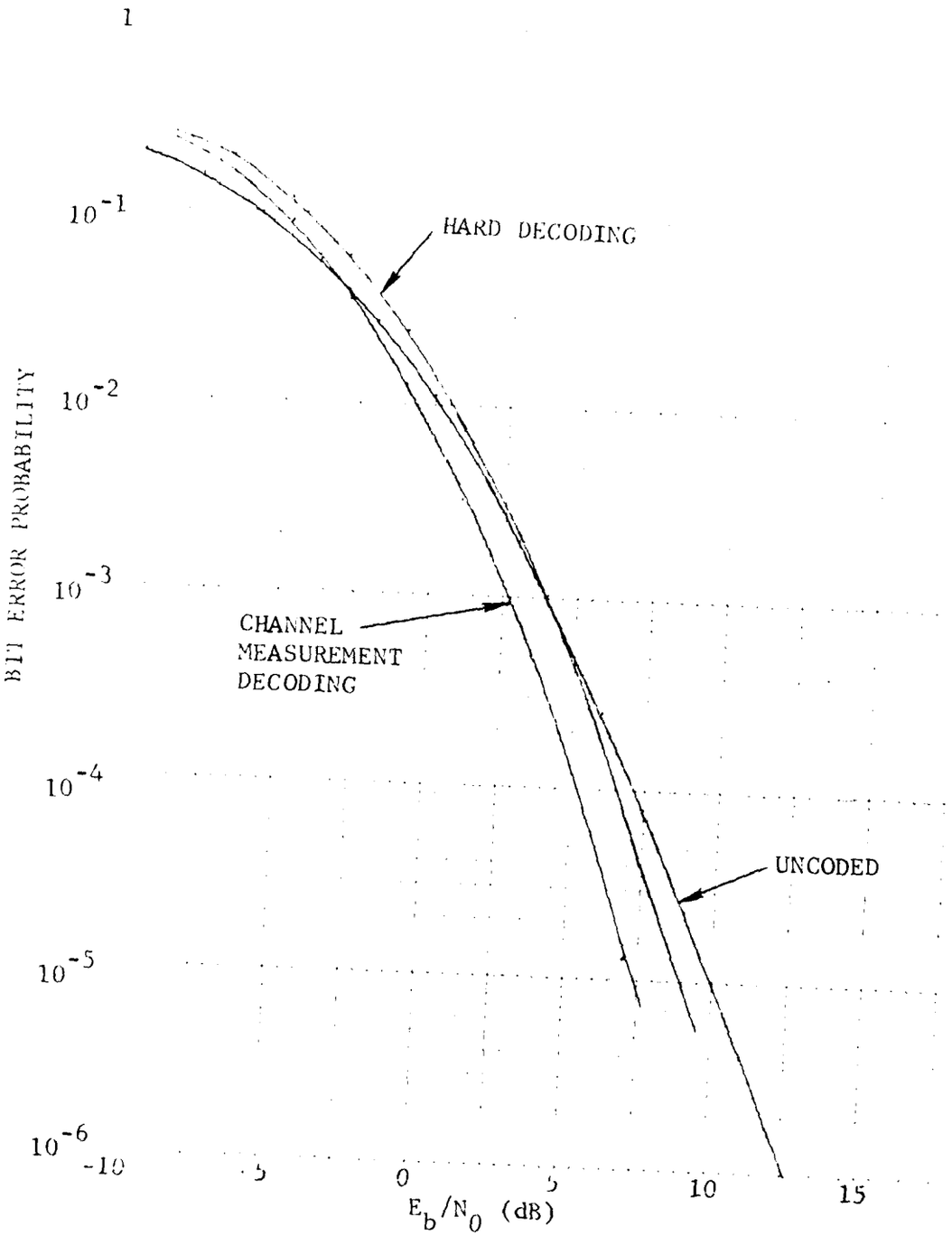

igure 2.21 Simulated Results for a Flat Fading Channel with Quad Diversity and Completely Correlated Code Bits

TABLE 2-5

CODING GAINS FOR COMPLETED CORRELATED BITS – COMPUTER-SIMULATED RESULTS

Order of Diversity	Binary Decoding	Channel Measurement Decoding
1	-1.0 dB	-0.5 dB
2	-0.5 dB	1.0 dB
3	0	1.5 dB
4	1.0 dB	2.5 dB

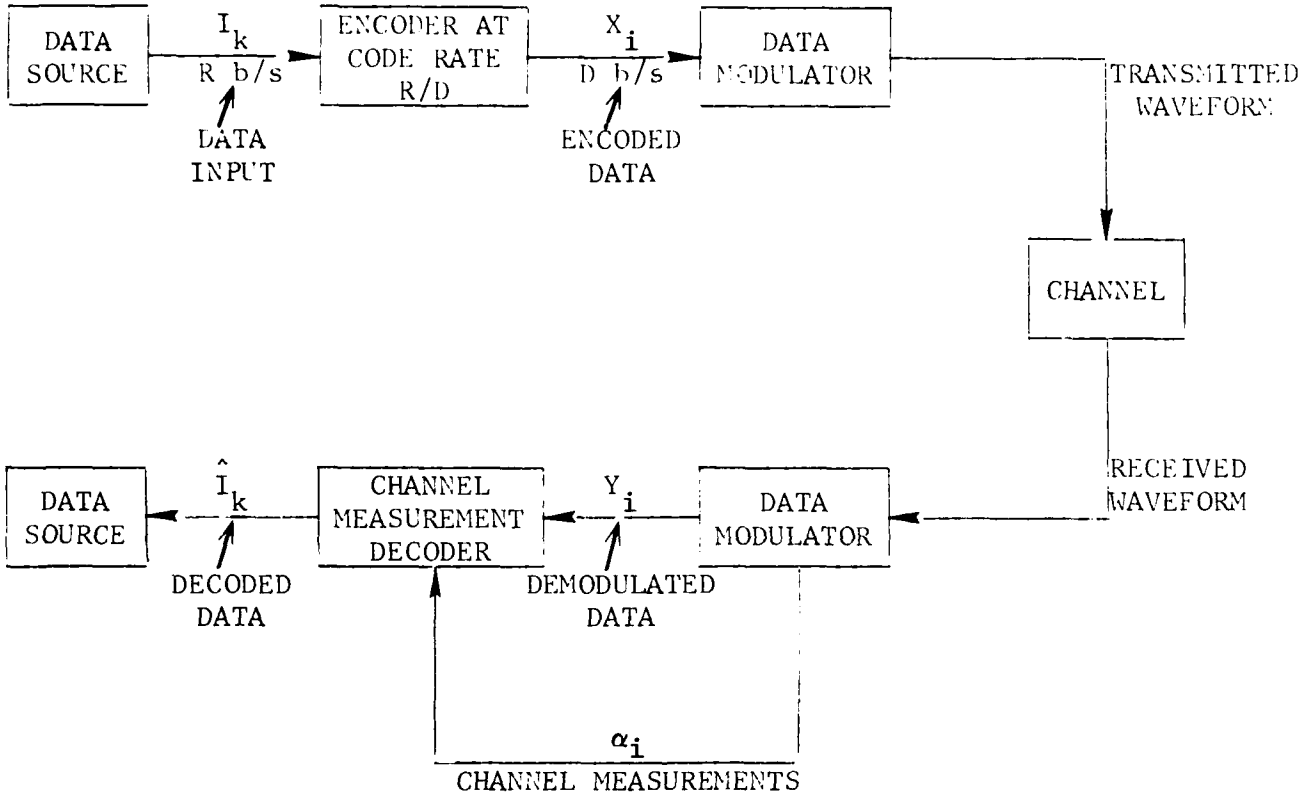

Figure 2.22 Communications System Block Diagram

$$x_i(t) = (-1)^{X_i} \varphi_i(t) = \begin{cases} \varphi_i(t) & \text{for } X_i = 0 \\ -\varphi_i(t) & \text{for } X_i = 1 \end{cases} \qquad 0 \le t \le T \tag{2.52}$$

where $\varphi_i(t)$ is just a sine wave for binary phase-shift-keying (BPSK) modulation. It is assumed that $\varphi_i(t)$ is normalized such that

$$\int_0^T \varphi_i^2(t)\, dt = 1 \tag{2.53}$$

where the interval (0,T) represents the time when $x_i(t)$ is transmitted.

The demodulator for the received signal,

$$y(t) = x_i(t) + n(t) \tag{2.54}$$

illustrated in Figure 2.23, is a synchronized matched filter whose analog output is given by

$$v_i = (-1)^{X_i} + n_i \tag{2.55}$$

The additive Gaussian noise component has the following properties:

$$\begin{aligned} \overline{n_i} &= 0 \\ \overline{n_i^2} &= \frac{N_0}{2} \end{aligned} \tag{2.56}$$

where the additive noise function n(t) is white Gaussian with

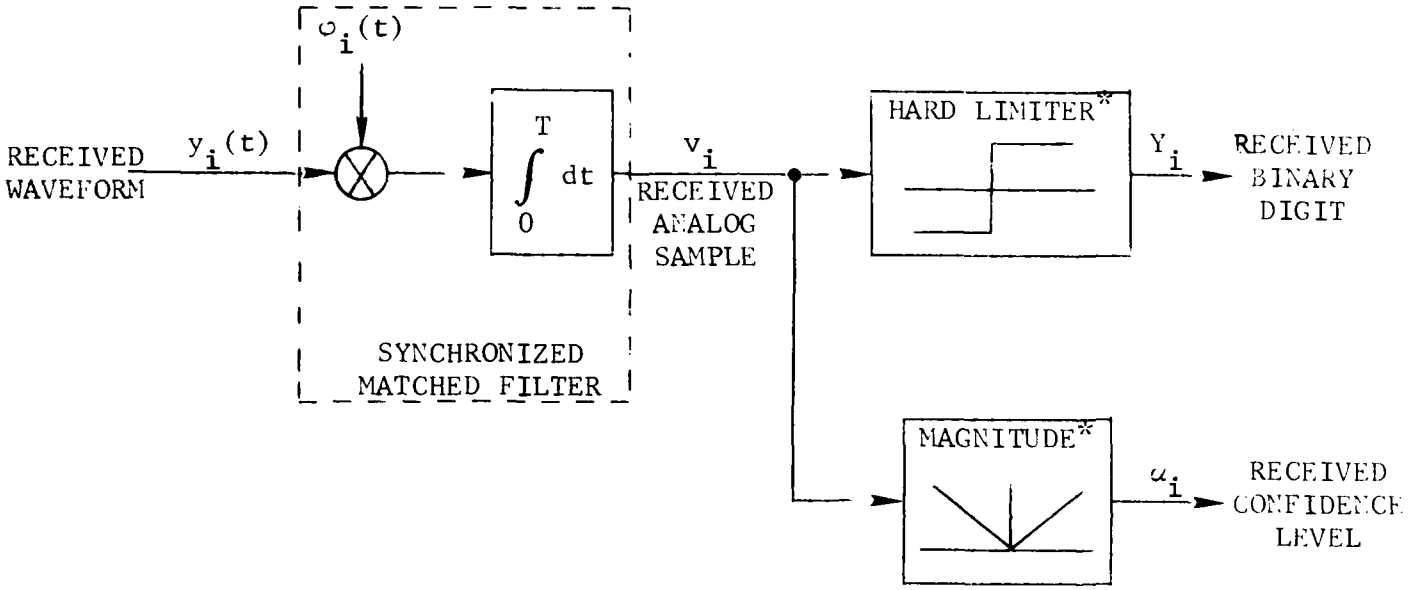

*THE HARDLIMITED AND MAGNITUDE FUNCTION CAN BE REPLACED BY A SIMPLE A-TO-D CONVERTER, WHERE Y_i IS JUST A SIGN BIT AND α_i IS A QUANTIZED CONFIDENCE LEVEL

Figure 2.23 Demodulation for a Binary Antipodal Waveform

$$\overline{n(t)n(\tau)} = \begin{cases} \frac{N_0}{2}\,\delta(t) & t = \tau \\ 0 & t \neq \tau \end{cases} \tag{2.57}$$

For this case, the signal-to-noise ratio per received digit is given by

$$\frac{E}{N_0} = \frac{\left[(-1)^{X_i}\right]^2}{2\,\overline{n_i^2}} = \frac{1}{N_0} \tag{2.58}$$

where the received signal energy is normalized to 1.

The received binary digit is obtained by the following decision rule:

$$Y_i = 0 \qquad \text{if} \qquad v_i \geq 0$$

and (2.59)

$$Y_i = 1 \qquad \text{if} \qquad v_i < 0$$

The confidence level is shown on Figure 2.23 to be just the magnitude (or quantized magnitude) of the decision statistic. This choice of confidence level can be justified from two points of view.

First we note that most channel measurement algorithms require a confidence level which is monotonically increasing with the probability that X_i is decoded correctly. This probability can be written as

$$P(Y_i=X_i \mid v_i) = \frac{P(v_i \mid Y_i=x_i)}{P(v_i)} \tag{2.60}$$

where

$$P(v_i \mid Y_i=X_i) = \frac{e^{-\frac{(v_i-1)^2}{N_0}}}{\sqrt{\pi N_0}} \quad \text{for} \quad v_i > 0 \text{ and } X_i = 0 \qquad (2.61)$$

and

$$P(v_i \mid Y_i=X_i) = \frac{e^{-\frac{(v_i+1)^2}{N_0}}}{\sqrt{\pi N_0}} \quad \text{for} \quad v_i < 0 \text{ and } X_i = 1 \qquad (2.62)$$

Thus, an expression for all values of v_i is given by

$$P(v_i \mid Y_i=X_i) = \frac{e^{-\frac{(|v_i|-1)^2}{N_0}}}{\sqrt{\pi N_0}} \qquad (2.63)$$

Similarly, we can write

$$P(v_i) = P(X_i=0)P(v_i \mid X_i=0) + P(X_i=1)P(v_i \mid X_i=1) \qquad (2.64)$$

which, for equally probable transmitted digits, becomes

$$P(v_i) = \frac{1}{2}\frac{e^{-\frac{(v_i-1)^2}{N_0}}}{\sqrt{\pi N_0}} + \frac{1}{2}\frac{e^{-\frac{(v_i+1)^2}{N_0}}}{\sqrt{\pi N_0}} \qquad (2.65)$$

Taking the required ratio given by (2.60) yields

$$P(Y_i=X_i|v_i) = \frac{1}{1+e^{-\frac{4|v_i|}{N_0}}} \tag{2.66}$$

for both $v_i \geq 0$ and $v_i \leq 0$.

From (2.66) we note that, by choosing $\alpha_i = |v_i|$, we have a confidence level which increases monotonically with the probability that Y_i is demodulated as X_i, i.e., that the received digit is demodulated correctly. A channel measurement decoder depends on α_i being small for those cases when $Y_i \neq X_i$, so that ultimately a correct decision on the transmitted data stream $\underline{I} = ---I_k---$ can be made. The argument used above to justify

$$\alpha_i = |v_i| \tag{2.67}$$

is valid for both block or convolutional codes.

A second justification of a confidence level is obtained by noting that a maximum likelihood decoder will select the encoded sequence, and thus the information sequence, which maximizes

$$P(\underline{v} \mid \underline{X}) = P(---v_i---|---X_i---) \tag{2.68}$$

For the white Guassian noise channel, (2.68) can be written as

$$P(\underline{v}|\underline{X}) = \prod_i \frac{e^{-\frac{\left[v_i-(-1)^{X_i}\right]^2}{N_0}}}{\sqrt{\pi N_0}} \tag{2.69}$$

Maximizing (2.69) is equivalent to finding the sequence which maximizes

$$\sum_i v_i(-1)^{X_i} \tag{2.70}$$

The above expression can be written as

$$\sum_{\substack{i \text{ such that} \\ X_i = Y_i}} v_i - \sum_{\substack{i \text{ such that} \\ X_i \neq Y_i}} v_i = \sum_{\substack{\text{all} \\ i}} v_i - 2\sum_{\substack{i \text{ such that} \\ X_i \neq Y_i}} v_i \tag{2.71}$$

When $X_i = Y_i$, the product $v_i(-1)^{X_i}$ must be positive for the bit decision rules given by (2.59). Maximizing (2.71) is equivalent to minimizing

$$\sum_{\substack{i \text{ such that} \\ X_i \neq Y_i}} v_i = \sum_{\substack{i \text{ such that} \\ X_i \neq Y_i}} \alpha_i \tag{2.72}$$

which is the desired expression for a maximum likelihood decision rule given in terms of α_i.

If we define the binary error sequence

$$\underline{Z} = ---Z_i--- = ---X_i \oplus Y_i--- \tag{2.73}$$

then we note that the error sequence which minimizes the "analog weight" given by

$$\sum_i Z_i \alpha_i \triangleq W_\alpha(\underline{Z}) \tag{2.74}$$

is equivalent to (2.72) and equivalent to a maximum-likelihood decoder. Again, these results hold for both block and convolutional codes even though the original formulation of this nature [2.4] was intended for the block coding case.

2.3.2 Binary Signaling over the Coherent Rayleigh Fading Channel

For this case we will assume an arbitrary correlation between the binary signals used to represent X_i and a channel which is perturbed by multiplicative Rayleigh-distributed noise and additive white Gaussian noise. Thus,

$$x_i(t) = \begin{cases} \varphi_{0i}(t) & \text{for} \quad X_i = 0 \\ \varphi_{1i}(t) & \text{for} \quad X_i = 1 \end{cases} \tag{2.75}$$

where

$$\int_0^T \varphi_{0i}^2(t)\, dt = \int_0^T \varphi_{1i}^2(t)\, dt = 1 \tag{2.76}$$

and

$$\int_0^T \varphi_{0i}(t)\varphi_{1i}(t)\, dt = \rho < 1 \tag{2.77}$$

The received signal is now given by

$$y_i(t) = r_i x_i(t) + n(t) \tag{2.78}$$

with the Rayleigh fading variable r_i normalized such that

$$\overline{r_i^2} = 1 \tag{2.79}$$

For the special case when we hold r_i fixed at 1 and let $\rho = -1$, this example reduces to the case considered in Section 2.3.1. When $\rho = 0$, the two waveforms represent the binary frequency-shift-keying (FSK) case.

An appropriate receiver for this fairly general case is given on Figure 2.24.

The decision statistic can be written as:

$$v_i = v_{0i} - v_{1i} = (1 - \rho)\, r_i (-1)^{X_i} + n_{0i} - n_{1i} \qquad (2.80)$$

In this case, the decision statistic is weighted by r_i which is not required for an optimum bit-by-bit demodulator but is required in order to obtain an optimum confidence level when r_i can vary from bit to bit.

The justification for this type of receiver follows along the lines outlined in Section 2.3.1, but is more involved since a decision on X_i involves the two decision statistics (see Figure 2.24):

$$v_{0i} = r_i \rho^{X_i} + n_{0i}$$

and (2.81)

$$v_{1i} = r_i \rho^{1-X_i} + n_{1i}$$

Note that for $X_i = 0$ we have

$$v_{0i} = r_i + n_{0i}$$

and (2.82)

$$v_{1i} = \rho r_i + n_{1i}$$

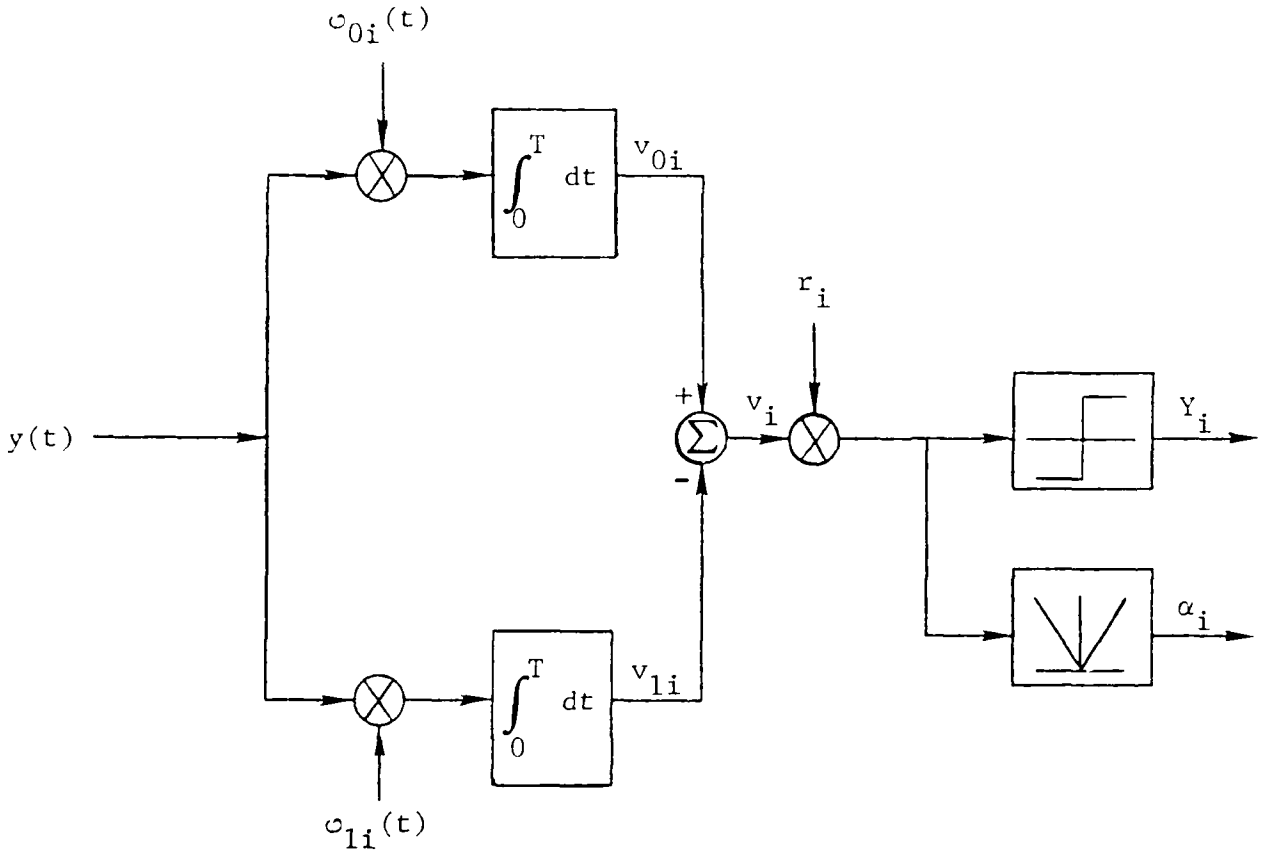

Figure 2.24 Demodulator for Binary Signaling over the Coherent Rayleigh Fading Channel

and for $X_i = 1$ we have

$$v_{0i} = \rho r_i + n_{0i}$$

and (2.83)

$$v_{1i} = r_i + n_{1i}$$

It should be noted in this case that the additive noise in these two decision statistics is correlated with

$$\overline{n_{0i} n_{1i}} = \iint \overline{n(t)n(\tau)}\, \omega_{0i}(t)\omega_{1i}(\tau)\, dt\, d\tau$$

$$= \frac{N_0}{2}\rho \qquad (2.84)$$

The variance of each noise term n_{0i} and n_{1i} is $N_0/2$ as before. Thus, the average signal-to-noise ratio for this case is given by

$$\frac{E}{N_0} = \frac{(1-\rho)^2\, \overline{r_i^2}\, \left[(-1)^{X_i}\right]^2}{2\left(\overline{n_{0i}^2} + \overline{n_{1i}^2} - 2\,\overline{n_{0i} n_{1i}}\right)} = \frac{1-\rho}{2}\,\frac{1}{N_0} \qquad (2.85)$$

The likelihood function for this case is given by

$$p(\underline{v}_0, \underline{v}_1 | \underline{X}) = \prod_i P(v_{0i}, v_{1i} | X_i) \qquad (2.86)$$

which involves a bivariate Gaussian probability density function which is complicated since v_{0i} and v_{1i} are correlated.

Holding X_i fixed and averaging over the additive noise, the following parameters can be defined:

$$m_0 = \overline{v_{0i}} = r_i \rho^{X_i}$$

$$m_1 = \overline{v_{1i}} = r_i \rho^{1-X_i}$$

$$\sigma_0^2 = \overline{(v_{0i} - m_0)^2} = N_0/2 \qquad (2.87)$$

$$\sigma_1^2 = \overline{(v_{1i} - m_1)^2} = N_0/2$$

$$\rho = \overline{(v_{0i} - m_0)(v_{1i} - m_1)}$$

Using the bi-variate probability density function, we can now write (2.86) as

$$P(\underline{v}_0, \underline{v}_1 | , \underline{X}) = \frac{e^{-\sum_i \frac{\sigma_1^2(y_0-m_0)^2 - 2\sigma_0\sigma_1\rho(y_0-m_0)(y_1-m_1) + \sigma_0^2(y_1-m_1)^2}{2\sigma_1^2\sigma_0^2(1-\rho^2)}}}{\prod_i 2\pi\sigma_1\sigma_0\left(1-\rho^2\right)^{1/2}} \qquad (2.88)$$

where, for convenience, $y_0 = v_{0i}$ and $y_1 = v_{1i}$. Maximizing (2.86) over all values of $\underline{X}$ is equivalent to minimizing

$$\sum_i \sigma_1^2(y_0 - m_0)^2 - 2\sigma_0\sigma_1\rho(y_0 - m_0)(y_1 - m_1) + \sigma_0^2(y_1 - m_1)^2 \qquad (2.89)$$

The terms which are not a function of X_i can be omitted from the above summation to give

$$\sum_i \sigma_1^2[-2y_0m_0 + m_0^2] - 2\sigma_0\sigma_1\rho[-y_1m_0 - y_0m_1 + m_0m_1] + \sigma_0^2(-2y_1m_1 + m_1^2) \tag{2.90}$$

Further simplification of (2.90) is possible by noting that

$$\sigma_1^2m_0^2 + \sigma_0^2m_1^2 = \frac{N_0}{2}\left(r_1^2\rho^{2X_i} + r_i^2\rho^{2-2X_i}\right) \tag{2.91}$$

is the same for $X_i = 0$ and $X_i = 1$, and that

$$2\sigma_0\sigma_1\rho m_0m_1 = N_0\rho r_i^2\rho \tag{2.92}$$

also, is not a function of X_i. Finally, dividing by N_0 and multiplying (2.90) by -1, we have shown that a maximum likelihood demodulator is obtained by maximizing the expression

$$\sum_i [y_0m_0 - y_1m_0\rho - y_0m_1\rho + y_1m_1] \tag{2.93}$$

which in terms of our original variable can be written as

$$\sum_i (v_{0i} - v_{1i})r_i\left(\rho^{X_i} - \rho^{1-X_i}\right) = \sum_i (v_i)r_i(1-\rho)(-1)^{X_i} \tag{2.94}$$

Since the factor $(1-\rho)$ is not a function of $\underline{X}$, Eq. (2.94) directly justifies the demodulation given on Figure 2.24 which weights v_i by the variable r_i.

For a minimum bit-by-bit decision, the weighting factor r_i need not be used, and a decision variable on X_i is obtained

based on the sign of v_i. However, when coding is applied and a decision variable on a sequence of bits is to be made, the weighting by r_i yields a confidence level of the form

$$\alpha_i = r_i v_i \tag{2.95}$$

which is equivalent to a maximum-likelihood decoder when the analog weight, given by (2.74), is used to select the most likely error pattern.

A justification of α_i in terms of finding a confidence level which is monotonically related to the probability that X_i is decoded correctly (as was done in Section 2.3.1) can be applied to this fairly general case as well.

2.3.3 Quaternary Signaling over the Troposcatter Channel

In this section we extend the theoretical considerations given on abstracting channel measurement information to the actual troposcatter demodulator. The modem of interest is a maximum-likelihood tropo (MLT) demodulator used in the analysis and test conducted for RADC [2.1],[2.2].

The abstraction of channel measurement information is complicated by the time-varying multipath structure prevelant over the troposcatter channel and the complex modulation format. The modulation format may be considered to be quaternary, i.e., four-phase, but, in fact, a low-level probe is combined with the basic data modulation signal. This probe is used to obtain channel measurement information which is used by the maximum-likelihood (Viterbi) demodulator. To a first approximation, the effects of this probe can be removed by the demodulator; thus, we are left with a quaternary data signal. Unfortunately, the multipath severely distorts this signal. Furthermore, as pointed out in [2.8], multipath also distorts the location of the actual bit errors and causes a dependence between bit errors. This effect can be minimized by using a certain amount of filtering to ensure that actual errors are covered by low confidence levels. While this filtering adds some extra low confidence levels, the performance impact is minimized since the interleaver spreads these confidence levels over independent codewords.

Following the previous theoretical considerations, the actual value of α_i used for the MLT demodulator is obtained by the following procedure:

(1) An estimate of the received complex sampled input sample $\tilde{Y}_i$ is constructed based on the demodulated data and the channel estimate. In fact, two estimates are constructed for each received bit since an early and late sample are used.

(2) The likelihood that this reconstructed sample is based on correctly demodulated data is estimated on a sample by sample basis by computing the difference between the actual and received samples as

$$|Y_i - \tilde{Y}_i|^2_{\text{Early}} + |Y_i - \tilde{Y}_i|^2_{\text{Late}} \tag{2.96}$$

(3) This difference term is normalized by subtracting off the term

$$|Y_i + \tilde{Y}_i|^2_{\text{Early}} + |Y_i + \tilde{Y}_i|^2_{\text{Late}} \tag{2.97}$$

which is analogous to the receiver shown on Figure 2.24.

(4) The actual confidence level is a filtered version of the difference between Eqs. (2.96) and (2.97) to give

$$4\,\text{Re}\left(Y_i * \tilde{Y}_i\right)_{\text{Early}} + 4\,\text{Re}\left(Y_i * \tilde{Y}_i\right)_{\text{Late}} \tag{2.98}$$

An equal weighting of the confidence levels over four data bits, i.e., box car filter, is implemented.

In the following section, experimental results are given for the above confidence level.

REFERENCES

[2.1] CNR, Inc., "Troposcatter Interleaver Study Report," Phase Report, RADC-TR-75-19, February 1975.

[2.2] CNR, Inc., "Troposcatter Interleaver," Final Technical Report for Rome Air Development Center, RADC-TR-76-213, July 1976.

[2.3] D. Chase, "A Combined Coding and Modulation Approach for Communication over Dispersive Channels," IEEE Trans. on Communications, Vol. COM-21, March 1973, pp. 159 - 174.

[2.4] D. Chase, "A Class of Algorithms for Decoding Block Codes with Channel Measurement Information," IEEE Trans. on Information Theory, Vol. IT-18, January 1972, pp. 170 - 182.

[2.5] Schwartz, Bennett, and Stein, Communication Systems and Techniques, McGraw-Hill, New York, 1966.

[2.6] J. G. Proakis, "Probabilities of Error for Adaptive Reception of M-Phase Signals," IEEE Trans. on Communications Techniques, February 1968.

[2.7] D. Chase and L. J. Weng, "Multiple Burst Correction Techniques for Slowly Fading Channels," IEEE Trans. on Information Theory, Vol. IT-22, September 1976, pp. 505 - 513.

[2.8] CNR, Inc., "Demod/Decoder Integration," Final Technical Report for Rome Air Development Center, RADC-TR-78-70, April 1978. AD#A053685.

SECTION 3

EXPERIMENTAL RESULTS

In this section, the equipment modifications, test procedures, and test results are discussed. Three categories of tests were performed.

The first tests were the soft decoder verification tests. These tests were performed on the soft decoder independent of the modem. The purpose of these tests was to insure proper operation of the soft decoder.

The second series of tests were performance tests over various simulated channels. These tests included the Gaussian noise channel as well as fading channels.

The final tests were with pulse interference. For these tests, a simulator was built and performance was measured over various pulse widths.

3.1 Tropo Interleaver Modifications

In order to carry out the investigation of channel measurement (soft decision) decoding for the tropo interleaver, it was necessary to add circuitry to the tropo interleaver. Figure 3.1 shows a diagram of the tropo interleaver. Changes were necessary in the soft decision generation of the demodulator and in the interleaved decoder.

The new interleaved soft decoder operates at an information bit rate of 16 kb/s. This corresponds to an encoded rate of 32 kb/s. A new interleaver and full soft decision deinterleaver were built with bit separation times of 0, 1.5, 2.25, 3, 4.5, 6, 12, 24, and 48 ms, which corresponds to 0, 34.5, 51.75, 69, 103.5, 138, 276, 552, and 1104 ms, respectively, of decoding delay. The channel data rate (to and from the modem) is 4.608 Mb/s. This is achieved by multiplexing the encoded data with PN fill to form the high-speed data stream. Testing at a channel rate of 4.6 Mb/s with an actual data rate of 16 kb/s is equivalent, as discussed in Contract F30602-74-C-0133, to testing at the full data rate (2.3 Mb/s), but less memory is required by the interleaver/deinterleaver.

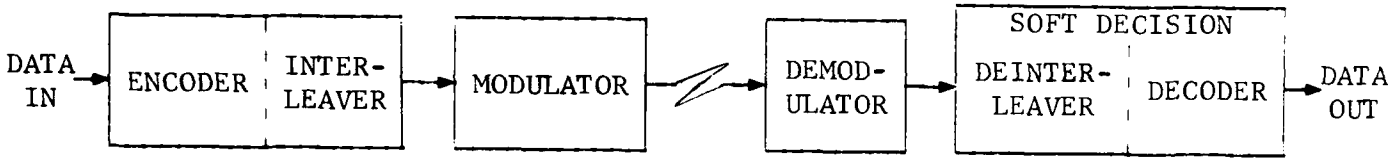

Figure 3.1 Tropo Interleaver

The channel measurements are generated by new circuitry in the demodulator. A single channel measurement value was generated for both in-phase and quadrature bit components of each baud. The first step in the generation of the channel measurement is the computation of a value α_i as follows.

$$\alpha_i = \left| \sum_{\rho=1} \left[\left| Y_i^{(\rho)} + \tilde{Y}_i^{(\rho)} \right|^2 - \left| Y_i^{(\rho)} - \tilde{Y}_i^{(\rho)} \right|^2 \right] \right| \qquad (3.1)$$

where

$Y_i^{(\rho)}$ = Received complex sample (output of A/D)

ρ = A number of samples per baud, $\rho = 1,2$

i = Baud position, $i = 1,2, \ldots$

$\tilde{Y}_i^{(\rho)}$ = Reconstructed complex sample (based on the Viterbi data estimate and the channel estimate)

The channel measurement values are computed from the α's by following the sliding average

$$\alpha_i' = \sum_{j=i-1}^{i+2} \alpha_i \qquad (3.2)$$

Figure 3.2 shows a block diagram of the demodulator with the new channel measurement circuits.

The input samples, Y, go into the maximum likelihood demodulator (MLD) and channel estimation circuits. Using a Viterbi algorithm, the MLD makes bit decisions for the input samples. The bit decisions and the channel estimates (h) are combined to form estimates of the input samples ($\tilde{Y}$). The actual input samples, Y, delayed by an amount equal to the delay through the MLD, are processed with $\tilde{Y}$ to produce the α's. The channel metric values are formed by a four-baud sliding average over the α's. The bit decisions from the MLD are delayed a small amount of times to line up with the channel measurement.

3.2 Soft Decoder Verification Tests

In order to verify the proper operation of the soft decision Golay decoder, a number of performance points were tested

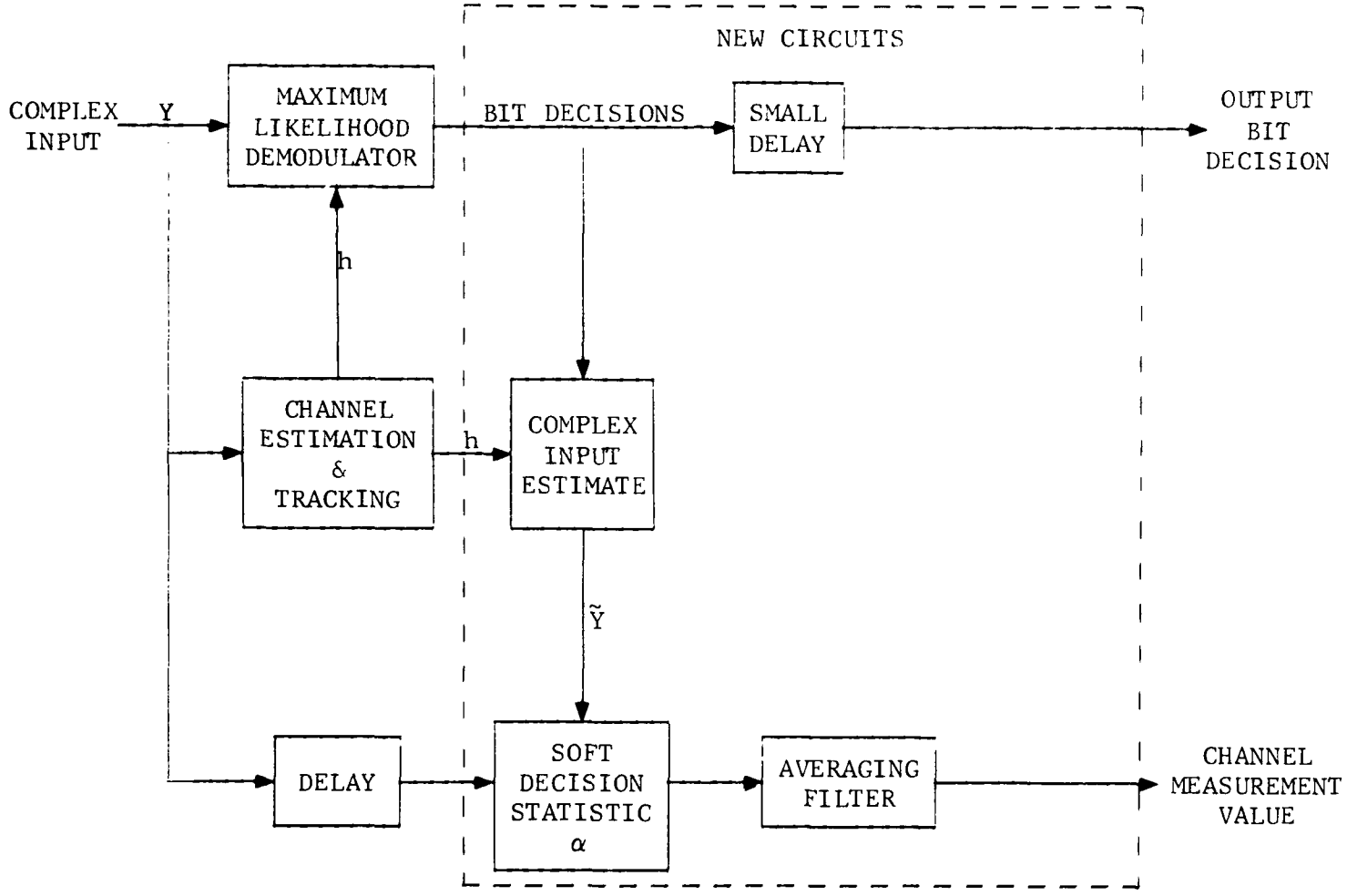

Figure 3.2 Demodulator with Channel Measurement Circuits

using the CNR Soft Decision Generator (SDG). Figure 3.3 shows the test setup using the SDG. A PN sequence at 16 kb/s (32 kb/s encoded rate) is generated by the transmit test set. The PN ata is encoded and merged into a 4.608 Mb/s data stream. Using an internal Gaussian noise source and A/D converter, the SDG generates Gaussian channel soft decision statistics. These soft decisions are received by the decoder where the data is decoded using the channel measurement decoding algorithm. The decoder can also be set to ignore the soft decisions and perform hard decision decoding on the data. The decoded data (hard or soft) and the raw data are sent to the test set where a local PN generator is used to check for errors.

Table 3-1 and Figure 3.4 show the results of the SDG tests. For these tests, raw error rate was set by adjusting the SDG. For each raw error rate point, the signal-to-noise ratio (E_b/N_0) for the corresponding code point is established by shifting down 3 dB from the E_b/N_0 of the raw point. The solid curves are the result of computer generated simulations. Since the performance points for hard and soft decoding correspond quite well with the computer-generated curves, the soft decoder is most likely operating properly.

3.3 Channel Simulator Tests

3.3.1 Equipment Interfacing

In order to perform any testing of the tropo interleaver, it is first necessary to connect all of the separate boxes. Figure 3.5 shows the correct point-to-point connections for coding tests. The dashed lines indicate that an external device other than that supplied by CNR, Inc. may be substituted; specifically, a separate test set consisting of a data generator and error detector/counter may be utilized to verify the operation of the equipment independently of the CNR, Inc. supplied test set

The test set, encoder, and decoder have many switches that need to be set for the various testing modes. Table 3-2 describes the necessary switch positions for the tests performed.

3.3.2 Simulator Adjustment

In this section, the setting of the simulator for the desired channel and signal-to-noise ratio will be discussed. Both additive Gaussian noise channels and fading dispersive channels will be covered.

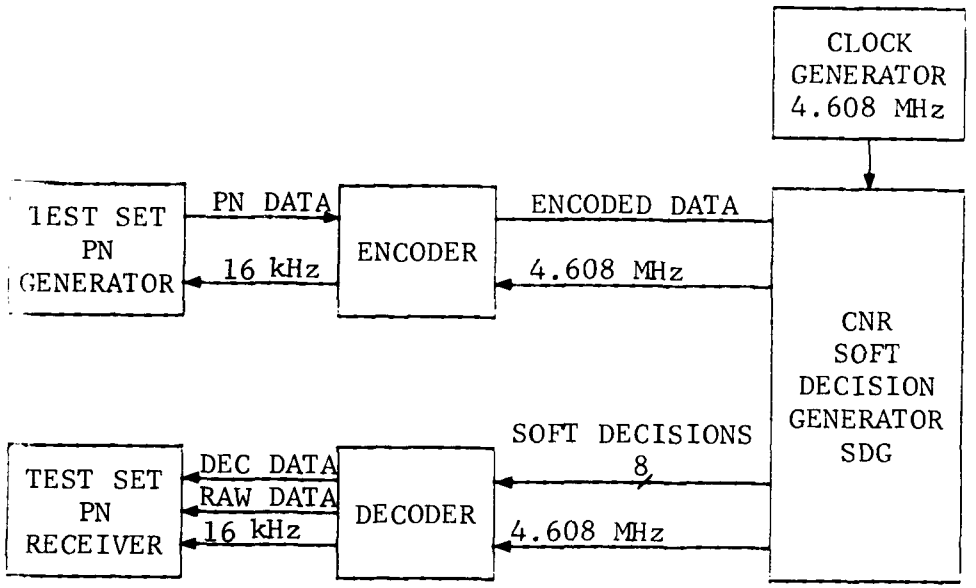

Figure 3.3 Soft Decoder Verification Test Setup

TABLE 3-1

ERROR RATES FOR GOLAY CODE

RAW	HARD	SOFT
8.1×10^{-2}	2.7×10^{-2}	5.80×10^{-3}
5.7×10^{-2}	9.3×10^{-3}	9.14×10^{-4}
3.9×10^{-2}	2.5×10^{-3}	7.12×10^{-5}

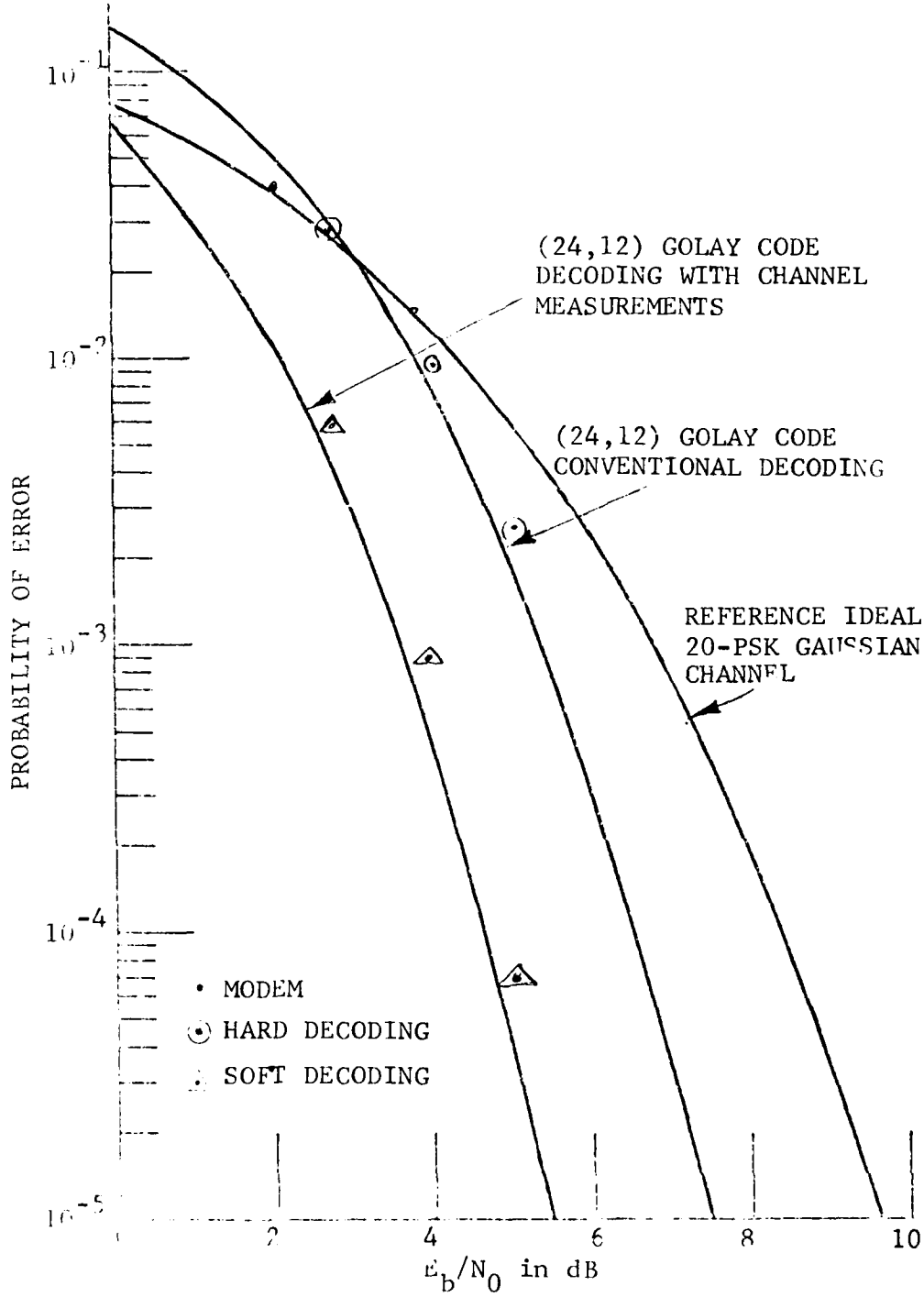

Figure 3.4 Performance Curves for the Rate-1/2 (24,12) Golay Code

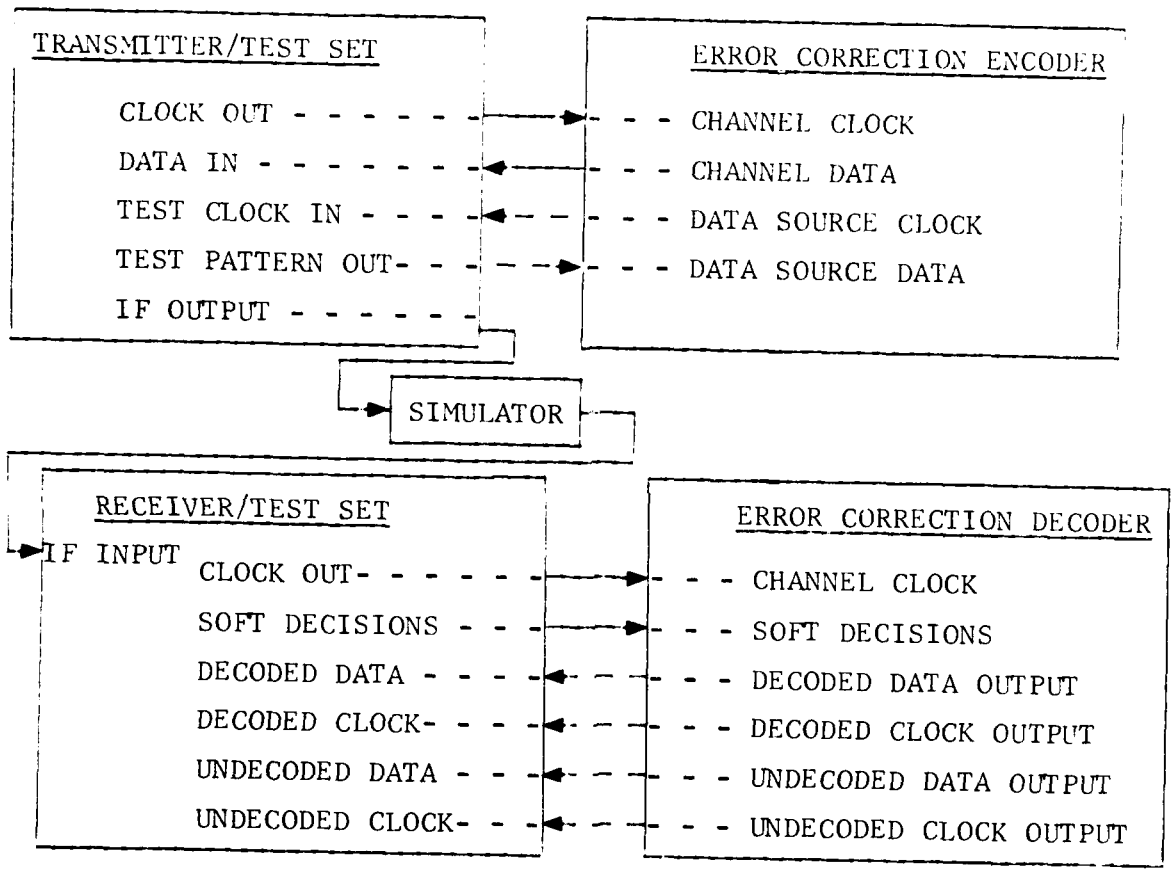

Figure 3.5 Connection Diagram for Troposcatter Interleaver Testing Using Coding

TABLE 3-2

TROPO INTERLEAVER SWITCHES

Error-Correcting Encoder Switches

Switch	Function
Main Breaker - ON	Controls line voltage to both logic and oscillator power supplies (Note: should normally be on at all times).
Power - ON	Controls line voltage to logic power supply - active only if main breaker is on.
Code	Allows selection of coding mode of operation.
PRODUCT	(24,12) Golay code with new interleaver
Data Rate	Controls selection of information bit rate (excludes parity) and required PN bit stuffing to match modem bit rate.
16 kb/s	Allowable Data Rate for Soft Decoding
Separation Time	Controls time between interleaved bits.
08	τ = 48 ms
Half Rate/Full Rate	Controls PN bit stuffing rate when matching coding bit rate to modem bit rate - set to match modem mode of operation.
Full	

Transmitter/Test Set Switches

Switch	Function
Power - ON	Controls line voltage to logic power supply
4.608 Mb/s/5.5296 Mb/s	Selects baud rate for modem.
4.608 Mb/s	2.304 M baud/s
Half Rate	Allows modem to transmit at half the baud rate.
Switch down (full rate)	2.304 M baud/s

TABLE 3-2 (Continued)

Transmitter/Test Set Switches (Continued)

Switch	Function
Pattern Selection Long	Selects pattern to be transmitted. Length $2^{20} - 1$, PN sequence

Receiver/Test Set Switches

Switch	Function
Main Breaker - ON	Controls line voltage to analog, digital, and oscillator power supplies.
Power - ON	Controls line voltage to analog and digital power supplies (functions only when main breaker is on).
Reset	Momentary contact switch to reset all counters to zero.
Resync	Momentary contact switch to sync local data sequence generators by injection loading.
Run/Halt Run Halt	Controls operation of test set. All enabled counters begin counting Suspends all counter operations
Undecoded Run Enable - ON	Controls undecoded data counter operation
Sampled Bit Run Enable - OFF	Controls sampled-bits counters operations
Signal Present Time Constant	Not implemented.
Modem Sync	Momentary contact switch which enables modem sync acquisition circuitry.
Decision Directed Feedback - ON	Selects decision directed feedback operation.
4.608 Mb/s/5.5296 Mb/s 4.608 Mb/s	Selects baud rate for receiver. 2.304×10^6 baud/s

TABLE 3-2 (Continued)

Receiver/Test Set Switches (Continued)

Switch	Function
Half Rate	Allows modem to receive at half the baud rate.
Switch down (full rate)	2.304 M baud/s
Int Time	Controls duration of probe correlation.
1	2032 baud
Loop Filter	Allows selection of tracking loop filter.
0	
Run Length	Controls duration of counting for decoded bit and undecoded bit counters from 10^4 to 10^{10}.
Pattern Selection	Selects local data sequence for error detection.
Long	Length 2^{20} - 1, PN sequence
BW Select	Controls selection of analog predetection filter (both 4 pole Butterworth).
NB	2.66 MHz 3 dB bandwidth

Error Correction Decoder Switches

Switch	Function
Main Breaker - ON	Controls line voltage to both logic and oscillator power supplies (Note: should normally be on at all times).
Power - ON	Controls line voltage to logic power supply - active only if main breaker is on.
Code	Allows selection of decoding mode.
PRODUCT	(24,12) Golay with new soft decision de-interleaver

TABLE 3-2 (Continued)

Error Correction Decoder Switches (Continued)

Switch	Function
Data Rate	Controls selection of information bit rate (excludes parity) and requires PN bit stuffing rate to match modem bit rate.
16 kb/s	Allowable data rate for soft decoding
Half Rate	Controls PN bit stripping rate - set to match modem mode of operation.
Switch down (full rate)	Modem operating at its full rate
Separation Time	Controls separation time for deinterleaver.
08	2τ = 48 ms
Resync	Momentary contact switch which enables code sync acquisition circuitry.
Channel Measurement	Selects channel measurement (soft decision) decoding or hard decision decoding.
Up	Soft decision decoding
Down	Hard decision decoding

3.3.2.1 Channel Selection

The simulator was placed in the I and Q test mode for the Gaussian noise tests. In this mode a single non-fading tap is selected.

For flat fading tests, the simulator was placed in its special flat fading mode. In this mode a single fading path is generated. RMS Doppler spreads of 1 Hz and 10 Hz were used in the tests.

In the selective fading test, the simulator was placed in the 16-tap, 4 diversity mode. However, only the A diversity was used, thus giving a single diversity with a maximum of 16 fading taps spaced at 100 ns intervals.

Table 3-3 shows the tap attenuator settings for a number of profiles. Taps with no indicated setting are turned off. Selective fading tests were conducted using profiles 3 and 5. Each profile was tested with 1 Hz and 10 Hz Doppler spreads.

3.3.2.2 Signal-to-Noise Ratio Adjustment

As a result of the extremely low power of the simulator's internal Gaussian noise source, a direct measurement of the noise level with a power meter was not possible. Instead, the noise was examined on a spectrum analyzer and a crude estimate of -70 dBm/MHz (-130 dBm/Hz) for noise spectral density was established. Since this was the nominal figure reported in the simulator operating manual, it was accepted as being accurate.

The simulator's average power output was measured using a power meter with the simulator in the I and Q mode. This mode freezes the pseudo-random tap modulators at their average values for just this purpose. The signal had a strength of -28 dBm.

From this information, the average signal-to-noise ratio for a one-path model can easily be calculated. E_b is the signal energy per bit. Hence, for the modem operating at 4.608 Mb/s

$$E_b = -28 - (10 \log 4.608 \times 10^6)$$

$$= -28 - 66.6$$

$$= -94.6 \text{ dBm} \qquad (3.3)$$

TABLE 3-3

SIMULATOR ATTENUATOR SETTINGS FOR TEST PROFILES (dB)

Tap Number (P_i)	Profile Number					
	1	2	3	4	5	6
1	0	0	0	0	-3	-1
2	-16	-6	-3	-1	0	0
3	-38	-14	-7	-4	-1	-1
4		-23	-12	-7	-3	-2
5		-34	-17	-11	-5	-3
6			-23	-14	-7	-5
7			-29	-18	-10	-7
8				-22	-12	-9
9				-25	-15	-11
10				-29	-18	-14
11					-21	-16
12					-24	-18
13					-27	-20
14						-23
15						-25
16						-28
P_{av} (dB)	0.1	1.1	2.5	4.0	5.5	6.6

Taking the noise spectral density as -130 dBm/Hz, the average signal-to-noise ratio with no signal attenuation after the tap modulators is

$$\frac{E_b}{N_0} = -94.6 - (-130) = 35.4 \text{ dB @ } 4.608 \text{ Mb/s} \tag{3.4}$$

For lower signal-to-noise ratios, the output signal is merely attenuated by the required amount.

The adjustment for the extra multipath power is made by increasing the above computed signal-to-noise ratio by P_{av} from Table 3-3. For example, suppose multipath profile 3 is set up on the simulator and the modem data rate is 4.608 Mb s. The single path calculation gives a signal-to-noise ratio of 35.4 dB with no attenuation. Table 3-3 indicates that multipath has added an additional 2.5 dB to the signal. Hence, the true signal-to-noise ratio is 37.9 dB. Adjustment for other signal-to-noise ratios must be made from this figure.

To compute E_b/N_0 for the coded systems, it is merely necessary to adjust the data rates in Eq. (3.3). This amounts to increasing the energy per bit, E_b, by the code rate. These adjustment figures are:

$$3 \text{ dB} = 10 \log \frac{12 \text{ information bits}}{24 \text{ codeword bits}} - \text{Golay} \tag{3.5}$$

For example, when running the code on a single path model with no attenuation in the signal path, the modem (raw) E_b/N_0 is 34.6 dB [Eq. (3.4)]. However, since the coded system has less information bits, it has an E_b/N_0 of

$$\begin{aligned} E_b/N_0 &= 34.6 \text{ dB} + 3.0 \text{ dB} \\ &= 37.6 \text{ dB} \end{aligned} \tag{3.6}$$

This penalization of the coded system allows a fair comparison to be made between coded and uncoded systems.

3.3.3 Simulator Test Procedure

The test procedure used with the simulator is summarized as follows:

(1) Connect RF power meter to simulator input test point and adjust input attenuator for -10 dBm at test point.

(2) Set up channel as indicated in Section 3.3.2.1 by adjusting tap attenuators, Doppler spread and mode switches.

(3) Set signal-to-noise ratio for test by adjusting the output attenuator (OATT). As was shown in Section 3.3.2.2, the signal-to-noise will be:

$$\frac{E_b}{N_0} = 34.6 - OATT + P_{av} \text{ (dB)} \quad \text{Raw}$$

and

$$\frac{E_b}{N_0} = 37.6 - OATT + P_{av} \text{ (dB)} \quad \text{Coded}$$

(4) Set decoder for hard decoding.

(5) Set test set run length to a value estimated to give at least 100 errors.

(6) Push Doppler spread RESET button on simulator (if fading channel).

(7) Test set RUN/HALT switch to HALT and RESET counters.

(8) RUN/HALT switch to RUN.

(9) At end of run, record results.

(10) Change to soft decoding; repeat 5 through 9.

(11) Change signal-to-noise ratio; repeat 3 through 10.

(12) Change channel; repeat 2 through 11.

3.3.4 Simulator Test Results

In this section, the data resulting from the various tests is presented. Figures 3.6 through 3.12 show performance curves derived from the data. On the curves, the raw modem data points are shown as "•", the hard decoding points are "⊙", and the soft decoding points are "△". For reference, the actual data taken is included in Tables 3-4 through 3-10.

3.4 Pulse Interference Tests

This series of tests is designed to show the improvement gained by channel measurement decoding when combating pulse interference. The pulse interference could be intentional or unintentional. In either case, the interference signal was modeled as a pulse of noise large enough to cause a 50% error rate. The power of the portion of the signal plus noise ratio was not changed during noise pulses.

3.4.1 Pulse Interference Test Setup

The setup for this series of tests is the same as that shown in Figure 3.5. The channel simulator for these tests is not the GFE Quad Diversity Simulator but is a CNR built interference simulator. Figure 3.13 shows a block diagram of this simulator. The 70 MHz IF output of the modulator is summed with a noise signal prior to being passed to the demodulator. The 70 MHz noise signal is gated by a mixer before summing with the data signal. The mixer is controlled by a pulse generator allowing noise pulses of widths 50 ms to 500 ms to be generated. A manual trigger is used for this pulse generator.

3.4.2 Pulse Interference Test Procedure

(1) Set proper parameters into modem and coding equipment, i.e., separation 48 ms (08), proper code, filter, etc.

(2) With noise off, synchronize modem, decoder, then test set. System should be error free.

(3) Turn noise on and verify a 50% error rate during noise pulses. This can be accomplished by setting the pulse generator to an arbitrary pulse with (T_p) and adjusting the noise level such that the following number of raw errors (N_e) is generated by each pulse.

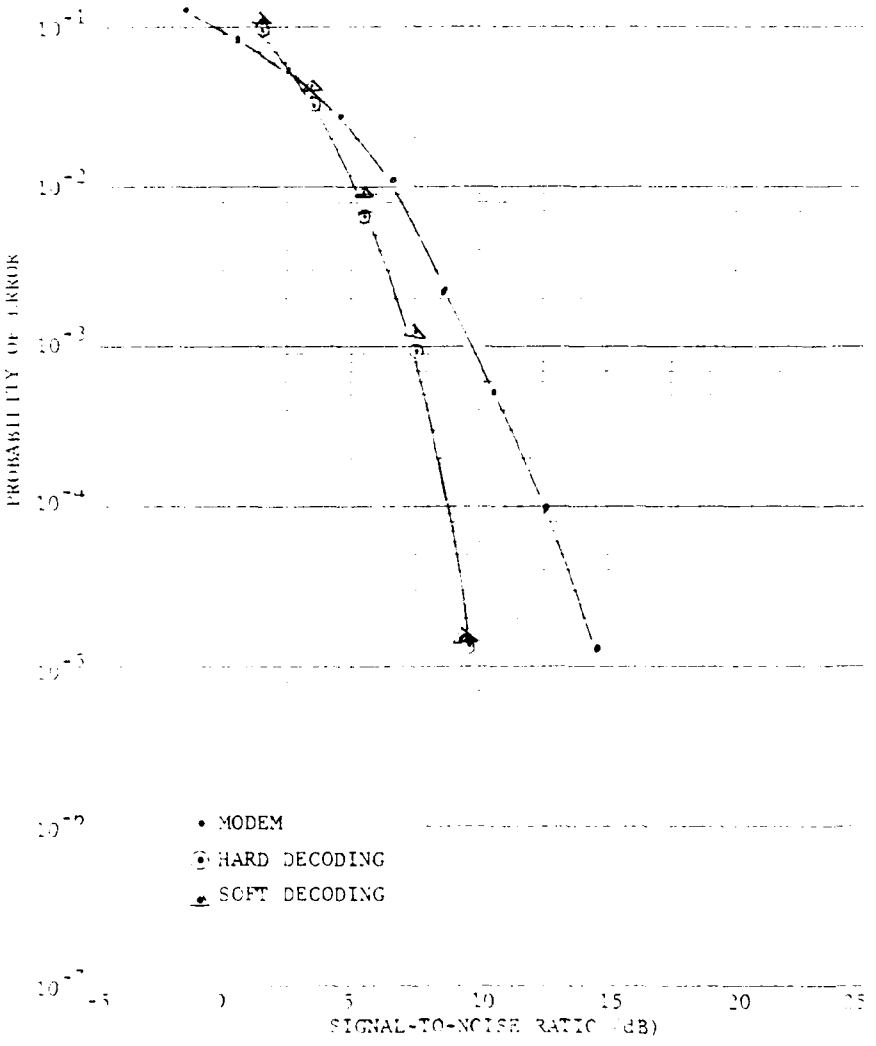

Figure 3.6 Performance over an Additive Gaussian Noise Channel

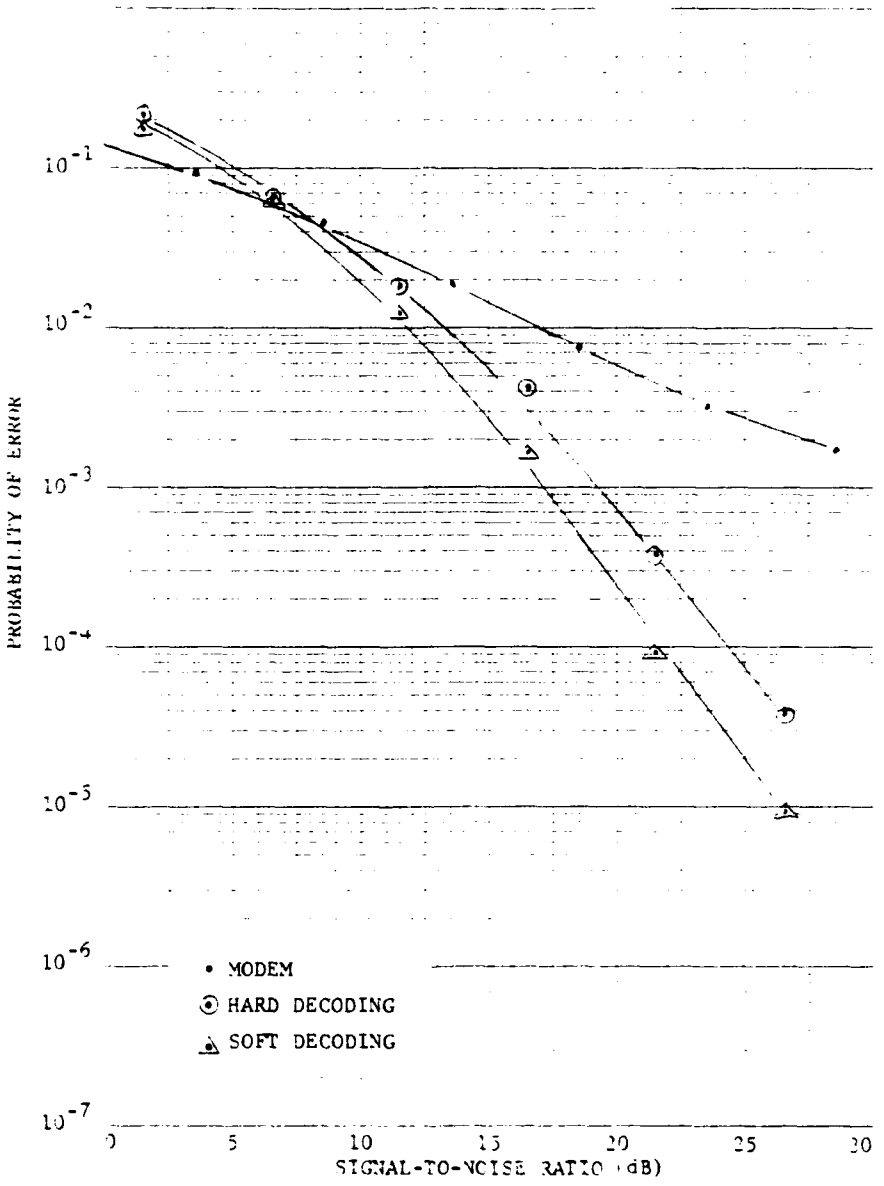

Figure 3.7 Performance over a Flat Fading Channel with 1 Hz RMS Doppler Spread

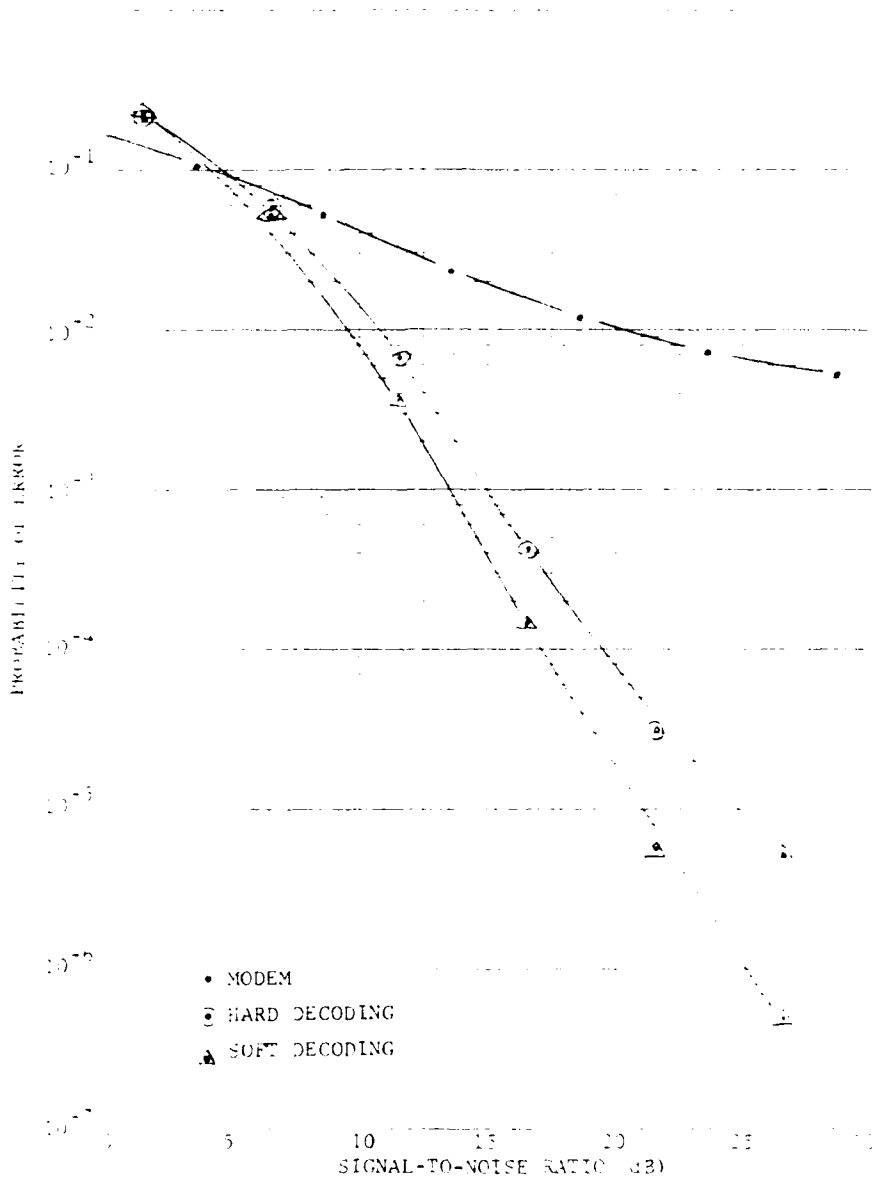

Figure 3.8 Performance over a Flat Fading Channel with 10 Hz RMS Doppler Spread

AD-A097 620 CNR INC NEEDHAM MA F/G 17/2
CHANNEL MEASUREMENT DECODING FOR TROPOSCATTER COMMUNICATIONS.(U)
FEB 81 D CHASE F30602-77-C-0182
UNCLASSIFIED RADC-TR-81-7 NL

2 OF 2
AD A097620

END
DATE FILMED
5 81
DTIC

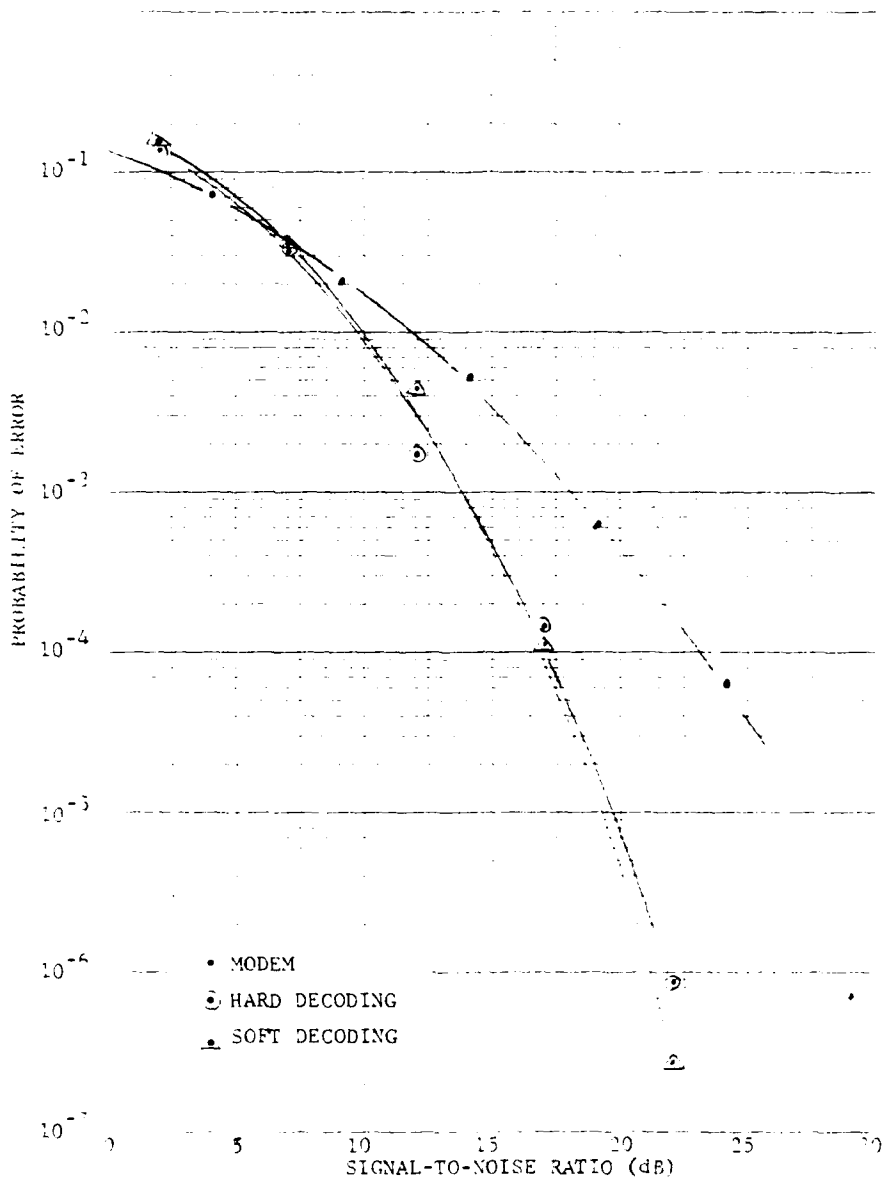

Figure 3.9 Performance over a Fading Channel with Multipath Profile 3 and 1 Hz RMS Doppler Spread

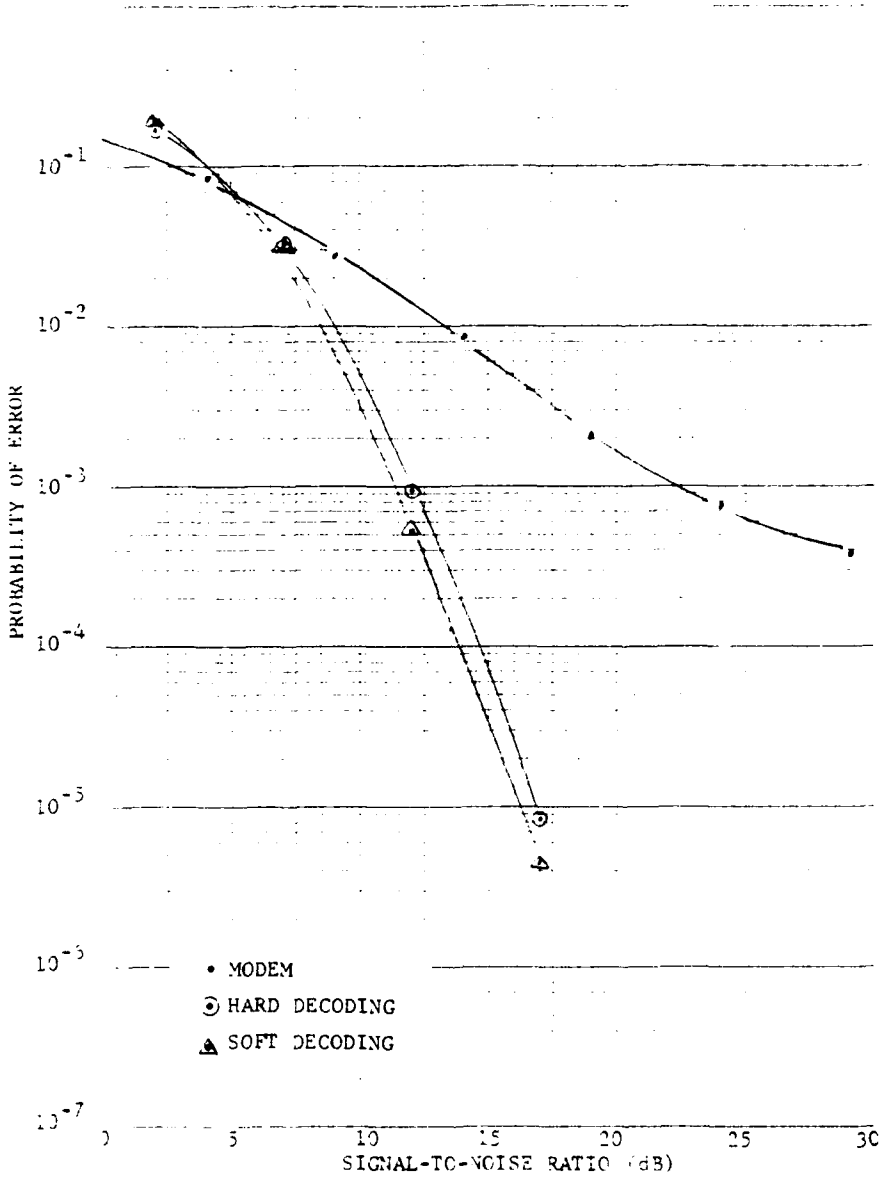

Figure 3.10 Performance over a Fading Channel with Multipath Profile 3 and 10 Hz RMS Doppler Spread

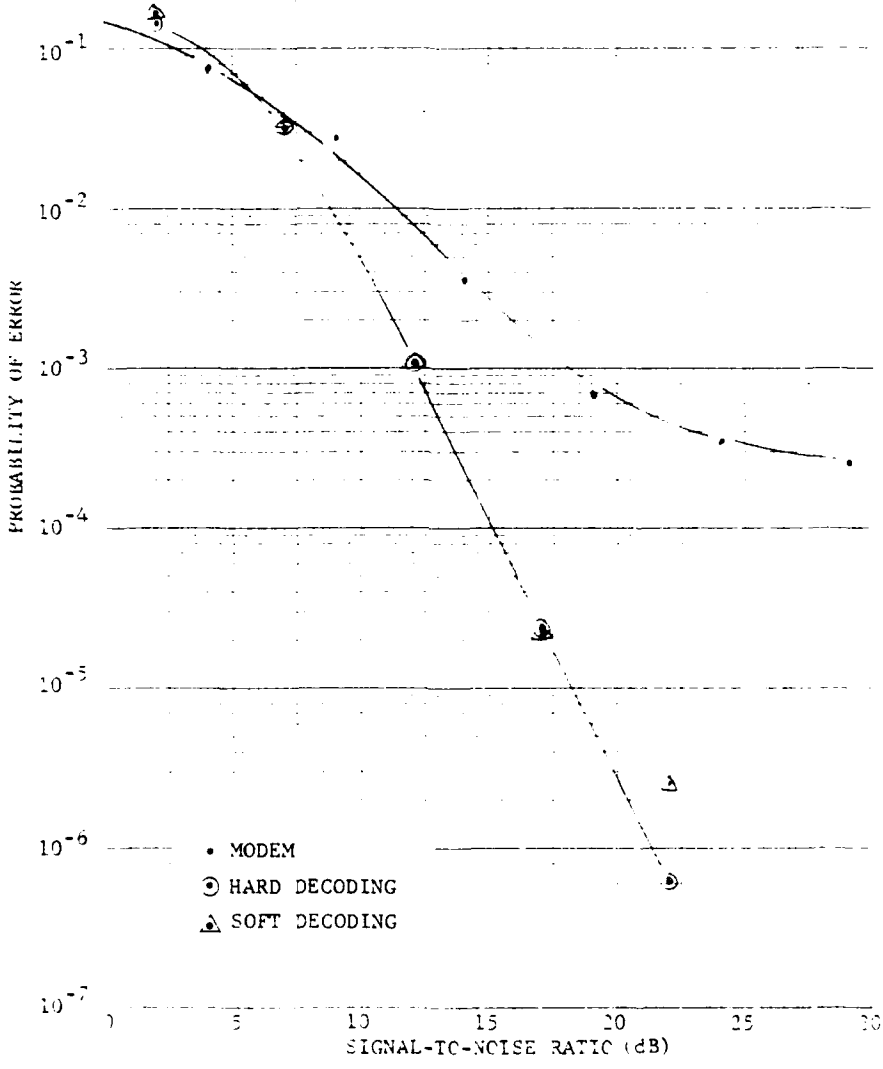

Figure 3.11 Performance over a Fading Channel with Multipath Profile 5 and 1 Hz RMS Doppler Spread

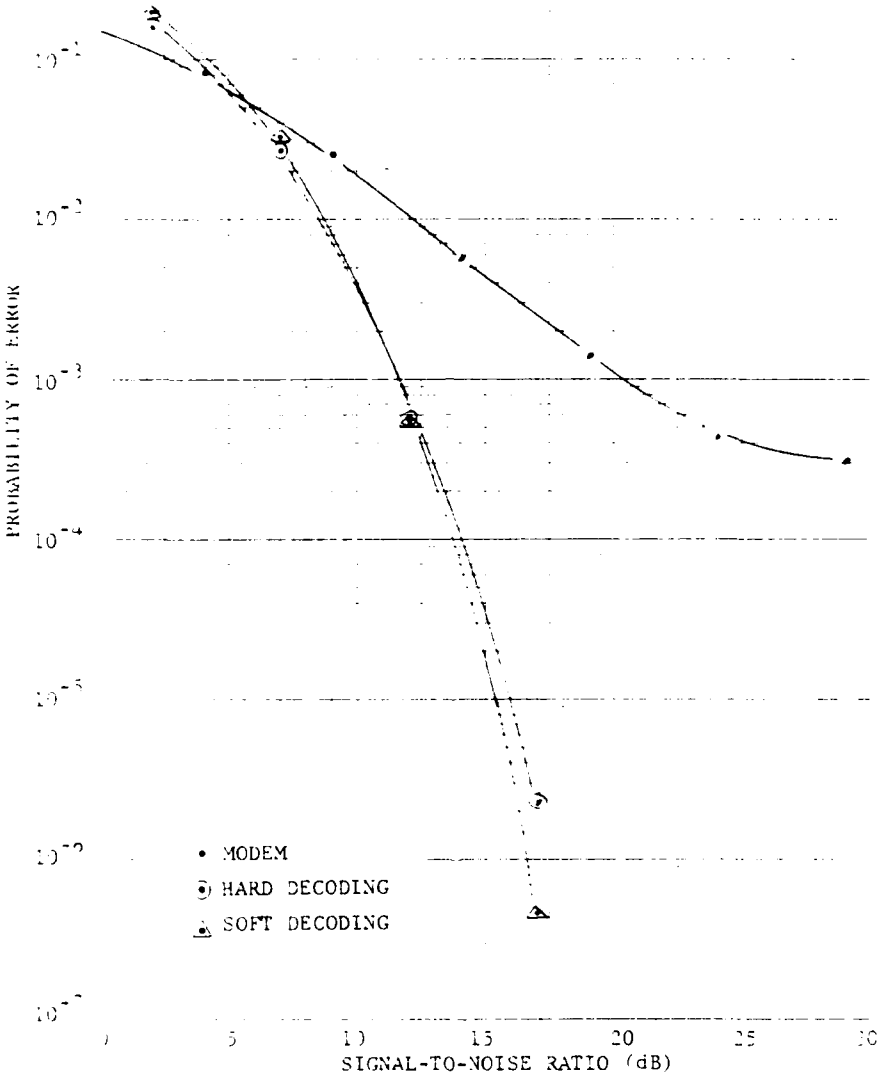

Figure 3.12 Performance over a Fading Channel with Multipath Profile 5 and 10 Hz RMS Doppler Spread

TABLE 3-4

GAUSSIAN NOISE TEST

Data Rate: 16 kb/s

Separation: 48 ms (08)

E_s/N_0 = 34.6 - Attn

Int: 1

Loop: 0

Filter: NB

Atten. Set	Signal to Noise		Hard Decoding			Soft Decoding		
	E_s/N_0	E_b/N_0	Run Length	Modem Error Rate	Decoder Error Rate	Run Length	Modem Error Rate	Decoder Error Rate
36	-1.4	1.6	10^6	1.32×10^{-1}	9.5×10^{-2}	10^6	1.32×10^{-1}	1.17×10^{-1}
34	0.6	3.6	10^6	8.67×10^{-2}	3.23×10^{-2}	10^6	8.64×10^{-2}	4.22×10^{-2}
32	2.6	5.6	10^6	5.19×10^{-2}	6.42×10^{-3}	10^6	5.22×10^{-2}	9.38×10^{-3}
30	4.6	7.6	10^6	2.93×10^{-2}	9.03×10^{-4}	10^6	2.88×10^{-2}	1.32×10^{-3}
28	6.6	9.6	10^7	1.02×10^{-2}	1.49×10^{-5}	10^7	1.00×10^{-2}	1.51×10^{-5}
26	8.6	11.6	10^6	2.11×10^{-3}				
24	10.6	13.6	10^6	5.07×10^{-4}				
22	12.6	15.6	10^6	9.7×10^{-5}				
20	14.6	17.6	10^7	1.35×10^{-5}				

TABLE 3-5

FLAT FADING 1 Hz TEST

Data Rate: 16 kb/s

Separation: 48 ms (08)

E_s/N_0 = 34.6 - Attn

Int: 1

Loop: 0

Filter: NB

Atten. Set	Signal to Noise		Hard Decoding			Soft Decoding		
	E_s/N_0	E_b/N_0	Run Length	Modem Error Rate	Decoder Error Rate	Run Length	Modem Error Rate	Decoder Error Rate
36	-1.4	1.6	10^6	2.13×10^{-1}	2.12×10^{-1}	10^6	1.34×10^{-1}	1.83×10^{-1}
31	0.6	3.6	10^6	9.71×10^{-2}	6.7×10^{-2}	10^6	9.62×10^{-2}	6.61×10^{-2}
26	2.6	5.6	10^6	4.38×10^{-2}	1.91×10^{-2}	10^6	4.3×10^{-2}	1.36×10^{-2}
21	4.6	7.6	10^6	1.98×10^{-2}	4.09×10^{-3}	10^6	1.99×10^{-2}	1.73×10^{-3}
16	6.6	9.6	10^7	7.54×10^{-3}	3.97×10^{-4}	10^7	7.51×10^{-3}	9.38×10^{-5}
11	8.6	11.6	10^7	3.18×10^{-3}	3.83×10^{-5}	10^7	3.2×10^{-3}	9.5×10^{-6}
6	10.6	13.6	10^8	1.72×10^{-3}	1.53×10^{-5}	10^8	1.47×10^{-3}	5.4×10^{-7}

TABLE 3-6

FLAT FADING 10 Hz TEST

Data Rate: 16 kb/s

Separation: 48 ms (08)

E_s/N_0 = 34.6 - Attn

Int: 1

Loop: 0

Filter: NB

Atten. Set	Signal to Noise		Hard Decoding			Soft Decoding		
	E_s/N_0	E_b/N_0	Run Length	Modem Error Rate	Decoder Error Rate	Run Length	Modem Error Rate	Decoder Error Rate
36	-1.4	1.6	10^6	2.01×10^{-1}	2.05×10^{-1}	10^6	2.02×10^{-1}	2.18×10^{-1}
31	0.6	3.6	10^6	1.06×10^{-1}	5.72×10^{-2}	10^6	1.1×10^{-1}	5.29×10^{-2}
26	2.6	5.6	10^6	5.18×10^{-2}	6.71×10^{-3}	10^6	5.22×10^{-2}	3.84×10^{-3}
21	4.6	7.6	10^6	2.34×10^{-2}	4.16×10^{-4}	10^6	2.34×10^{-2}	1.52×10^{-4}
16	6.6	9.6	10^7	1.23×10^{-2}	3.01×10^{-5}	10^7	1.22×10^{-2}	5.9×10^{-5}
11	8.6	11.6	10^7	7.01×10^{-3}	5.0×10^{-6}	10^7	7.10×10^{-3}	4.8×10^{-6}
6	10.6	13.6	10^6	5.05×10^{-3}				

TABLE 3-7

FADING PROFILE 3 1 Hz TEST

Data Rate: 16 kb/s

Separation: 48 ms (08)

E_s/N_0 = 37.1 - Attn

Int: 1

Loop: 0

Filter: NB

Atten. Set	Signal to Noise		Hard Decoding			Soft Decoding		
	E_s/N_0	E_b/N_0	Run Length	Modem Error Rate	Decoder Error Rate	Run Length	Modem Error Rate	Decoder Error Rate
38	-0.9	2.1	10^6	1.62×10^{-1}	1.46×10^{-1}	10^6	1.61×10^{-1}	1.61×10^{-1}
33	4.1	7.1	10^6	7.1×10^{-2}	3.19×10^{-2}	10^6	7.11×10^{-2}	3.41×10^{-2}
28	9.1	12.1	10^6	2.01×10^{-2}	1.82×10^{-3}	10^6	2.82×10^{-2}	4.47×10^{-3}
23	14.1	17.1	10^7	5.02×10^{-3}	1.5×10^{-4}	10^7	5.08×10^{-3}	1.09×10^{-4}
18	19.1	22.1	10^8	6.26×10^{-4}	8.6×10^{-7}	10^8	6.4×10^{-4}	2.7×10^{-7}
13	24.1	27.1	10^7	6.57×10^{-5}				
8	29.1	32.1	10^7	7.0×10^{-7}				

TABLE 3-8

FADING PROFILE 5 10 Hz TEST

Data Rate: 16 kb/s

Separation: 48 ms (08)

E_s/N_0 = 37.1 - Attn

Int: 1

Loop: 0

Filter: NB

Atten. Set	Signal to Noise		Hard Decoding			Soft Decoding		
	E_s/N_0	E_b/N_0	Run Length	Modem Error Rate	Decoder Error Rate	Run Length	Modem Error Rate	Decoder Error Rate
38	0.9	2.1	10^6	1.78×10^{-1}	1.71×10^{-1}	10^6	1.78×10^{-1}	1.92×10^{-1}
33	4.1	7.1	10^6	8.52×10^{-2}	3.14×10^{-2}	10^6	8.46×10^{-2}	3.2×10^{-2}
28	9.1	12.1	10^6	2.89×10^{-2}	9.51×10^{-4}	10^6	2.89×10^{-2}	5.17×10^{-4}
23	14.1	17.1	10^7	8.50×10^{-3}	8.1×10^{-6}	10^7	8.55×10^{-3}	4.4×10^{-6}
18	19.1	22.1	10^7	2.01×10^{-3}		10^7	1.98×10^{-3}	
13	24.1	27.1	10^6	7.73×10^{-4}				
8	29.1	32.1	10^6	3.97×10^{-4}				

TABLE 3-9

FADING PROFILE 5 1 Hz TEST

Data Rate: 16 kb/s

Separation: 48 ms (08)

E_s/N_0 = 40.1 - Attn

Int: 1

Loop: 0

Filter: NB

Atten. Set	Signal to Noise		Hard Decoding			Soft Decoding		
	E_s/N_0	E_b/N_0	Run Length	Modem Error Rate	Decoder Error Rate	Run Length	Modem Error Rate	Decoder Error Rate
41	-0.9	2.1	10^6	1.71×10^{-1}	1.51×10^{-1}	10^6	1.71×10^{-1}	1.82×10^{-1}
36	4.1	7.1	10^6	7.43×10^{-2}	3.11×10^{-2}	10^6	7.46×10^{-2}	3.53×10^{-2}
31	9.1	12.1	10^6	1.95×10^{-2}	1.06×10^{-3}	10^6	1.93×10^{-2}	1.02×10^{-3}
26	14.1	17.1	10^7	3.57×10^{-3}	2.52×10^{-5}	10^7	3.7×10^{-3}	2.27×10^{-5}
21	19.1	22.1	10^7	6.92×10^{-4}	6.0×10^{-7}	10^7	7.02×10^{-4}	1.60×10^{-6}
16	24.1	27.1	10^6	3.50×10^{-4}				
11	29.1	32.1	10^6	2.70×10^{-4}				

TABLE 3-10

FADING PROFILE 5 10 Hz TEST

Data Rate: 16 kb/s

Separation: 48 ms (08)

E_s/N_0 = 41.18 - Attn

Int: 1

Loop: 0

Filter: NB

Atten. Set	Signal to Noise		Hard Decoding			Soft Decoding		
	E_s/N_0	E_b/N_0	Run Length	Modem Error Rate	Decoder Error Rate	Run Length	Modem Error Rate	Decoder Error Rate
41	-0.9	2.1	10^6	1.81×10^{-1}	1.77×10^{-1}	10^6	1.81×10^{-1}	2.01×10^{-1}
36	4.1	7.1	10^6	8.17×10^{-2}	2.79×10^{-2}	10^6	8.13×10^{-2}	3.22×10^{-2}
31	9.1	12.1	2×10^6	2.59×10^{-2}	5.71×10^{-4}	2×10^6	2.59×10^{-2}	5.37×10^{-4}
26	14.1	17.1	6×10^7	5.66×10^{-3}	2.33×10^{-6}	6×10^7	5.58×10^{-3}	4.83×10^{-7}
21	19.1	22.1	10^6	1.41×10^{-3}				
16	24.1	27.1	10^6	4.14×10^{-4}				
11	29.1	32.1	10^6	3.05×10^{-4}				

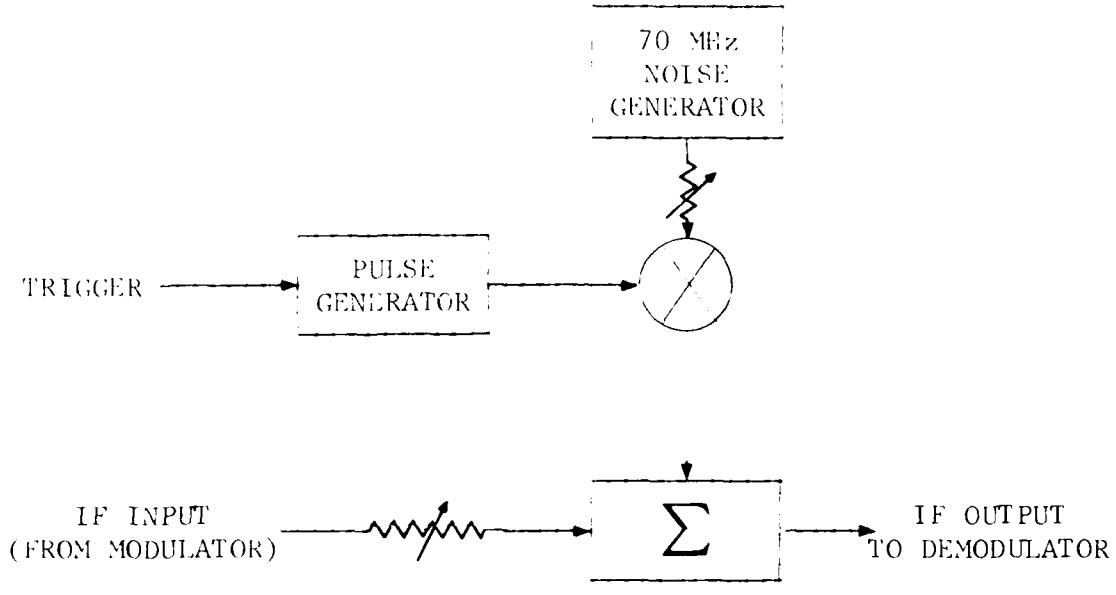

Figure 3.13 Pulse Interference Test Setup

$$N_e = 16 \times 10^3 \times T_p \times 0.5$$

(4) Make sure all units are still in sync.

(5) Set the pulse width, T_p, to 50 ms.

(6) Set the decoder for hard decoding.

(7) Reset error counters.

(8) Trigger pulse generator 10 times waiting approximately five seconds between each trigger.

(9) Record the number of errors.

(10) Set the decoder for channel measurement decoding.

(11) Repeat 7 through 9.

(12) Repeat 6 through 11 for pulse widths of 100, 140, 150, 160, 200, 250, 280, 290, 300, 310, 320, 350, 400, 450 ms.

3.4.3 Pulse Interference Test Results

Table 3-11 lists the results of the pulse interference tests. The number of errors listed for each entry is the total number of errors after ten pulses are transmitted. The data is plotted in Figure 3.14. This plot is on semi-log paper and gives the average number of errors per pulse vs. the pulse width.

From the curve, it can be seen that hard decoding goes error free for pulse widths below 140 ms and soft decoding for pulse widths below 280 ms. At a separation time of 48 ms, this corresponds to the correction of three errors per codeword for hard decoding and slightly more than six errors per codeword for soft decoding. Even for larger pulse widths, soft decoding maintains a significant advantage over hard decoding.

TABLE 3-11

PULSE INTERFERENCE TEST RESULTS

Data Rate: 16 kb/s
Separation: 48 ms (08)

Int: 1
Loop: 0
Filter: NB

PULSE WIDTH T_p	NUMBER OF ERRORS IN 10 PULSES			
	HARD DECODING		SOFT DECODING	
	MODEM ERRORS	DECODER ERRORS	MODEM ERRORS	DECODER ERRORS
50	3.99×10^3	0	3.93×10^3	0
100	7.83×10^3	0	7.90×10^3	0
140	1.11×10^4	0		0
150	1.17×10^4	2.99×10^2	1.19×10^4	0
160	1.25×10^4	5.02×10^2	1.25×10^4	0
200	1.59×10^4	2.28×10^3	1.56×10^4	0
250	1.97×10^4	6.54×10^3	1.98×10^4	0
280			2.20×10^4	0
290			2.25×10^4	8.70×10^1
300	2.35×10^4	1.22×10^4	2.34×10^4	1.37×10^2
310			2.41×10^4	1.66×10^2
320			2.53×10^4	2.26×10^2
350	2.76×10^4	1.91×10^4	2.73×10^4	1.23×10^3
400	3.14×10^4	2.55×10^4	3.13×10^4	5.63×10^3
450	3.56×10^4	3.14×10^4	3.54×10^4	1.22×10^4

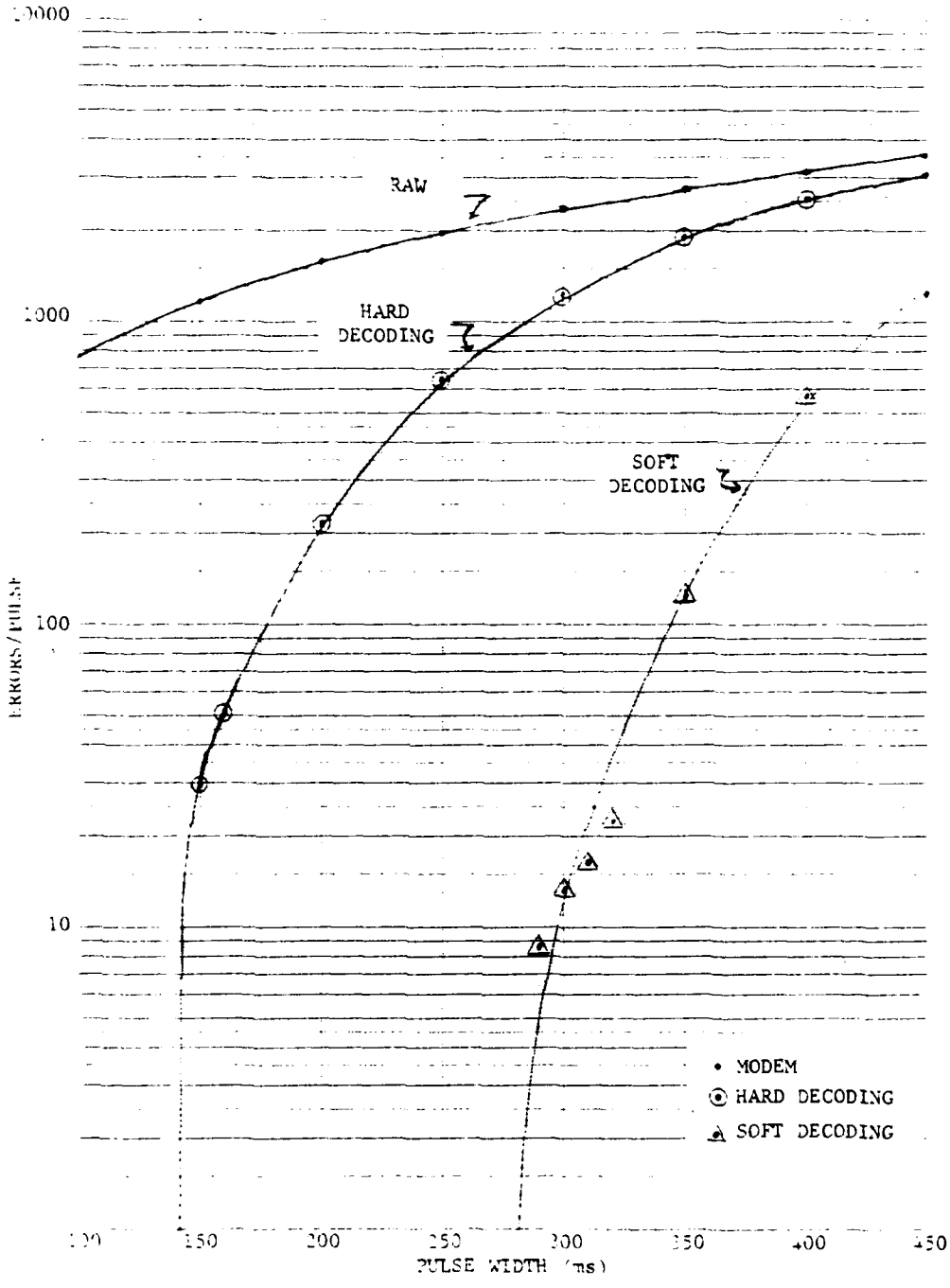

Figure 3.14 Performance with Pulse Interference

SECTION 4

CONCLUSIONS AND RECOMMENDATIONS FOR FUTURE WORK

The experimental results obtained during this effort indicate that under certain conditions, such as pulse jamming, significant gains can be achieved by the use of channel measurement decoding. For typical multipath profiles, significant coding gains have been achieved by fairly simple binary decoding techniques. Unfortunately, the predicted theoretical gains due to the use of channel measurement decoding have not been achieved by the experimental results. While channel measurement decoding did offer a 3-dB gain over binary decoding for flat fading, this gain is well below the theoretical prediction of 7.2 dB. Similarly, for multipath profiles 3 and 5, the performance gain obtained from the use of channel measurement decoding was small and well below the expected theoretical gain of 3.4 dB predicted in Section 2.2 The discrepancy between the theoretical and experimental results is still an open question, which may be resolved by future work in this area. Modifying an existing troposcatter demodulator to extract meaningful channel measurement information, as was done on this contract, is not an effective way to resolve these issues. Indeed, one of the important conclusions of this work is that one must consider the abstraction of channel measurement information during the start of the demodulator design. It is believed that in a fresh design of a troposcatter modem, the performance gains due to the use of channel measurement decoding will be significantly greater than the experimental results obtained during this contract. Furthermore, the significant performance gains in the presence of pulse jamming indicated that a new modem design can be very attractive for ECCM applications.

MISSION
of
Rome Air Development Center

RADC plans and executes research, development, test and selected acquisition programs in support of Command, Control Communications and Intelligence (C^3I) activities. Technical and engineering support within areas of technical competence is provided to ESD Program Offices (POs) and other ESD elements. The principal technical mission areas are communications, electromagnetic guidance and control, surveillance of ground and aerospace objects, intelligence data collection and handling, information system technology, ionospheric propagation, solid state sciences, microwave physics and electronic reliability, maintainability and compatibility.

END

DATE
FILMED

5 81

DTIC